2012

Fatigue Failure Evaluation of Tie Plates due to Secondary Deformations on Steel Plate Girder Bridges

Xiang Li
Lehigh University

Fatigue Failure Evaluation of Tie Plates due to Secondary Deformations on Steel Plate Girder Bridges

by

Xiang Li

A Thesis
Presented to the Graduate Research Committee
of
Lehigh University

In Candidacy for the Degree of
Master of Science
In
Civil Engineering

Lehigh University
Bethlehem, Pennsylvania
May 2012

Copyright

Certificate of Approval

This Thesis is accepted and approved in partial fulfillment of the requirements for the Master of Science.

_____

Clay J. Naito, Ph. D., P. E.
Thesis Advisor

_____

Sibel Pamukcu, Ph. D.
Chair of Civil and Environmental
Engineering Department

_____

Date

Acknowledgements

I'd like to first express my gratitude to my academic advisor, Professor Clay Naito, for his continuous support and guidance throughout my M.S. study at Lehigh University. He is always available for discussion and meetings with him are always welcoming and thought-provoking.

I would also wish to thank Dr. Ben Yen and Ian Hodgson for their contribution, support, and encouragement throughout my M.S. study.

The support of the Department of Civil and Environmental Engineering at the P.C. Rossin College of Engineering, and ATLSS (a National Center for Engineering Research on Advanced Technology for Large Structural Systems, Lehigh University) are gratefully acknowledged.

Table of Contents

Acknowledgements iv

Abstract 1

1. Introduction 3

1.1 Background on Steel Plate Girder Bridge System 3

1.2 Overview of Secondary Deformations 4

1.3 Previous Cases of Fatigue Failures 5

1.4 Monitoring Method 7

1.5 Finite Element Method in Bridge Study 7

1.6 Study Objectives 11

1.7 Outline of Thesis 11

2. Overview of Study 13

2.1 Bridge Description 13

2.2 Field Damage Conditions 17

2.3 Testing Plan 18

2.3.1 Instrumentation Locations 19

2.3.2 Controlled-Load Testing 22

2.3.3 Long-Term Monitoring 24

3. Field Measured Results 25

3.1 Crawl Test Results 25

3.1.1 Longitudinal Girder Response 25

3.1.2 Tie Plate Response 27

3.1.3 Cantilever Floor Beam Web Response 31

3.2 Long-Term Monitoring Results 34

3.2.1 Location A: Connection with Bolts Removed 36

3.2.2 Location B: Retrofitted Connection 38

3.2.3 Location C: As-Built Connection 40

3.3 Summary of Short-Term and Long-Term Monitoring Results 41

4. Development and Validation of FEM 42

4.1 Simulation Overview 42

4.1.1 Geometry and Element Type 42

4.1.2 Mesh and Element Size 43

4.1.3 Assembly and Constraints 44

4.1.4 Loads and Boundary Conditions 46

4.2 Preliminary Examination on Model Behavior 47

4.3 Comparison between Measured and Computed Results 49

4.3.1 Primary Girder Response 51

4.3.2 Tie Plate Response 54

4.3.3 Cantilever Bracket Web Response 59

4.4 Adjustment of FE Model 64

4.5 Summary of Comparison 66

5. Examination of Bridge System using FEM 68

5.1 Cause of Tie-Plate Bending 68

5.1.1 Girder Rotation 70

5.1.2 Stress and Displacement Envelops 73

5.2 Examination of Skew 76

5.2.1 The “Right” Bridge 78

5.2.2 Floor Beams Parallel to Abutments 78

5.3 Examination of Stringer Spacing 80

5.4 Summary of Parametric Studies 87

6. Recommendation for Retrofit 88

6.1 Recommended Retrofit Location 88

6.2 Recommended Retrofit Procedures 90

6.2.1 “Softening” 91

6.2.2 “Stiffening” 92

6.3 Summary 94

7. Conclusions and Limitations 96

References 99

Appendix A: Instrumentation Details 101

Appendix B: Mathcad Computation Sheet 105

Vita 108

List of Tables

Table 3-1: Fatigue-life estimates for tie plate and cantilever bracket web at Location A 37
Table 3-2: Fatigue-life calculations for strain gages installed on tie plate and cantilever bracket web at Location B 39
Table 3-3: Summary of fatigue-life calculations for strain gages installed on tie plate at Location C 41

List of Figures

Figure 2-1: Bridge location (Google Maps 2010) and view of bridge looking east from Abutment 1 14
Figure 2-2: Bridge layout 15
Figure 2-3: Cross-section of bridge 16
Figure 2-4: Cantilever bracket to tie plate to floor beam connection details 17
Figure 2-5: Location of the three cracked tie plates discovered on the bridge 18
Figure 2-6: Sensors placed on critical locations of the bridge 19
Figure 2-7: Location plan showing tie-plates selected for instrumentation 20
Figure 2-8: Strain gages installed on the tie plate (A3, A4) after 7 of the 8 bolts removed and on the cantilever bracket web (A5, A6) 21
Figure 2-9: Strain gages installed on the tie plate (B3, B4), on the top flange of the girder (B1) and on the cantilever bracket web (B5, B6) 22
Figure 2-10: Test truck used during controlled load tests 23
Figure 3-1: Stress location-history plot for strain gages installed on the top and bottom girder flanges 27
Figure 3-2: Stress location-history plot for strain gages installed on the tie plates at Location A before bolt removal (BBR), after bolt removal (ABR) and at Location B 29
Figure 3-3: Displacement location-history plot for LVDTs installed at Location A before bolt removal (BBR), after bolt removal (ABR) and at Location B 31
Figure 3-4: Stress location-history plot for strain gages installed on cantilever bracket web at Location A before bolt removal (BBR), after bolt removal (ABR) and at Location B 34
Figure 3-5: Stress-range histogram for strain gages installed on the tie plate at Location A 37
Figure 3-6: Potential web cracking (in red) locations in web of cantilever bracket 40
Figure 4-1: Detailed mesh and constraint at floor beam-girder connection 44
Figure 4-2: Wireframe of the model with load and boundary conditions 47
Figure 4-3: Bridge deformation and structural components' interaction 48
Figure 4-4: Strain gage location 50
Figure 4-5: Computed and measured stress in the top and bottom girder flange at locations at Location A 52
Figure 4-6: Computed and measured stress in the top and bottom girder flange at locations at Location B 52
Figure 4-7: Computed and measured stress in the top and bottom girder flange at locations at Location C 53
Figure 4-8: Computed and measured stress in the tie plate at locations at Location A before bolt removal 55
Figure 4-9: Computed and measured stress in the tie plate at locations at Location B 56
Figure 4-10: Computed and measured stress in the tie plate at locations at Location C 57
Figure 4-11: Computed and measured stress in the tie plate at locations at Location A after bolt removal 57

Figure 4-12: Displacement location-history plot for test data and FEA of tie plate at Location A before bolt removal (BBR), after bolt removal (ABR) 59
Figure 4-13: Computed and measured stress in the cantilever bracket web at locations at Location A before bolt removal 61
Figure 4-14: Computed and measured vertically-oriented stress in the cantilever bracket web at locations at Location B 62
Figure 4-15: Computed and measured vertically-oriented stress in the cantilever bracket web at locations at Location A before bolt removal 63
Figure 4-16: Computed and measured vertically-oriented stress in the cantilever bracket web at locations at Location A after bolt removal 63
Figure 4-17: Bridge cross-section after adding parapets to FE model 64
Figure 4-18: Stress in the top and bottom girder flange at locations at Location A without and with parapets 65
Figure 4-19: Model (with parapets) exaggerated deformed shape with frequency of 1.57 Hz 66
Figure 5-1: Sketch of tie plate bending due to global action [Fisher 1984, Page 188] 69
Figure 5-2: Comparison of stress history in tie plate with influence line for girder slope for Location A (floor beam 13) 71
Figure 5-3: Neutral axis and zero rotation location of south girder and stress envelope of the associated tie plate 73
Figure 5-4: Envelope of horizontal displacement at each tie plate over the length of the bridge 74
Figure 5-5: Envelope of normal stress at each tie plate over the length of the bridge 74
Figure 5-6: Envelope of normal stress at each tie plate after shortening the span length 75
Figure 5-7: Plan views of three proposals for skewness investigation 77
Figure 5-8: Comparison of stress in tie plate at Location A with three skewness arrangements . 77
Figure 5-9: Magnified plan view of floor beam system deformation and structural components' interaction 79
Figure 5-10: Plan view of stringer-to-floor-beam connection and fixed-end beam theory 81
Figure 5-11: Relative displacement between tie plate and stringers at Location A with tie plate connected and not connected to girder using FEA 82
Figure 5-12: Bending stress in tie plate with stringer fixed at various spacing when the tie plate is bolted to girder 84
Figure 5-13: Maximum and minimum bending stress of tie plate vs. stringer spacing at Location A with tie plate connected and not connected to girder 84
Figure 5-14: The envelope of girder slope at the tie-plate 85
Figure 5-15: Estimation of maximum bending stress by design computation of tie plate at Location A with tie plate connected to girder 86
Figure 6-1: Estimated stress range for tie plates over south girder 89
Figure 6-2: Recommended retrofit strategies 90
Figure 6-3: Stress in tie plate at Location A prior to and after bolt removal (BBR)/ (ABR) 92
Figure 6-4: Bridge cross-section after adding additional stringers to FE model 93
Figure 6-5: Stress in tie plate at Location A prior to bolt removal without and with additional stringers 94

Abstract

Prevention of fatigue induced fracture of steel bridge systems represents an important criterion of bridge design. Unfortunately in some cases unanticipated secondary deformations can occur on portions of the bridge structure. One form of fatigue induced fracture from secondary deformations was first identified in 1967 when out-of-plane deformations were induced on tie plates connecting transverse floor beams and cantilever brackets across the primary longitudinal girders.

This fatigue condition has been identified on a number of bridges over the past 40 years. The most recent occurrence was found in the bridge carrying route 422 over the Schuylkill River in Berks County Pennsylvania, United States. A field and forensic investigation conducted by Pennsylvania Department of Transportation crews and personnel from the ATLSS Center of Lehigh University in 2009 to determine the cause of the crack formation and to develop a recommendation on a repair approach for the bridge.

The results of the study revealed that the steel bridge construction consisting of a concrete deck supported by stringers supported by floor beams can result in unanticipated secondary deformations of the tie plates crossing the girders. The magnitudes of the displacements are large enough to produce cyclic stresses that result in fatigue induced fracture. Field measurements and finite element analysis indicated that the deck system is rigid with respect to the displacement of the girder and tie plate and the tie plates were highly stressed near the supports due to their relative movement in compliance with the top flange of the girder resulting

in the limited fatigue life. Building on the verified finite element model, a series of parametric studies on steel plate girder bridge system were conducted to assess the potential of this failure mode for bridges with different geometries. Results demonstrated that skewness of floor beam system and constrain from stringers may contribute to the tie plate in-plane bending stress. In addition, two optional retrofit strategies are executed and evaluated with the aid of finite element method. A retrofit consisting of removal of the restraint between the tie plate and the girder was recommended to minimize secondary displacements and associated stresses.

1. Introduction

The study is carried out to evaluate fatigue cracking in tie plates in a multi-span, non-redundant, steel plate girder bridge. The tie plates are needed to provide continuity for the transverse floor beam, which were originally designed to perform as tension connectors. Fatigue cracking in the tie plates has raised concerns that the tie plates are being subjected to stresses that are significantly different than those assumed in design. The occurrence of cracks in the tie plates of the bridge carrying State Route 422 provides a unique opportunity to investigate the cause of cracking.

1.1 Background on Steel Plate Girder Bridge System

It has been generally recognized that a steel plate girder bridge is an economical and efficient type of structure for spans ranging from 15 to 80 ft., carrying roads or railways.

A great number of steel bridges designed in the United States are of this type, a type evidently possessing advantages justifying its adoption to such a large extent.

In the first place, plate girders are so simple that there is little possibility of error in the calculation of either stresses or design. Secondly, the cost of manufacture is considerably less than any other kind of construction, while the risks of defects due to faulty material and workmanship are reduced to a minimum. They can be transported with little difficulty, oftentimes in one piece, and erected at site in a short time without great trouble, and at a small cost. When erected they require little attention beyond occasional painting, the only maintenance necessary for a properly designed bridge.

The joint qualities of simplicity, economy, endurance, and low maintenance costs are combined to such an extent in plate girder bridges that their adoption for moderate spans has become the standard practice of most engineers.

This non-redundant bridge system has two main longitudinal girders set back from the edges. There are transverse floor beams, both between the longitudinal girders and that cantilever out from the longitudinal girders. The top flanges of the longitudinal girders, the floor beams and cantilever bracket are connected by tie plates. To simplify construction longitudinal stringers are placed on top of this assembly and used to support the reinforced concrete deck.

1.2 Overview of Secondary Deformations

When designing a bridge system, two-dimensional evaluation assumptions are often made to simplify the design process while still providing a level of conservatism to the design approach. While in some cases, the resulting bridge system can produce unexpected secondary deformations under service. These deformations occur due to compatibilities in displacement as the members transfer loads in three dimensions.

Take the tie plate in a steel plate girder bridge system as an example. The tie plate is originally designed to function as tension connectors, the designers expected that these bolted plates would act in simple tension, which is a reasonable assumption based on the plans and actual bridge. Fatigue cracking in the tie plates has drawn attentions to fellow bridge engineers.

Although the magnitudes of the secondary deformations are often small, for stiff components the imposed deformations can result in moderate stress cycles. Over time the unexpected stress

cycles can result in fatigue induced cracking and failures prior to the service expectancy of the bridge.

1.3 Previous Cases of Fatigue Failures

Since 1967 a number of highway and railroad bridge structures in the United States have experienced fatigue cracking which sometimes resulted in brittle factures as a result of service loading [Fisher 1984]. In many cases these failures can be attributed to unanticipated secondary displacements of the structural elements which in turn produce cyclic displacement-induced stresses

Cases of similar damage have occurred in a number of bridges in Pennsylvania. Failures such as these were found in the Lehigh River and Canal Bridges located in Bethlehem, Pennsylvania [Fisher 1984, Demers and Fisher 1989], the Allegheny River Bridge located in Pittsburgh [Fisher 1984], the Edison Bridge on Route 9 over the Raritan River [Fisher et. al. 1995], and, most recently, the Schuylkill River Bridge carrying Route 422 in Berks County, PA [Naito et. al. 2010].

The Lehigh River and Canal Bridges consist of two adjacent identical structures. The twin bridges were constructed in 1953. In 1972, Pennsylvania Department of Transportation personnel discovered several fatigue cracks in the tie plates connecting the floor beams and the cantilever brackets across the main girders. Analysis showed all cracks initiated from the edge of the tie plates where a tack weld was used to connect the plates to the cantilever bracket during fabrication, and the fatigue cracks developed and propagated slowly from the ends of the tack

welds through the bolt holes, where it experienced the largest changes in rotation. To resolve this issue, all the cracked plates were replaced with a new design that eliminated bolted connection between the tie plate and girder, and decreased the midsection width to decrease the stiffness and associated service stresses.

Similarly, the Allegheny River Bridge was a four-span continuous beam-girder bridge and a five-span truss bridge over the Allegheny River outside of Pittsburgh, Pennsylvania, which also consists of the cantilever brackets. All fatigue cracks found in the tie plates of the Allegheny River Bridge originated from rivet holes caused by the same secondary displacement observed in the Lehigh River and Canal Bridges case. The cracked plates were repaired on site through welding and the addition of a reinforcement plate bolted on top of the pre-existing plate. Post inspection measurements revealed continued levels of high stress in the retrofitted connection. Further cracking was expected to occur within 10 or 20 years, however the bridge was replaced prior to further deterioration.

The Edison Bridge on Route 9 over the Raritan River in New Jersey is a riveted two-girder floor beams structure that was built in 1944. Cracks were also discovered in several tie plates that connected the cantilever brackets to the main girder and floor beam. Field testing confirmed that in-plane bending of the tie plate was caused by the secondary displacement of the main girder, and that the cantilever bending stresses were negligible. The cracks initiated from the flame-cut tapered edge, therefore, the replacement plate edges were smoothened to provide an edge without the flame-cut serration.

1.4 Monitoring Method

For over four decades, Pennsylvania Department of Transportation and ATLSS Center of Lehigh University have been conducting both short-term and long-term structural health monitoring on bridges throughout the State. Short-term studies have involved strain monitoring on a variety of bridges ranging in age, construction type, and usage. These strain monitoring studies have been a useful tool in assessing the behavior and structural integrity of a variety of bridges in the State's infrastructure. The results have provided information needed for repairs and renovations.

Other researchers have also used strain monitoring to evaluate bridges. Nowak, Sanli, and Eom analyzed steel multi-girder bridges and determined that the American Association of State Highway and Transportation Officials (AASHTO) load distribution factors are conservative [Nowak et. al. 1999]. Shenton, Jones, and Howell developed a web-based system for measuring live load strain in bridges that was used for load rating, fatigue assessment, and permit vehicle monitoring [Shenton et. al. 2004]. Bhattacharya, Li, Chajes, and Hastings used a strain monitoring system to determine load ratings using in-service data from normal traffic loading [Bhattacharya et. al. 2004]. Chajes and Shenton conducted controlled load tests in order to determine load ratings [Chajes et. al. 2005].

1.5 Finite Element Method in Bridge Study

Proper modeling of the bridge structure using finite element method has been adopted to investigate the unexpected fatigue cracks and to evaluate retrofit strategies during several case studies performed by research institutes in cooperation with DOTs (Department of

Transportation). The broader goals of these research programs are to develop applicable FE procedures for the analysis of bridge fatigue, especially in the aspects of stress prediction and repair recommendation, and to extend the same analytical procedures to the study of other bridges as an alternative to experimental testing.

In recent years, Kansas Department of Transportation (KDOT) welded plate girder bridges have experienced fatigue cracking at locations where transverse structural members are framed into longitudinal girders through connection stiffeners. Sometimes the connection stiffener was not attached to the compression flange, which caused a small portion of the girder web between the flange and the stiffener end left unstiffened for lateral movement. These small web gaps can be easily pulled or pushed out-of-plane under traffic loading. Unexpected distortion-induced fatigue cracks then developed either along the horizontal flange-to-web welds or the vertical stiffener-to-web welds [Zhao et. al. 2003]. FE studies were performed for this diaphragm-girder bridge that developed distortion-induced fatigue cracks at unstiffened web gaps. Using coarse-to-fine sub-modeling procedures in ANSYS, local stress conditions of the crack-prone details were explored and the corresponding repair methods were examined. Both the distortion-induced stresses and displacements generated in the research using FE methods indicate a good match with the observed in the field studies. Research discovered that the diaphragm-girder connections of the two interior girders are subject to stress amplitudes that can cause fatigue cracking. A bolted repair was recommended for the positive moment region connections and a welded repair was recommended for the transition and negative moment region connections. Through comparison between pre- and post-retrofit stresses in the positive and transition moment

regions at the bottom horizontal and vertical diaphragm-to-stiffener weld intersection, coarse-to-fine sub-model analysis predicted a new crack initiation site might develop after the repair.

Floor beam to girder connection in steel plate girder system has always been high fatigue-cracking risk region, even after retrofit performed. Finite element method has been used to test the effectiveness of the proposed second retrofit schemes. Recent cases include an elevated section of I-345 near the interchange of I-45 and I-30 in downtown Dallas, Texas, of which the transverse floor beams frame over the two main girders and support the concrete slab [Barrett et. al. 2009]. Cracking occurred in the girder web where the bottom floor beam flange is welded to the girder web. A retrofit was performed in 2004 by TxDOT (Texas Department of Transportation) in an attempt to mitigate the cracking by welding the cracks, drilling the arrestor holes and adding retrofit stiffeners on top of the stiffeners connecting the floor beams to the girders. New cracks developed in the retrofit stiffener's area and between the bearing stiffeners and the bottom flange of the floor beams. In 2009's technical report, a supplementary numerical study via ABAQUS was conducted to compare the stresses from the field tests and the three-dimensional finite element model. The local stress at the critical sections was in reasonable agreement between the field and analytical results. Proposed retrofit schemes were evaluated in the analytical model. In general, the proposed schemes appear to reduce the stresses at the critical locations, however high stresses are generated in other areas that have not cracked. The model predicted the high risk region, though failing to consider the damages caused by previous retrofit might weaken the argument.

Through 2006 to 2009, the University of Connecticut and the Connecticut Department of Transportation conducted a strain monitoring study on a 1964-built non-redundant steel plate-girder bridge carrying four lanes of traffic of a major state route over the Connecticut River and an AMTRAK Railroad [Troiano et. al. 2009]. There are five simply supported spans at the ends and a continuous three-span segment in the center portion. The fatigue cracks occurred in the tie plate connections on the transverse floor beam connections located at the ends of the simple spans. The field monitoring was used to better understand the cause of the large strains inducing cracks and to explain the behavior. The field data was correlated with a three-dimensional ABAQUS model to fully explain how deformations were occurring and to provide insight into potential repairs. Only one simple span of the system was simulated, and a static load was designed to model the controlled test truck load. A study of the deformations confirmed qualitatively that the tie plate was bending in the horizontal plane, and that these deformations are consistent with the field strain data. This behavior reinforced the fact that the first, and highest, peak of the strain data collected occurs when the load was in the center of the span, which is where the longitudinal girder is at its largest deflection, and therefore, it largest end rotation.

In general, it has been proven by previous studies that an appropriate FEA of a structure by using an adequate model is essential and necessary for the evaluation of the behavior of a bridge structure.

1.6 Study Objectives

The overall objective of this study is to determine the root cause of the observed cracks discovered in the tie plates and to examine the implications of the proposed retrofitting schemes on the long term performance of the bridge. This is to be accomplished by the following scope of work:

1. Install sensors on bridge at key locations (retrofitted tie plate, as-built tie plate, tie plate with girder bolts removed)
2. Perform controlled-load tests to determine the response of the bridge to a test truck of known weight and geometry.
3. Conduct finite element analysis to explain the behavior causing fatigue fracture.
4. Move on to a sequence of parametric studies to assess the potential of this failure mode for bridges with different geometries and structural layouts.

1.7 Outline of Thesis

Lehigh University and the Pennsylvania Department of Transportation have established a long-term bridge health monitoring system to monitor critical vulnerabilities in a group of bridges throughout the state. This research focuses on a single bridge carrying State Route 422 over the Schuylkill River in Cumru Township, Berks County. The bridge is a four-span continuous composite steel girder bridge carrying five lanes of highway traffic.

In order to monitor the critical vulnerabilities of the bridge, it is important to quantify anticipated changes in measurements resulting from different types and levels of damage. Section 2 of the

paper presents a description of bridge damage conditions and the testing plan, including the types and locations of all sensors, as well as the controlled-load testing and long-term monitoring procedures. Section 3 provides results of the controlled-load testing and long-term monitoring.

Section 4 focuses on the identification of fatigue cracking for the composite steel girder bridge using a finite element model. In order to incorporate the stress measurements into the automated bridge monitoring system of this bridge, the analytical measures obtained in Section 4 must be compared to the inherent variability of actual bridge measurements to determine the feasibility and the effectiveness of the finite element model.

Studies in Section 5 and Section 6 distinguish this thesis from previous investigation reports by a series of examination on bridge system. In section 5, the cause of tie plate in-plane bending is determined, the maximum and minimum in-plane displacements and bending stresses at each tie plate are obtained. In addition, arguments regarding suspicion of the defect in steel plate girder bridge system design are made. The structural components' arrangements are modified and their contributions to fatigue failure are determined. The two optional retrofit strategies are evaluated with the aid of FEA in section 6. The locations with high bending demand are identified. The optional retrofit paths are performed and examined.

Finally, results, conclusions, and limitations are summarized in Section 7.

Appendix A provides the instrumentation details for controlled load testing and long-term monitoring program.

Appendix B provides design computation procedure to estimate tie-plate bending stresses.

2. Overview of Study

The first half of this section provides an overview of the project background.

Then, for the second half, the detailed instrumentation plan, controlled-load testing plan and long-term monitoring program were developed to produce results for further forensic evaluation.

2.1 Bridge Description

The bridge discussed in this paper is the eastern most bridge carrying State Route 422 over the Schuylkill River in Cumru Township, Berks County, Pennsylvania (BMS ID: 06 0422 0440 0638). The location of the bridge is illustrated in Figure 2-1. All three bridges are of similar construction, which dated back to 1959. A photograph of the bridge, which represents a typical structural layout of steel plate girder bridge system, is shown on upper right side in Figure 2-1. For this system the primary longitudinal girders are framed into transverse floor beams. To simplify construction longitudinal stringers are placed on top of this assembly and used to support the reinforced concrete deck. The outside lanes and shoulders of the bridge are supported by cantilevered floor beam brackets.

Figure 2-1: Bridge location (Google Maps 2010) and view of bridge looking east from Abutment 1

The bridge is a four-span continuous two-girder bridge with end span lengths of 127.5 feet and interior span lengths of 153 feet. The bridge supports are skewed at an angle of 63-degrees. After transforming the original shop drawings prepared by PennDOT, the arrangement of stringers, floor beams, girders and supports are illustrated in Figure 2-2. The stringers were supported on equally spaced transverse riveted built-up floor beams with cantilever brackets. The cantilever bracket has a similar shape as the pork chop, so often referred by bridge engineers as “pork chop”.

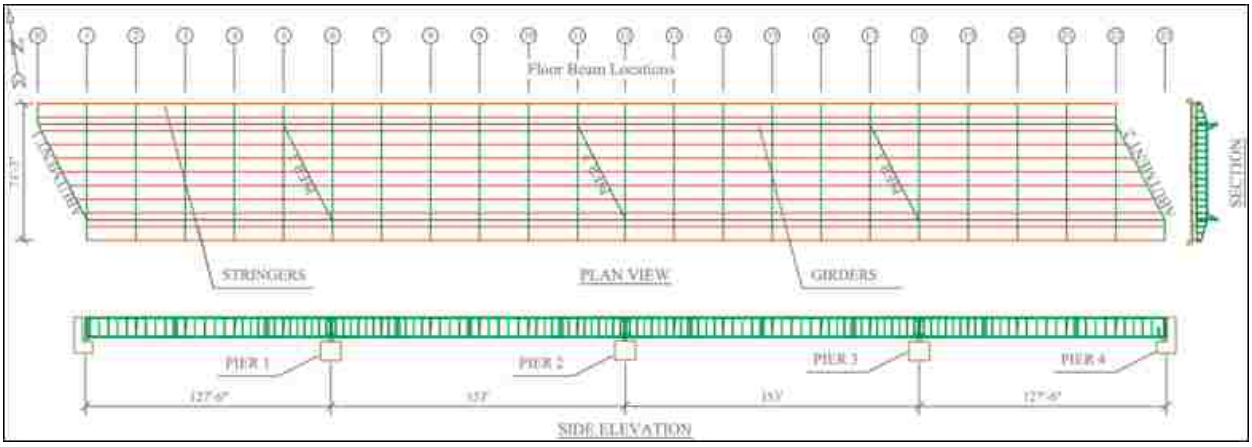

Figure 2-2: Bridge layout

The transverse floor beams span the interior between the longitudinal plate girders with cantilever brackets exterior to the longitudinal girders on each side. The top flange of the floor beam is made continuous with the top flange of the bracket using a tie plate. A cross-section of the deck-to-floor beam system is illustrated in Figure 2-3. The total width of cross section is 71.25 ft, and the spacing between twin girders is 50 ft. The concrete deck was cast on 24WF76 rolled beam stringers, with the thickness of 7.75 inches. The bridge carries 5 lanes of traffic, three in the East bound direction and two in the West bound direction. The extreme south lane is the acceleration lane for the east bound onramp before the bridge. Note that the centerline of traffic does not coincide with the centerline of the structure.

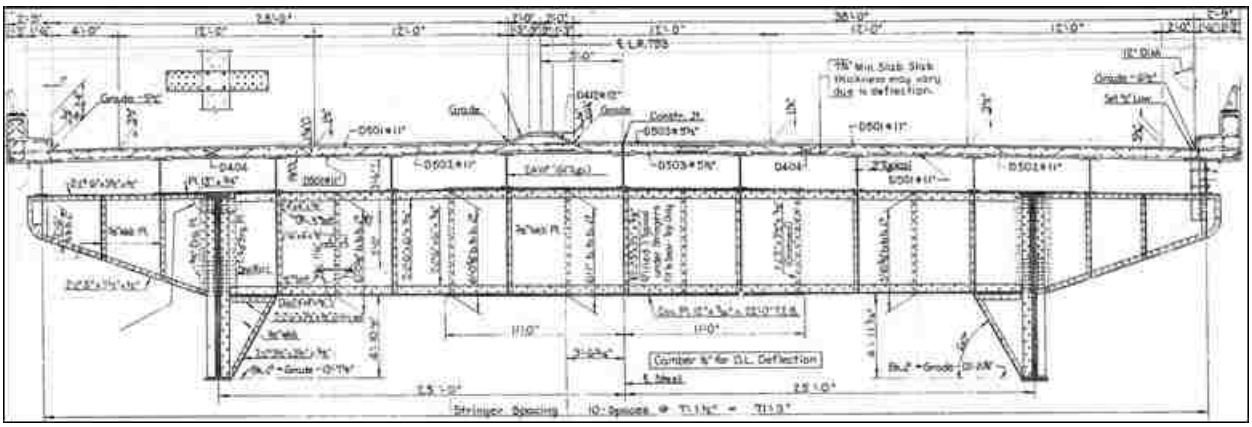

Figure 2-3: Cross-section of bridge

Shop details and structural drawings indicate that shop connections such as built up sections and stiffeners were riveted using 7/8 in. diameter ASTM A141-58 rivets in 15/16 in. diameter holes. All field connections such as the floor beam to tie plate connections were made with high strength bolts. All structural steel was specified as ASTM A7-58T. The A7 specification required a minimum yield point of 33 ksi and a tensile strength from 60 to 72 ksi. Fracture toughness requirements were not defined in the 1958 specification.

The tie plates were shop installed on the cantilever floor bracket with riveted connections. Attachment to the bridge girder and floor beams were made in the field with high strength bolts as illustrated in Figure 2-4.

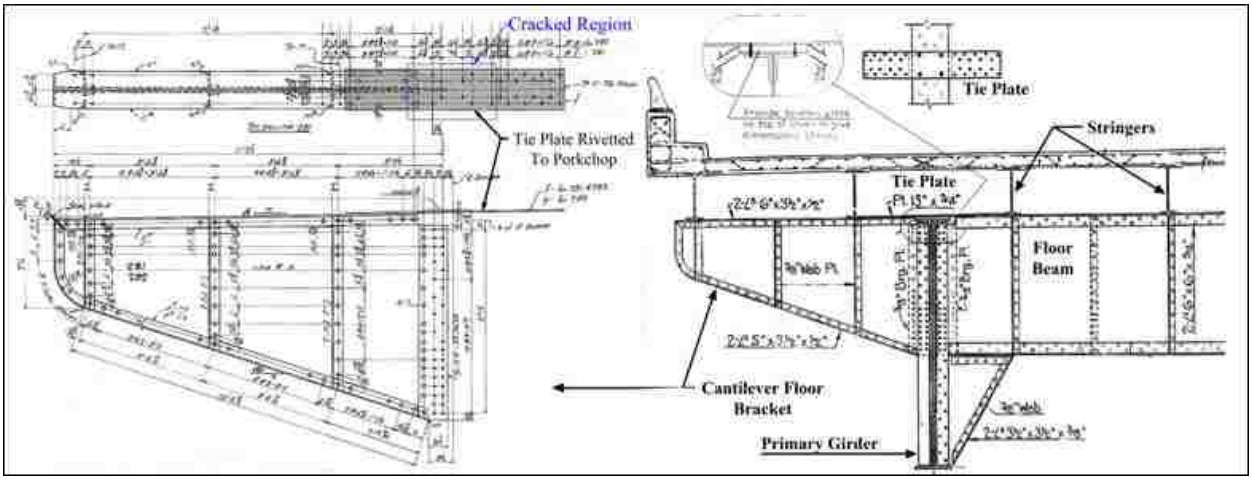

Figure 2-4: Cantilever bracket to tie plate to floor beam connection details

2.2 Field Damage Conditions

A 2009 inspection of the bridge revealed a crack of a tie plate connecting the main floor beam to the cantilever bracket over the top flange of the girder (see Figure 2-4). The crack was discovered in the tie plate at floor beams 2, 7 and 22 at the south girder (see Figure 2-5). The crack at floor beam 2 was approximately 5.5 in. long and was removed from the bridge and replaced with a similar tie plate by PennDOT. This new tie plate with identical dimensions as the one it replaced is not connected to the girder and the beveled fill plate has been removed. The cracked tie plate at floor beam 7 was removed from service and replaced using the same procedures as floor beam 2. The crack at floor beam 22 was located at the inside tie plate to girder bolt hole and propagated only to the edge of the plate. This tie plate remains in service.

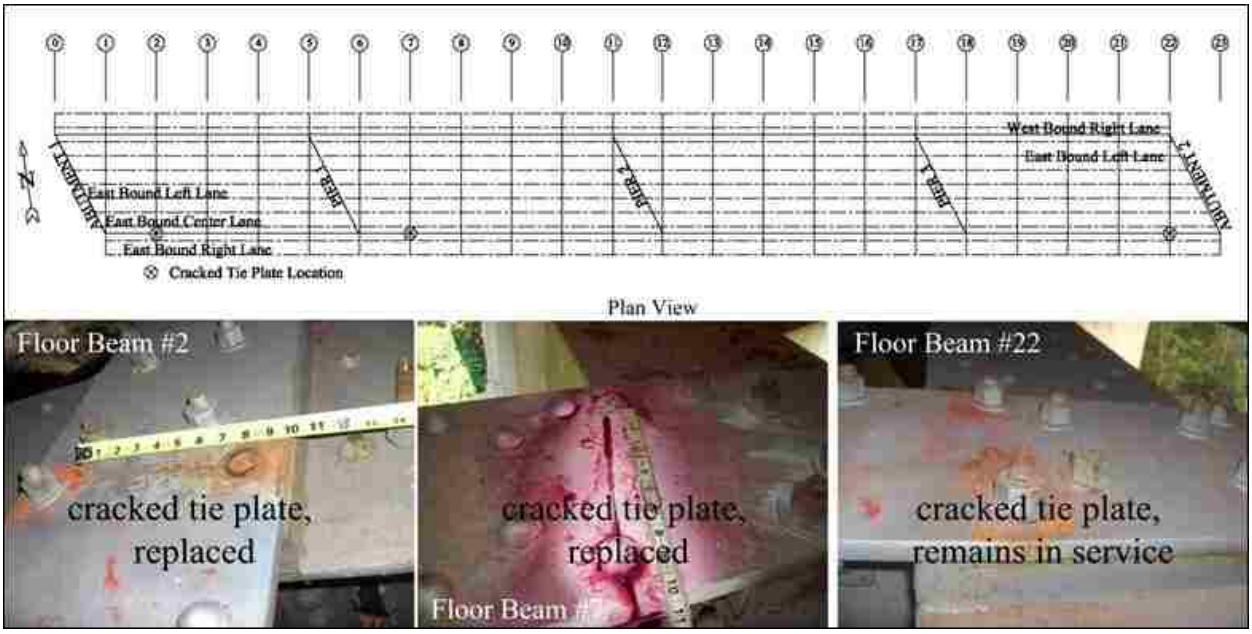

Figure 2-5: Location of the three cracked tie plates discovered on the bridge

2.3 Testing Plan

Strain gages were placed at fatigue sensitive details and at locations that provide global load distribution characteristics and general behavior of the bridge. The majority of the strain gages installed in the field were 0.25 in. gage length (see left picture in Figure 2-6). Weldable-type strain gages were selected due to the ease of installation in a variety of weather conditions.

Spring-loaded linear variable differential transformers (LVDTs) were used to measure the relative longitudinal displacement between the centerline of the tie plate at the girder and the connection points at the stringers on either end. The sensors have a displacement range of ±1/4 in. (see the right picture in Figure 2-6)

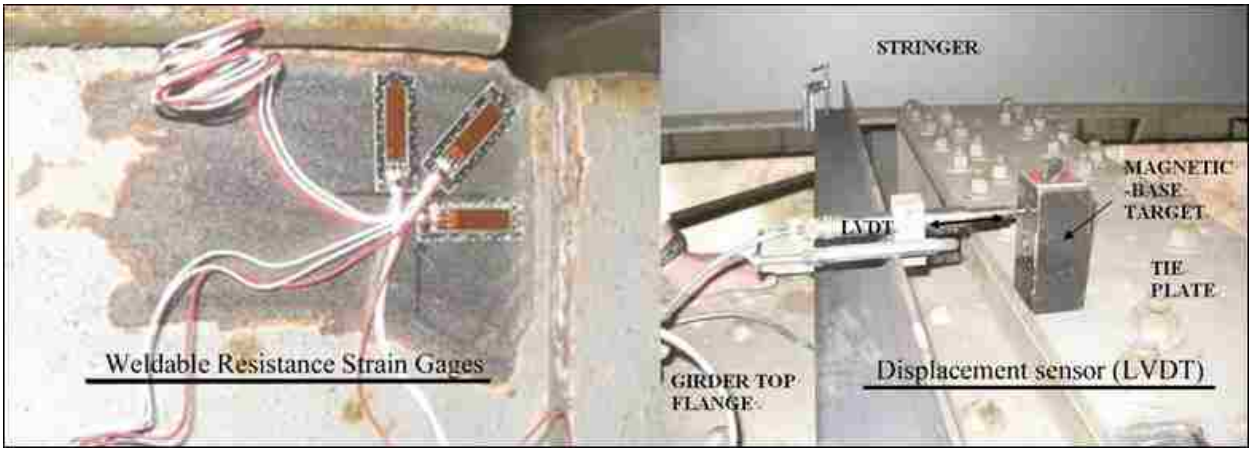

Figure 2-6: Sensors placed on critical locations of the bridge

A Campbell Scientific CR9000 data logger was used for the collection of data at the bridge. Remote communications with each data logger was established using broadband wireless modems. Data download was performed automatically each via a server located in the ATLSS laboratory of Lehigh University in Bethlehem, PA.

2.3.1 Instrumentation Locations

Three tie plate locations were selected for instrumentation, and were identified as Locations A, B, and C (Figure 2-7). Each of the locations was selected to be in an area suspected of high in-plane bending demand on the tie plate.

At each location, two strain gages were installed on the top surface of the tie plate at each location. These strain gages were oriented parallel to the axis of the tie plate (i.e., transverse direction with respect to the bridge) one inch from either side of the tie plate above the outside edge of the flange. In addition, to measure the primary bending stress in the girder at the tie plate, two strain gages were installed at the top and bottom flange of the girder at a cross-section

adjacent to the tie plate. At Locations A and B only, strain gages were installed on the web of the cantilever bracket web adjacent to the cope at the top flange. Complete instrumentation plans are presented in Appendix A.

To further aid in the study of the behavior leading to the cracking, displacement sensors were installed at each of the three locations to measure the relative longitudinal displacement between the tie plate and the supporting bottom flanges of the adjacent stringers.

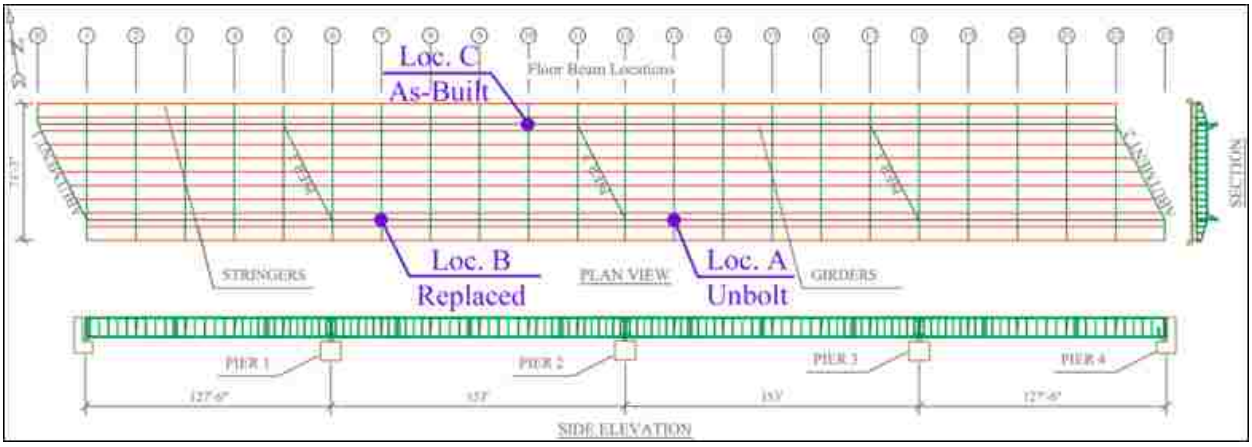

Figure 2-7: Location plan showing tie-plates selected for instrumentation

2.3.1.1 Location A

Location A represents an as-built location which was modified during the investigation. The region was instrumented and monitored before and after the removal of the tie plate-to-girder bolts. The performance of this section is used to assess the change in stress range on the connection detail as a result of the retrofit strategy.

However, it should be noted that the PennDOT bridge crew was not able to remove all eight bolts connecting the tie plate to the girder. One bolt remained in place (without the nut). A

photograph of this tie plate with the single bolt in place is shown in Figure 2-8. The expected lateral deformation of the plate was expected to be less than 0.05 in., which is less than the distance between the remaining bolt and the bolt hole. Consequently, the remaining un-tensioned bolt was deemed to be acceptable for the evaluation. Horizontally- and vertically-oriented strain gages were installed on both sides of the cantilever bracket web (back-to-back). In addition, back-to-back diagonally-oriented strain gages were installed. The three strain gages installed on one side of the bracket web at Location A was also shown in Figure 2-8.

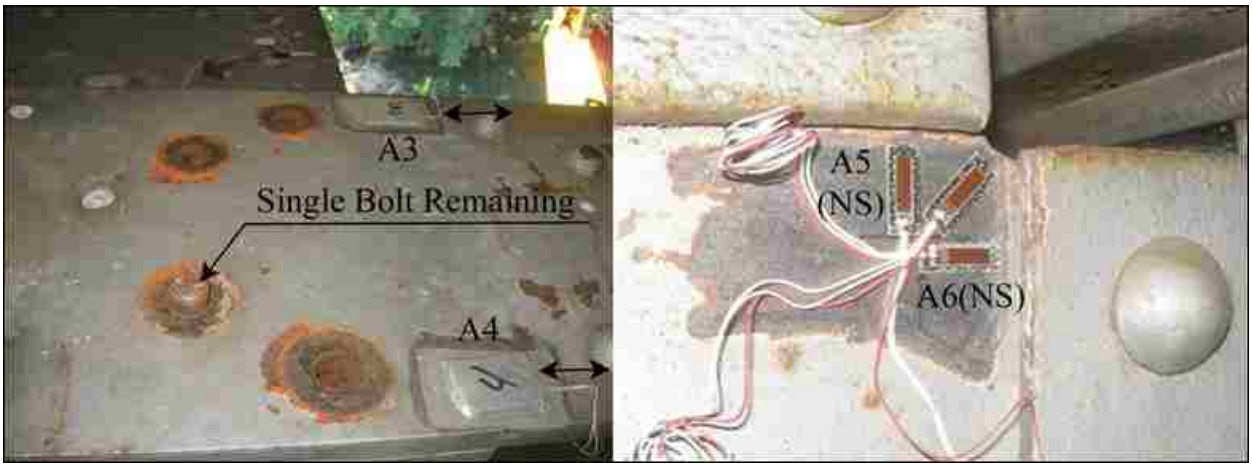

Figure 2-8: Strain gages installed on the tie plate (A3, A4) after 7 of the 8 bolts removed and on the cantilever bracket web (A5, A6)

2.3.1.2 Location B

Location B represents a retrofitted connection. This area represents a cracked region that was retrofitted with a new plate prior to installation of instrumentation and monitoring. The tie plate replacement was of identical geometry to the original plate but was not reconnected to the girder top flange (see Figure 2-9). The photograph was taken after the strain gages were weatherproofed. Similar as Location A, horizontally- and vertically-oriented strain gages were

installed on both sides of the cantilever bracket web (back-to-back). The performance of this section is used to assess the retrofit strategy.

Figure 2-9: Strain gages installed on the tie plate (B3, B4), on the top flange of the girder (B1) and on the cantilever bracket web (B5, B6)

2.3.1.3 Location C

Location C represents an as-built tie plate connection. No modifications were made at this location during the monitoring period. The performance of this section is used to assess the remaining fatigue life of the as-built details.

2.3.2 Controlled-Load Testing

A series of controlled load tests were conducted using a fully loaded PennDOT dump truck (see Figure 2-10). The truck had a front steering axle, a rear tandem axle and a fourth floating axle ahead of the tandem. The test truck was fully loaded with a gross vehicle weight (GVW) of 66,950 pounds. Figure 2-10 contains the weight at each wheel. Figure 2-10 also provides the

key dimensions of the test truck. Note that the fourth floating rear axle was raised for the duration of the load tests.

During each of the tests, all eastbound and westbound traffic was temporarily stopped off the entire bridge. Traffic queues were cleared between tests. The test truck was driven slowly across the bridge (in a designated span and lane) at crawl speeds (3-5 mph). This test was performed to establish the near-static response of the bridge. Each crawl test was repeated twice to evaluate the repeatability of the data.

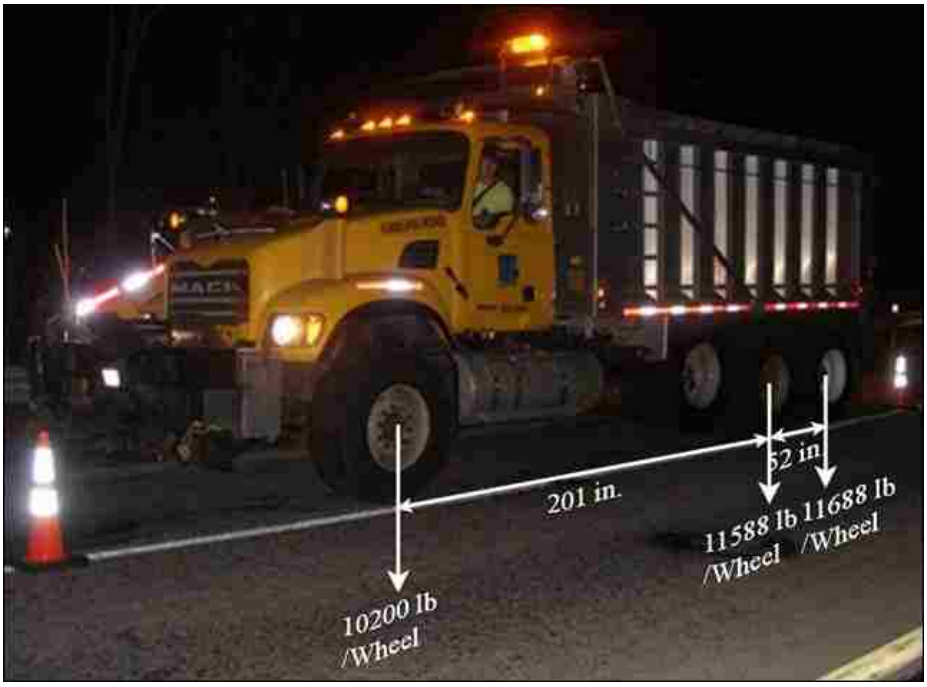

Figure 2-10: Test truck used during controlled load tests

One possible retrofit strategy entails removal of bolts between the tie plate and top girder flange. To evaluate the effectiveness of this retrofit, the crawl tests were performed both before and after bolts were removed from the tie plate at Location A.

2.3.3 Long-Term Monitoring

Finally, a long-term monitoring program was developed so that stress-range histograms at all strain gages could be collected that would be representative of the demands experienced by the bridge over its life.

The stress range bin histogram data are collected by rain-flow counting method from monitoring data at the selected locations of structural members. During the monitoring program, since small cycles do not contribute to the overall fatigue damage, the rain-flow analysis algorithm can be programmed to ignore any stress ranges less than 0.5 ksi.

These stress range histograms form the basis of the calculations of the remaining fatigue life on the bridge. These results will also aid in the forensic evaluation of the cracked tie plates. As noted previously, three tie plate locations were selected for instrumentation. Location C represents the as-built condition. Location B represents a repaired condition where the tie plate has been replaced without connection to the girder. Finally, Location A represents a repair condition where the bolts between the tie plate and girder are removed.

3. Field Measured Results

This section provides a summary of the short-term and long-term monitoring of this bridge. Results from controlled load tests will be used in determining the response of the bridge to a test truck of known weight and geometry. Generating stress range spectra from long-term monitoring program will aid the fatigue evaluation of the tie plate and the cantilever bracket web.

3.1 Crawl Test Results

The global and local behaviors of the bridge are examined utilizing data collected during the controlled load tests. The test was performed with the test truck traveling at crawl speed (5mph) to establish the near-static response of the bridge.

Note that during the short-term monitoring program, the original real-time data collected by ATLSS laboratory consisted of time versus strain. The time-frame was representing the location of the operating test truck, while the strain data from each sensor indicated the bridge performance at certain location. The data is well presented in this section with location versus stress after taking crawl speed of test truck and stiffness of structural members into consideration.

3.1.1 Longitudinal Girder Response

As noted in Section 2 (also see Appendix A), strain gages were installed on the bottom and top flanges of the girder at Locations A and B (on the south girder) and Location C (on the north girder). During the crawl test the strain gages and transducers were monitored continuously. The truck starting location and speed was recorded to determine the location of the vehicle along

the span during the time history. The strains were converted to stress by multiplying by a modulus of 29000 ksi. The results are presented as stress versus the location of the front of the truck on the span (see the elevation view of the bridge at the lower part of Figure 3-1, Figure 3-2 and Figure 3-3). Note that the dashed lines in the following figures are representing the interior piers.

Presented in Figure 3-1 are the stress location-history plots for the six strain gages installed on the girders at the three locations for crawl tests with the test truck travelling eastbound in the acceleration lane (i.e., far right lane). Sensors A1, B1, and C1 are on the top girder flanges and sensors A2, B2, and C2 are on the bottom girder flanges.

The far right lane tests produces the highest stresses in the south girder (Locations A and B). Stresses in the north girder (Location C) were very small. The measured response with the test truck in interior lanes was similar except that a greater portion of the load was distributed to the north girder and therefore lower peak stresses were measured in the south girder.

It can be seen that when the test truck passed through the span in which a given sensor was located, the stress in the girder flange was the highest, with the strain sensors on the top flanges (B1, C1, and A1) in compression. The sensors on the bottom flange (B2, C2, and A2) were correspondingly in tension. There was a reversal in the stress (e.g., consider gages A1 and A2, located in Span 3) as the truck travelled the bridge. This is consistent with the expected influence line for a four-span structure and the given sensor location within the span.

The peak stresses at Locations A and B were similar, equal to approximately 1 ksi. The response at the top and bottom flange of the girder is generally equal-and-opposite as a result of the non-composite nature of the girder.

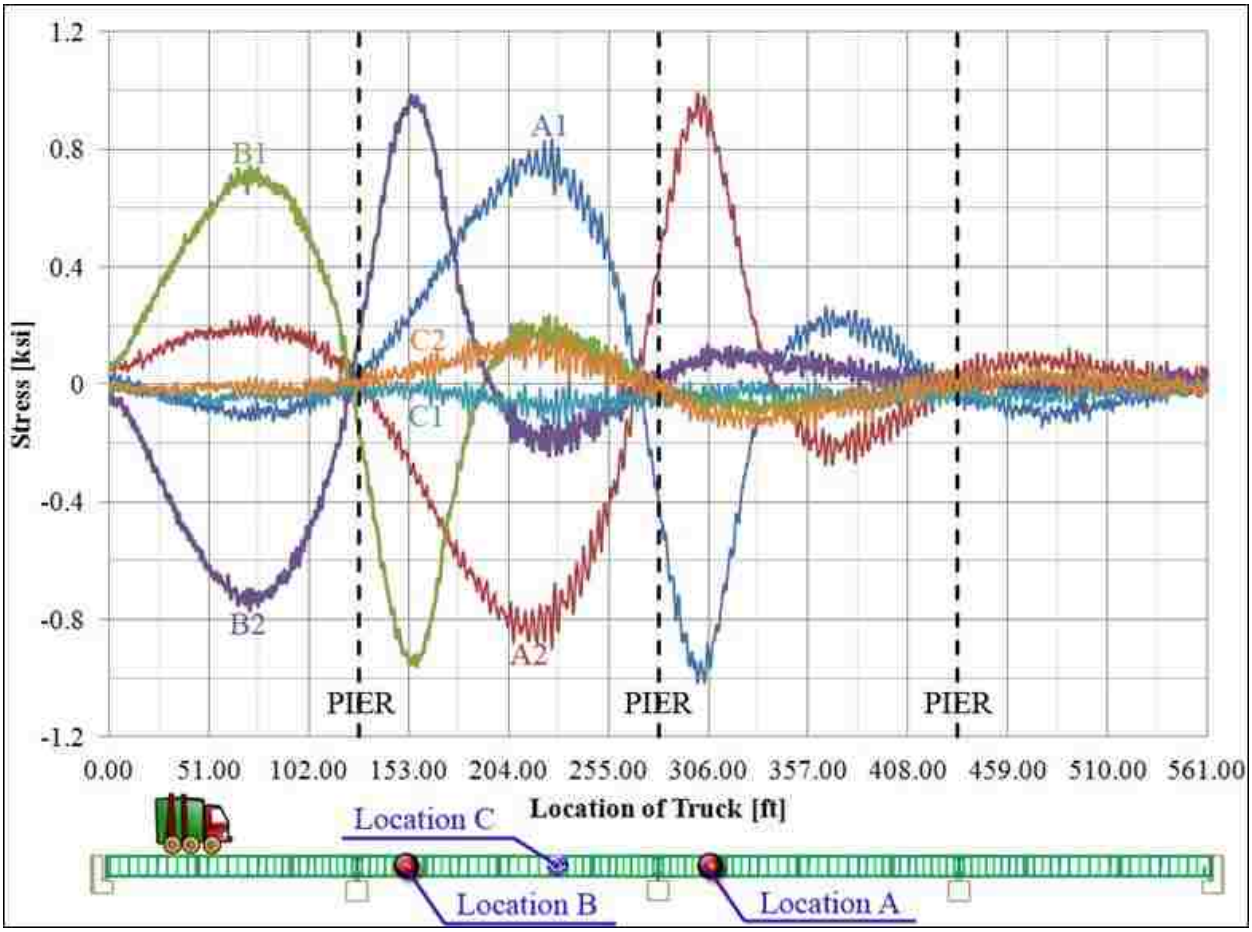

Figure 3-1: Stress location-history plot for strain gages installed on the top and bottom girder flanges

3.1.2 Tie Plate Response

Two strain gages were installed on the tie plate at each of the three instrumented locations. All gages were oriented along the axis of the tie plate (transverse to the bridge axis) and were

mounted on the top surface, 1 inch from the side of the tie plate and directly above the exterior edge of the girder flange.

As noted in Section 2, after the initial crawl tests were performed, 7 of the 8 tie plate-to-girder flange bolts were removed from the connection Location A. The nut on the last bolt was removed however the bolt itself remained in place.

To assess stress changes in the tie plate at Location A before and after bolt removal (BBR/ABR), stress location-history data is gathered in Figure 3-2. Comparing A3 (ABR) and A4 (ABR) to A3 (BBR) and A4 (BBR), it can be seen that removal of the bolts resulted in significantly reduced stresses in the tie plate as well as displacement of the tie plate. After bolt removal, peak stresses of 1.5 ksi were measured (compared to 8 ksi prior to bolt removal).

To evaluate the retrofit strategy operated on the tie plate at Location B, Figure 3-2 also presents the stresses in the tie plate for the same load test. After tie place being replaced with a new identical one without bolt-connect, the girder is free to move longitudinally relative to the tie plate, the stresses are significantly reduced from the as-built condition (A3 (BBR) and A4 (BBR) in Figure 3-2). The maximum measured stress was just over 1.0 ksi.

It is also worth mentioning that stresses in the tie plate at Location B are in the same stress range as the ones in the tie plate at Location A after bolt removal, which provides a practical evidence that the “softening method” (removal of the bolts) can effectively reduce high stress in the tie plates regardless of their locations.

Response of tie plate at Location C, which represents as-built condition, is similar to Location A prior to bolt removal. Longitudinal movement of the girder relative to the deck and stringers is imposed on the tie plate resulting in high measured stresses. Stress location-history plot of Location C is considered redundant.

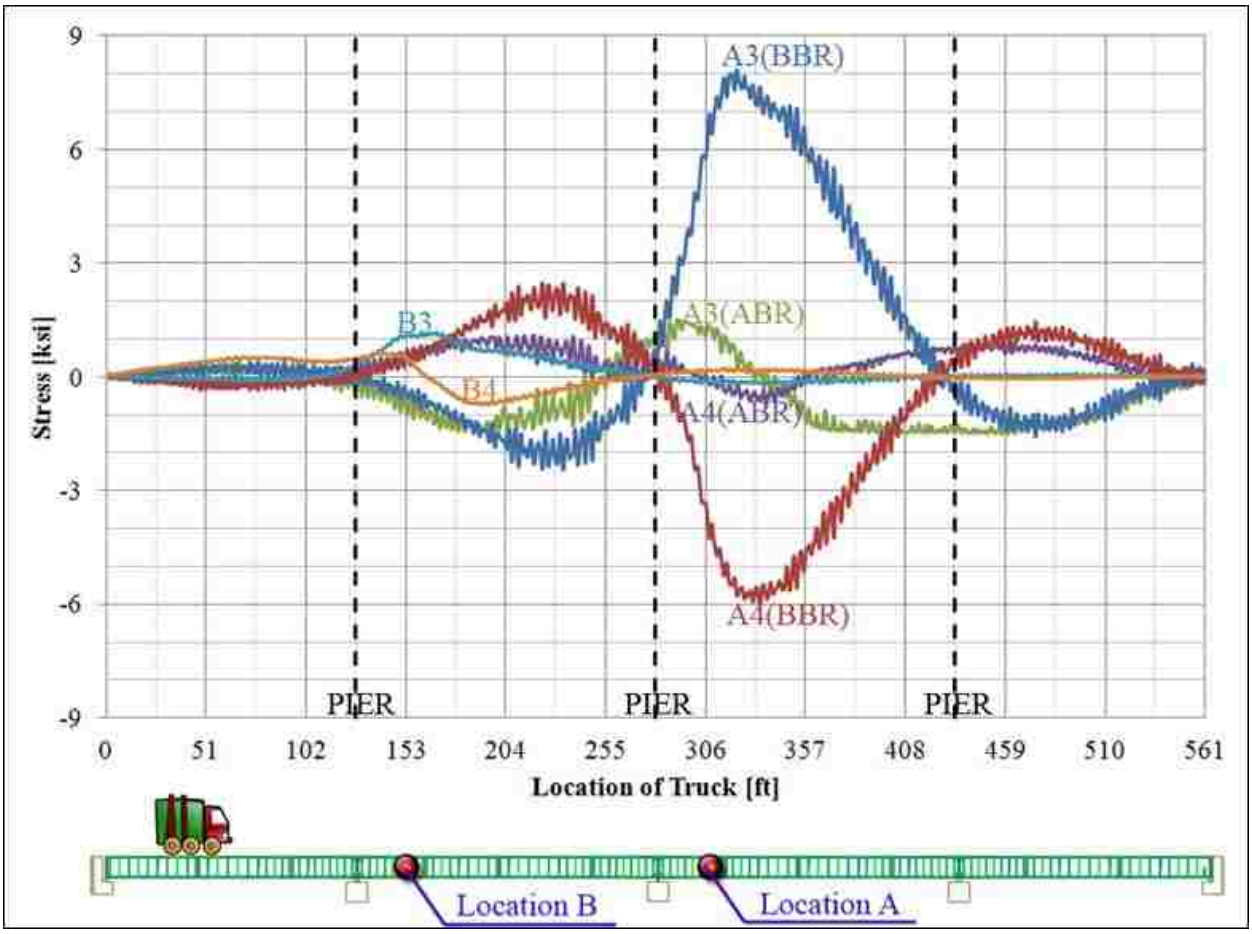

Figure 3-2: Stress location-history plot for strain gages installed on the tie plates at Location A before bolt removal (BBR), after bolt removal (ABR) and at Location B

LVDT measured the relative displacement between mid length and the end of the tie plate span. As shown in Figure 3-3 is the displacement plot for the sensors on the tie plate at Location A, prior to and after removal of the tie plate-to-girder flange bolts(BBR/ABR). For better

comparison, performance at Location B, with the same loading as Location A before bolt removal, is also provided in the same figure. The maximum relative displacement of the tie plate prior to bolt removal was about 24 mils (0.024 in.), compared to 4 mils (0.004 in.) after unbolting. It is proved that removal of the bolts resulted in significantly reduced stresses in the tie plate as well as displacement of the tie plate. Peak displacement at Location B was 5 mils (0.005 in.), which wss similar to A (ABR), but with a reversed sign. Ploted in blue, the relative displacement between tie plate and its adjacent stringers at Location A when tie plate still connecting to girder reveals poor coordination between tie plate and stringers, especially when test truck passing above (span three and four). It might be imposed by longitudinal girder action. It is also suspected that the sensor wasn't well-attached to structural components.

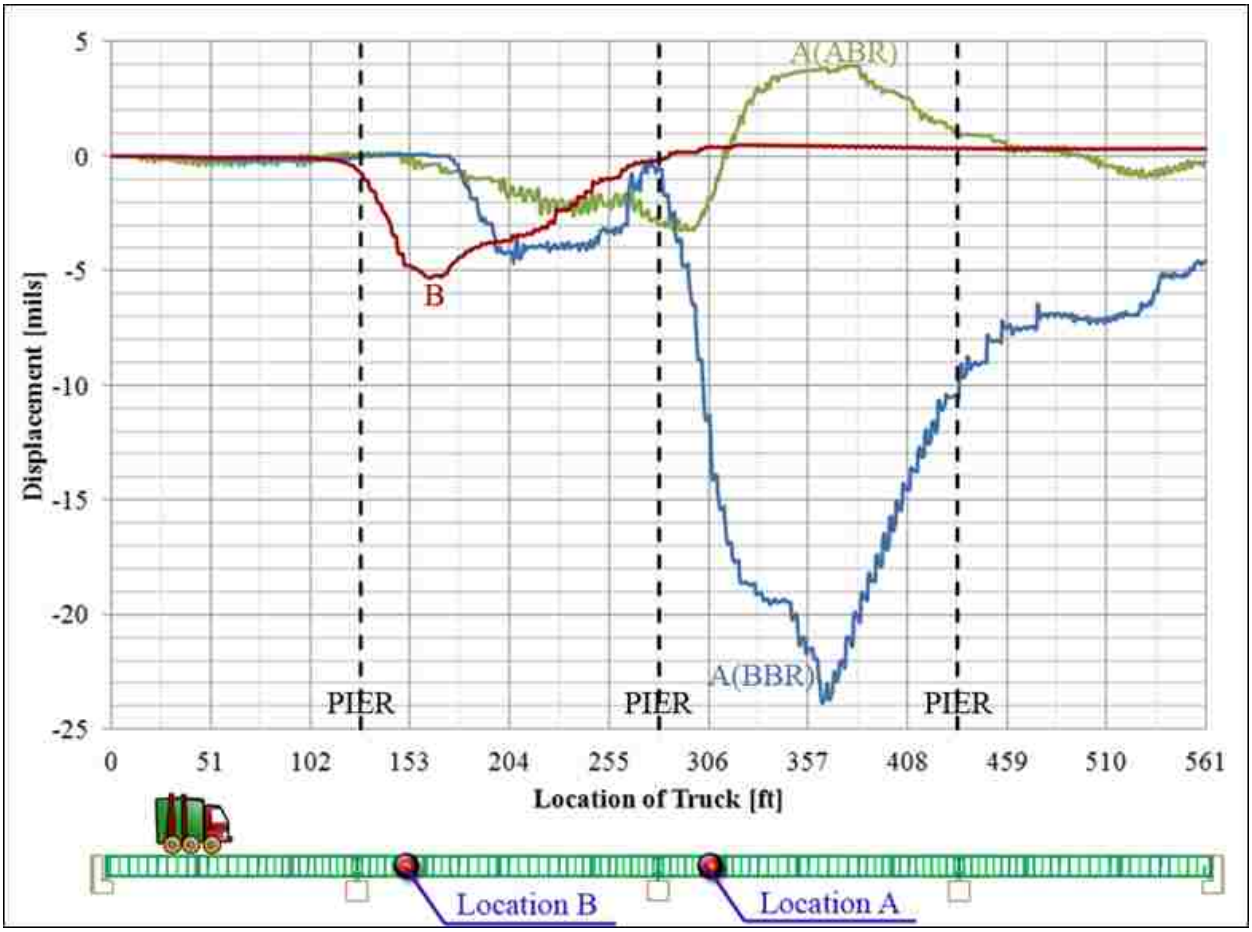

Figure 3-3: Displacement location-history plot for LVDTs installed at Location A before bolt removal (BBR), after bolt removal (ABR) and at Location B

3.1.3 Cantilever Floor Beam Web Response

As detailed previously in Section 2, "Test Plan", six strain gages installed on the web of the south cantilever bracket adjacent to the cope at the top flange of the girder at Location A for a crawl test both prior to and after the removal of the tie plate-to-girder connection bolts. Strain gages A5 and A7 are vertically oriented back-to-back on the web at the cope. Strain gages A6 and A8 are horizontally oriented back-to-back on the web. Finally strain gages A9 and A10 are diagonally oriented back-to-back on the web. To include as much as information in one figure,

and at the same time to make it better present itself, only data obtained from one side of the web are plotted. A5 (BBR) and A6 (BBR) represent vertically and horizontally stress in the web before unbolting, respectively. A5 (ABR) and A6 (ABR) represent vertically and horizontally stress in the web after unbolting, respectively.

With the tie plate connected, it can be seen in Figure 3-4 that the stresses are low, with highest measured stresses at all locations of less than 1 ksi. Peak stresses occur when the test truck is directly over the instrumented location, and are in the horizontal direction (gages A6). Out-of-plane bending dominates the response of the web. Figure 3-4 also presents stress location-history plots after seven of the eight tie plate-to-girder connection bolts were removed. By comparing with A5 (BBR) and A6 (BBR), it can be seen that removal of the bolts resulted in a significant increase in the stresses in the web. The largest stress was nearly 7 ksi with a maximum stress range of over 8 ksi.

Based on observation and comparison, a conclusion can be drawn that fatigue cracking can initiate in this region as a result of relative displacements between the deck/stringers and girder. Stress location-history from sensors A5 and A6 have provided enough information about stress changes in the cantilever bracket web for the study of web stresses, thus, data from sensors A9 and A10 is no longer listed in study scope.

Similar examination is also operated for Location B. The original cracked tie plate was replaced by PennDOT with a bolted tie plate without a connection to the top flange of the girder. As a result, the girder is free to move longitudinally relative to the tie plate. This movement causes

stresses in the web of the cantilever bracket since it is connected to the girder but restrained by the stringers. It can be seen in Figure 3-4 that the stresses in the web are significantly higher than those measured at A5 (BBR) and A6 (BBR). This is due to the release of the tie plate from the girder flange. The highest stresses were horizontal (B6) with a magnitude of nearly 6 ksi. The response of the web is dominated by out-of-plane bending, which is consistent with that of web at Location A after bolt removal.

Shown in plots colored pink and purple, data from horizontally oriented Strain gages A6 reveals a reversal in the stress before and after disconnecting girder to the tie plate (A6 (BBR) and A6 (ABR)). This is imposed by the change in longitudinal deformations as girder is freed to move without constrain from tie plate.

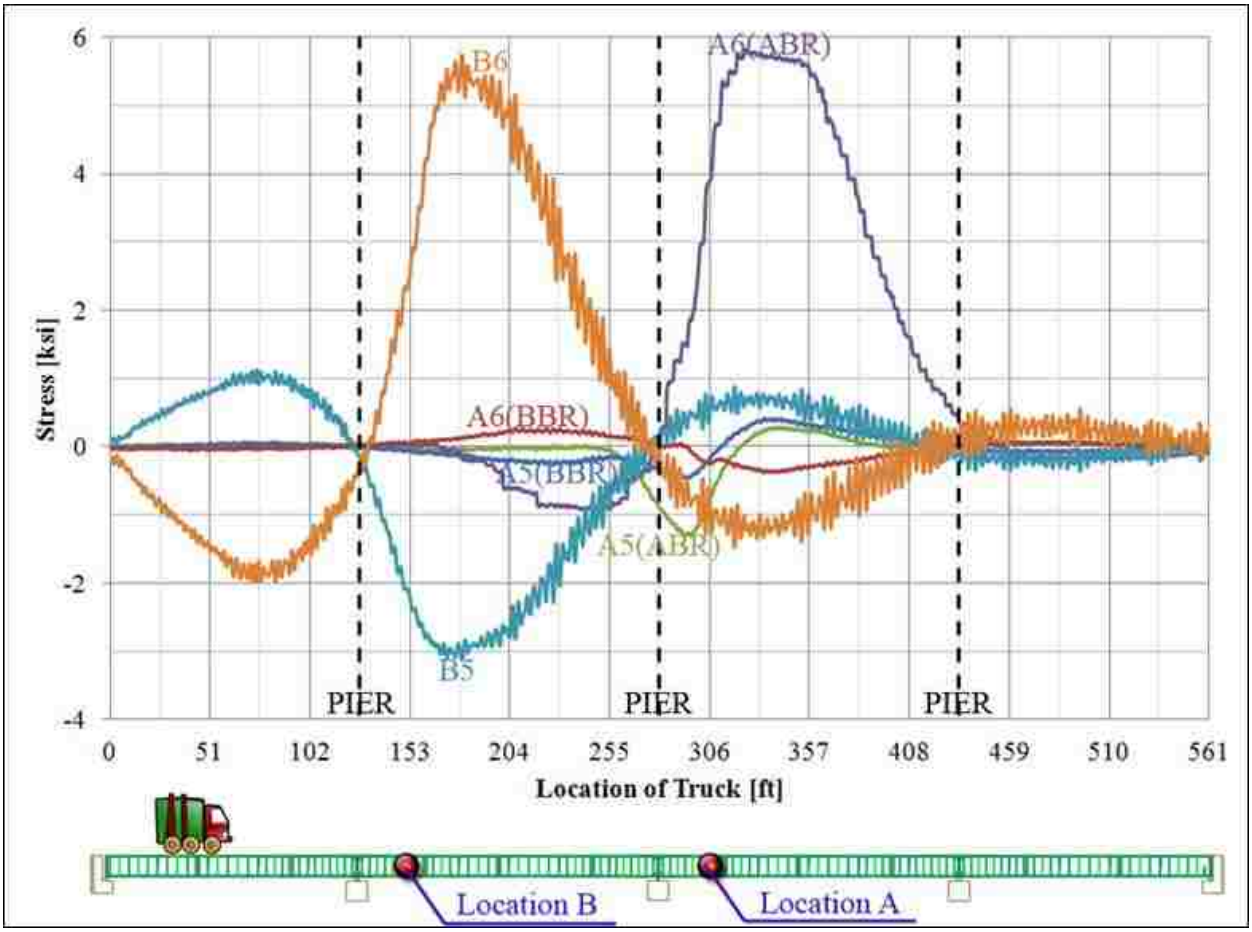

Figure 3-4: Stress location-history plot for strain gages installed on cantilever bracket web at Location A before bolt removal (BBR), after bolt removal (ABR) and at Location B

3.2 Long-Term Monitoring Results

During the long-term monitoring of this bridge, the stress-range histograms were developed for each strain gage. The histograms for key sensors are presented graphically. A total of 28.7 days of data were collected. As described previously, three tie plate locations were selected for instrumentation. Location A represents a repair condition where the bolts between the tie plate and girder are simply removed (all but one bolt out of eight have been removed from the tie plate-to-girder connection for the duration of the monitoring). Location B represents a repaired

condition where the tie plate has been replaced without connection to the girder. Finally, Location C represents the as-built condition.

Using the measured stress-range histogram (numbers of cycles and corresponding stress ranges) an effective stress range can be calculated. The AASHTO is based on the S-N (i.e., stress-life) relationship and Miner's rule [Miner 1945]. The basic equation for the resistance is:

$$\Delta F = \left(\frac{A}{N}\right)^{1/m}$$

where ΔF is nominal fatigue resistance, A is the fatigue detail coefficient for each category, N is number of stress range cycles, and m is material constant representing the slope of the S-N curves, which can be assumed as m=3 for all fatigue categories. Effective stress range, s_{eff}, can be calculated from stress-range bin histogram and Miner's rule as follows:

$$s_{eff} = \left[\sum \frac{n_i}{N_{total}} \cdot s_{ri}^3\right]^{\frac{1}{3}}$$

where n_i is number of observations in the predefined stress-range bin, S_{ri}, and N_{total} is the total number of observations during the monitoring period.

Given the fatigue category and the calculated effective stress, an estimate of the total fatigue life of the detail is made using the AASHTO fatigue curves. If the maximum stress range measured in the entire stress range spectrum is less than the constant amplitude fatigue limit (CAFL) of the detail, infinite life can be expected. Assuming the current rate and magnitude of stress cycles from the monitoring are representative of those experience by the bridge over its life an estimate can be made of the expected remaining fatigue life of each instrumented detail. For the

remaining-life calculations, it has been assumed that the bridge has been in service for 51 years and that the rate of cycle accumulation is constant over the life of the bridge (equal to that measured during the monitoring period).

3.2.1 Location A: Connection with Bolts Removed

Plot in Figure 3-5 provides the stress-range histograms for the two strain gages installed on the tie plate at Location A after 7 of the 8 tie plate-to-girder flange bolts being removed from the connection. It can be seen in the figure that the measured stress ranges were similar at A3 and A4. Similarly, the stress-range histograms for the six strain gages installed on the web of the cantilevered floor beam bracket at Location A (strain gage installation details are shown in Figure 2-8 and Appendix A) were developed.

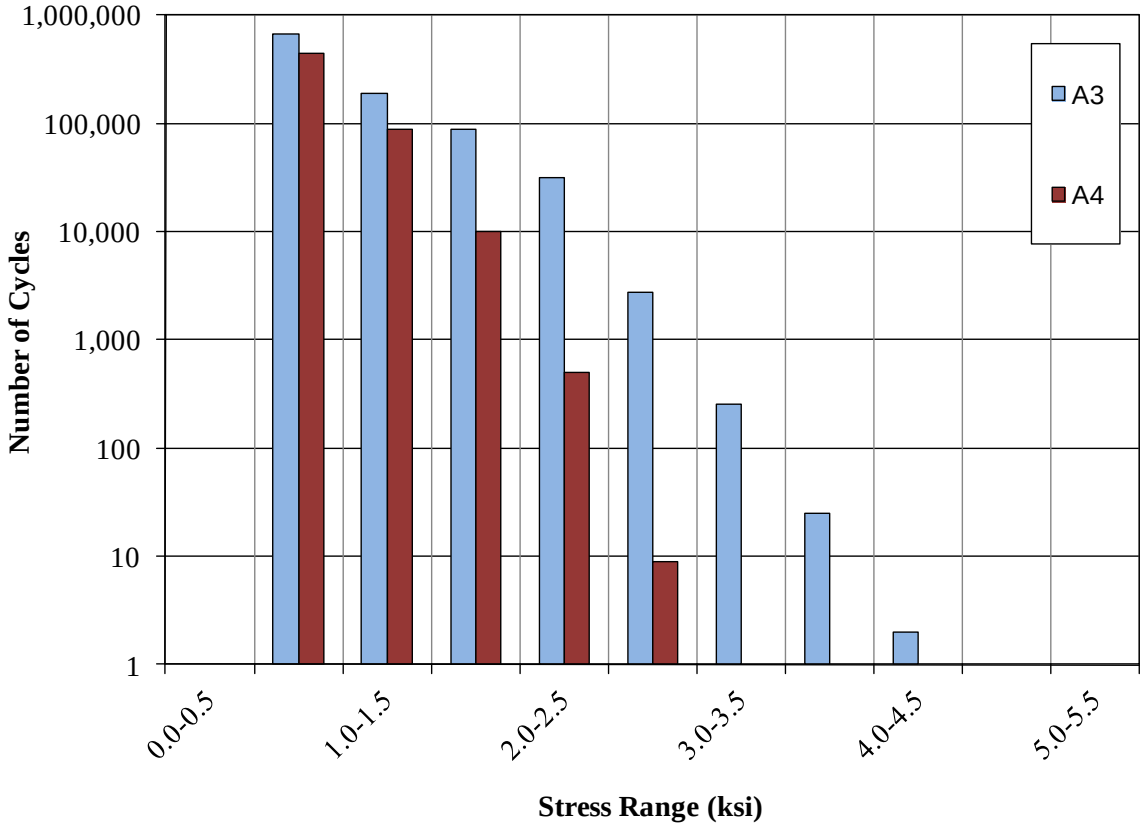

Figure 3-5: Stress-range histogram for strain gages installed on the tie plate at Location A

Strain Gage	Location	Detail Category	s_{Reff} [ksi]	s_{Rmax} [ksi]	Cycles/ day	CAFL [ksi]	Cycles > CAFL		Remaining Life (years)
							#	%	
A3	Location A - Tieplate East	D	1.16	4.5	34,450	7	0	0.00%	infinite
A4	Location A - Tieplate West	D	0.92	3.0	18,914	7	0	0.00%	infinite
A5	Location A - West Web - Vert.	C	0.81	2.5	325	10	0	0.00%	infinite
A6	Location A - West Web - Horiz.	C	2.78	10.5	1,439	10	3	0.01%	infinite
A7	Location A - East Web - Vert.	C	0.83	2.5	286	10	0	0.00%	infinite
A8	Location A - East Web - Horiz.	C	3.44	14.5	1,702	10	58	0.12%	123
A9	Location A - West Web -Diag.	C	0.90	2.0	162	10	0	0.00%	infinite
A10	Location A - East Web - Diag.	C	0.78	2.0	354	10	0	0.00%	infinite

Table 3-1: Fatigue-life estimates for tie plate and cantilever bracket web at Location A

A summary of the fatigue life calculations for the two strain gages on the tie plate and the six strain gages on the cantilever bracket web is presented in **Error! Reference source not found.**. To be conservative, the tie plate details were considered an AASHTO Fatigue Category D. The cantilever bracket web is conservatively considered a Category C, due to the unusual out-of-plane bending of the web plate in combination with the riveted bracket attachments. As shown in the table, the stress ranges measured on the tie plate were all less than 4.5 ksi. Since this is less than the CAFL of 7 ksi for Category D [AASHTO 2008], infinite fatigue life can be expected. The data collected from the web gages on the cantilever bracket web indicate that the CAFL of 10 ksi for Category C was exceeded on one gage location A8. The maximum stress range was 14.5 ksi at strain gage A8, horizontal gage on the east side of the web. For this location a remaining life of 123 years was estimated.

3.2.2 Location B: Retrofitted Connection

In any case, the retrofit actions taken at location B resulted in a similar behavior to that of location A. A summary of the fatigue life calculations for the two strain gages on the tie plate and the four strain gages on the cantilever bracket web is presented in Table 3-2. The tie plate locations were considered an AASHTO Fatigue Category B as a bolted detail (it is a new tie plate). The cantilever bracket web is conservatively considered a Category C to account for the riveted connections. As shown in the table, the stress ranges measured on the tie plate were all less than 3 ksi. Since this is less than the CAFL of 16 ksi for Category B, effectively infinite fatigue life can be expected. The data collected from the web gages on the cantilever bracket

web indicate that the CAFL of 10 ksi for Category C was exceeded at both horizontal gages. The horizontal gage B8 on the east side of the web resulted in a remaining life of 41 years.

Strain Gage	Location	Detail Category	s_{Reff} [ksi]	s_{Rmax} [ksi]	Cycles/ day	Cycles > CAFL		Remaining Life (years)
						#	%	
B3	Location B - Tie Plate East	B	6.00	17.24	684	0	0.00%	infinite
B4	Location B - Tie Plate West	B	6.96	20.68	720	0	0.00%	infinite
B5	Location B - West Web - Vert.	C	8.83	48.26	10,244	0	0.00%	infinite
B6	Location B - West Web - Horiz.	C	11.17	86.18	25,547	22	0.00%	infinite
B7	Location B - East Web - Vert.	C	9.58	48.26	7,901	0	0.00%	infinite
B8	Location B - East Web - Horiz.	C	11.93	96.53	25,519	76	0.01%	41

Table 3-2: Fatigue-life calculations for strain gages installed on tie plate and cantilever bracket web at Location B

Estimates for the remaining fatigue life for A8 and B8 in **Error! Reference source not found.** and Table 3-2 reveal that removal of the tie plate-to-girder connection removes the restraint between the tie plate and the girder. This results in longitudinal displacement on the floor beam and cantilever bracket webs causing the region to bend out of plane. This additional demand can result in fatigue cracking of the web region (sketched in Figure 3-6). The strain gages measurements indicate that a vertical crack along the connection angle would occur before a horizontal crack (higher stresses in the horizontally oriented gages).

Figure 3-6: Potential web cracking (in red) locations in web of cantilever bracket

3.2.3 Location C: As-Built Connection

The summary of the fatigue life calculations for the two strain gages on the tie plate is given in Table 3-3. The tie plate details are considered an AASHTO Fatigue Category D due to the riveted connections.

As shown in the table, the stress ranges measured on the tie plate were very high, finite fatigue life is expected. By using the recorded stress magnitudes and rate of cycling, calculations in accordance with AASHTO indicate that the detail should have cracked 39 years ago. This particular tie plate is not presently cracked. This discrepancy could be attributed to: (1) the stress magnitude or rate were lower in the past, (2) the actual condition may be better than specified AASHTO fatigue category D which is based on the assumption of poor clamping force from the rivets, (3) the AASHTO design fatigue curves are based on a 97.5% confidence limit and

therefore represent a conservative estimate of fatigue life, and (4) stresses at the suspected crack initiation point at the rivets are lower than the location of the strain gage (closer to the neutral axis of the plate). However, the measurements indicate that cracking is likely at this detail. This is confirmed by the cracks found in three tie plate on this bridge at other locations.

Strain Gage	Location	Detail Category	s_{Reff} [ksi]	s_{Rmax} [ksi]	Cycles/ day	Cycles > CAFL		Remaining Life (years)
						#	%	
C3	Location C - Tie Plate East	D	2.22	22.5	46,222	8,239	0.62%	-39
C4	Location C - Tie Plate West	D	2.09	22.0	45,858	6,722	0.51%	-37

Table 3-3: Summary of fatigue-life calculations for strain gages installed on tie plate at Location C

3.3 Summary of Short-Term and Long-Term Monitoring Results

In summary, the results indicate that removal of the bolts between the tie plate and girder will reduce the restraint in the tie plate and the associated stresses. The stresses in the tie plate of the unbolted configuration are below the AASHTO fatigue limit for the detail thus indicating that the system will have an infinite fatigue life. The stresses in the web however increase. These stresses indicate the possibility of a vertical fatigue crack formation. The stresses measured in the web however indicate a worse case fatigue life of 41 years.

4. Development and Validation of FEM

To provide better insight on in-plane bending of tie plate due to the secondary out-of-plane displacement of the floor beam and cantilever bracket, a finite element model of the bridge was developed. The model is based on the bridge dimensions provided in the PennDOT design drawings for the bridge. The system is modeled in three-dimensions to provide an accurate representation of the global stiffness and the occurrence of secondary deformations. The effects of skew, cross-section geometry, controlled test truck load, connection of cantilever brackets and riveting of tie plates are all accounted for in the model.

4.1 Simulation Overview

Analyzing displacement-induced fatigue behavior using a combination of field monitoring and finite element method (FEM) has been done previously by others [Zhao et. al. 2003, Barrett et. al. 2009, Troiano et. al. 2009]. It has been proven by previous studies that an appropriate finite element analysis (FEA) of a structure by using an adequate model is essential and necessary for the evaluation of the behavior of a bridge structure. Although this study has not been conducted in a vacuum, it manages to distinguish itself by three-dimensional full-scaled structural layout combining with detailed localized simulation using finite element software ABAQUS, version 6.9-3.

4.1.1 Geometry and Element Type

During the process of developing finite element model, the relevant information including all dimensions and material properties are obtained from both as-built shop drawings and actual

field measurements. To establish a standard unit system for data input as well as result output, foot and kip are used.

The study examines only the service level response of the system, thus, all the structural component including longitudinal girders, floor beams, cantilever brackets, stringers, angles at cantilever bracket to floor beam connection and concrete deck are modeled as linear-elastic. An elastic modulus of 29,000 ksi is assumed for the steel and an elastic modulus of 4,000 ksi is assumed for the concrete. Four-node reduced integration linear quadrilateral shell elements (S4R) are used to create each component. Note that after defining section properties, the thickness of shell element cannot be recognized in the display window in ABAQUS (see Figure 4-1 as a typical example). The edge represents the centre line of the section.

Benefitted from practical assumption about structural behavior and reasonable choice of element type, the amount of CPU time necessary for analysis of the model is reduced, while at same time, more accurate results are produced. The outcome result will be presented later in this section.

4.1.2 Mesh and Element Size

Apart from reduced integration, variable mesh method also contributes to the efficiency of computation while still providing enough accuracy in the region of the tie plate connection. Partitions are used to produce various mesh sizes The shorter edge of element is as fine as 2.5 inches on tie plate and 4.5 inches near beam-girder connection, versus 12 inches somewhere else. There are a total of over 92,000 elements and 95,000 nodes in the developed Finite Element

model. Figure 4-1 shows elements with different mesh size at cantilever bracket to girder to floor beam connection.

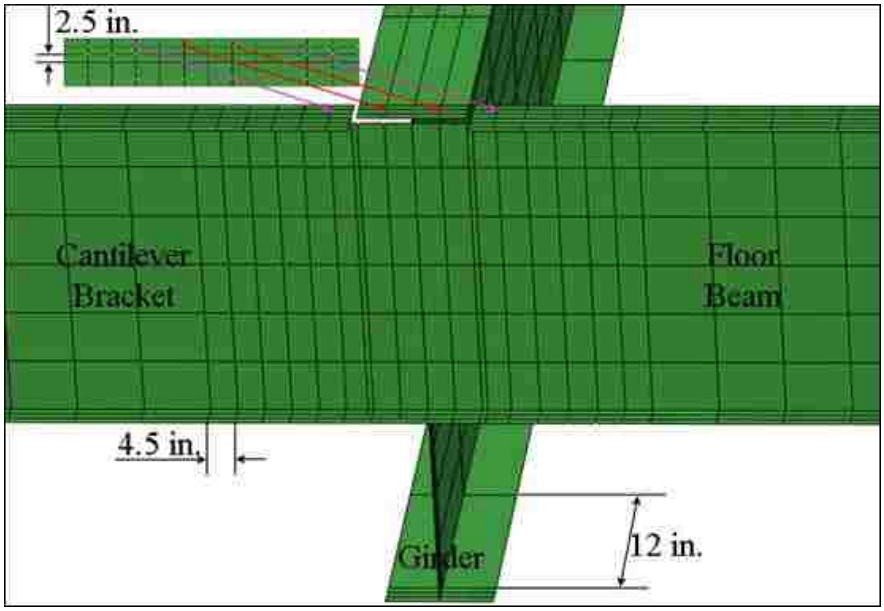

Figure 4-1: Detailed mesh and constraint at floor beam-girder connection

4.1.3 Assembly and Constraints

In regions around cantilever bracket to girder to floor beam connection, cuts are made to disconnect the top flanges of the three components (see Figure 4-1) to match the actual shop details. In addition, to avoid high in-plane stress level at webs of cantilever brackets, the connection angles are developed to accommodate the stress level.

Although the connection details are designed as the true "pin" connections, the actual behaviors of the connection details based on the field monitored data reveal that the connections provide some restraints to the rotations of the web of the floor beam [Connor et. al. 2004]. Therefore, the webs of cantilever bracket, girder and floor beam are merged together.

As clarified before, given the nature of shell element, the center lines of adjacent steel plates of structural members will be merged together if the distance between them within the tolerance (0.001 ft), resulting reducing the height of overall cross-section. The height difference between model and field measure is approximate 5 inches. The shortening might cause a change in stiffness of composed bridge system, leading the model becoming more flexible than actual condition. This discrepancy is accepted in this study since the objective of the FEA is to provide insight on in-plane tie plate bending due to the secondary out-of-plane displacement of the floor beam and cantilever bracket.

Tie constraints are created to simulate the bolt connection between tie plates and top flanges of cantilever brackets and floor beams. Tie Constraint in ABAQUS restricts all degrees of freedom, fusing the bodies together. Figure 4-1 also provides stretches of the master nodes on the tie plate tying to the slave nodes on the corresponding top flanges of girders, floor beams and cantilever brackets. Not all of which are shown in Figure 4-1, constraint locations are selected based on the tie plate bolt and rivet details provided by PennDOT (also see Figure 2-4).

Deck to stringer to floor beam connections are not discretely modeled, given which is not priority in this study. The adjacent steel plates (shell element) are merged, so that the simulated test truck load applied on deck surface can be transferred to lower structural components. The loading and boundary conditions will be discussed further.

4.1.4 Loads and Boundary Conditions

Because of further study including comparison of analytical and measured data, the finite element model is also subjected to a moving fully loaded tri-axle dump truck, similar as the test truck in controlled load testing. Recall that the test was performed with the test truck traveling at crawl speed (5mph) to establish the near-static response of the bridge, the weight and geometry of the truck is shown in Figure 2-10. As for the model, six vertical static concentrated loads, each represents one wheel, are applied at each of five lanes. The magnitudes of the six loads are defined based on truck axle load, which are 20400 lb for front axle, 23175 lb for first rear axle and 23375 lb for second rear axle. The distance between two adjacent loads matches the dimension of the truck.

The abutments are fixed in longitudinal, horizontal, and vertical three directions, while interior piers are only fixed vertically, allowing displacements in other directions. The bridge was designed 63-degree skewed, which is also taken into consideration during boundary definition. Figure 4-2 presents the finite element model with skewed support in one load case.

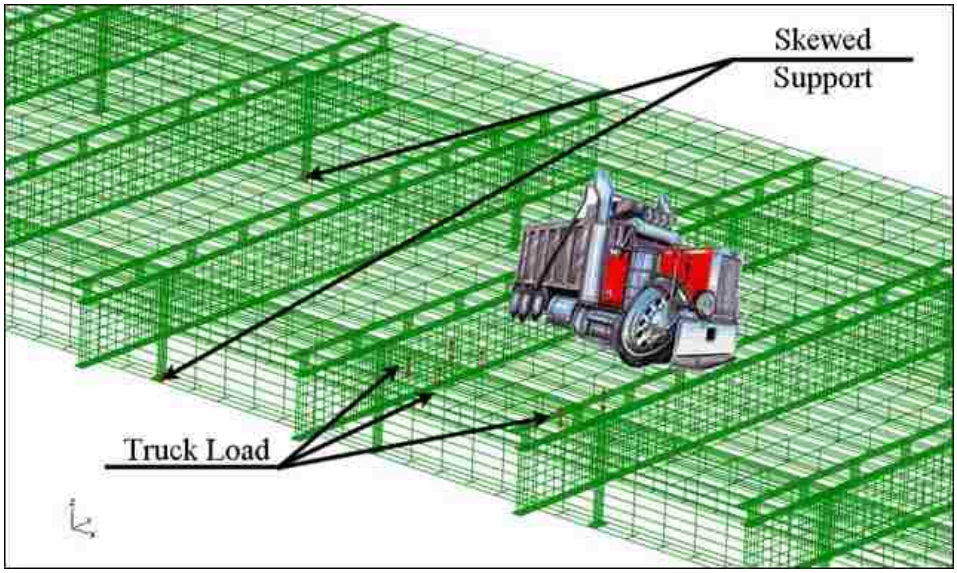

Figure 4-2: Wireframe of the model with load and boundary conditions

4.2 Preliminary Examination on Model Behavior

A study of the deformations confirms qualitatively that the tie plate is bending in the horizontal plane, which validates the feasibility and the rationality of the finite element model.

Shown in Figure 4-3 is an exaggerated deflected shape of the structure when the loads are applied on far right lane. View cut has been made at approximate half height of the stringers, leaving the lower structural components exposed. By uncovering the understructure, deformations caused by compatibilities in displacement as the members transfer loads in three dimensions can be examined. Figure 4-3 demonstrates that the longitudinal girder deflects in bending when the load is applied on the span. This deflection causes the end of the girder to rotate toward the center of the span, about the bearing located at the bottom flange of the girder. As the longitudinal girder rotates inward, the top of the transverse floor beam's web, which is

enhanced by angles and connected to the longitudinal girder, is pulled toward the center of the span. The stringers, which are connected to the top flange of the transverse floor beam, provide lateral bracing restraint and resist the inward movement of the transverse floor beam. This forces the tie plate to bend in the horizontal plane, creating tension on the leading edge of the tie plate and compression on the trailing edge of the tie plate.

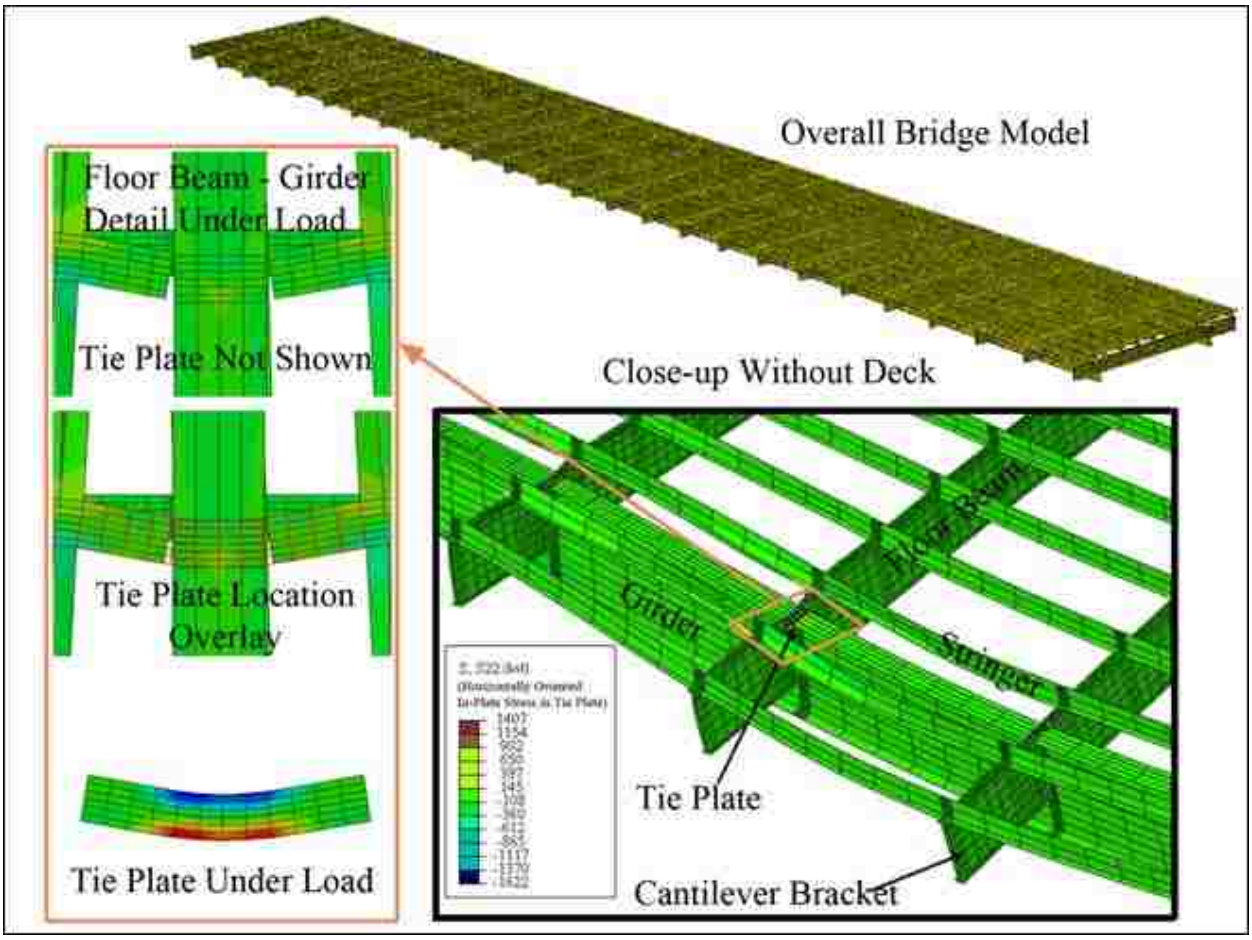

Figure 4-3: Bridge deformation and structural components' interaction

The comparison of the two details indicates that the high cyclic stresses in tie-plate are caused by in-plane displacement of the tie-plate, which generated by flexural bending of the girder as well as out-of-plane bending of floor beam and cantilever bracket.

On the basis of qualitative analysis, quantitative evaluation will be conducted further to assess the accuracy of the model.

4.3 Comparison between Measured and Computed Results

After the feasibility of FEM being reinforced, the analytical and field measured stresses are compared to verify its effectiveness.

With targeted elements at similar locations in the FE model as field instrumentation, the results from preliminary evaluation are applicable in this comparison. The stresses in these elements are corresponding to the discrete stress measurements in the tie plates, cantilever brackets and girders acquired at Locations A, B and C during field measurement. Figure 4-4 shows instrumentation plan of controlled load testing, which is also used as reference to isolate a sequence of elements in ABAQUS for stress plotting.

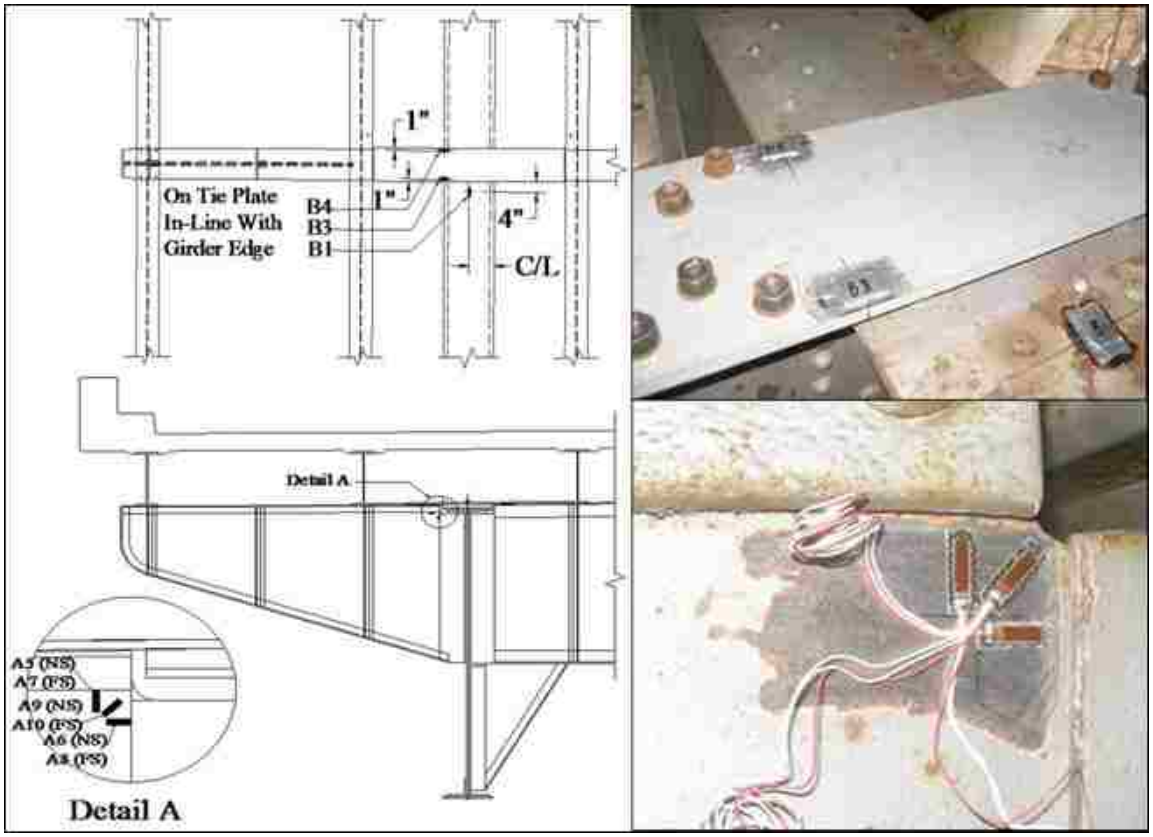

Figure 4-4: Strain gage location

Recall that test data at Location A and B were collected when the test truck was travelling eastbound in the far right lane, while test data at Location C was collected when the test truck was travelling westbound in the right lane. To simulate the loading condition, all together the six concentrated loads in ABAQUS are applied at twelve (12) locations along the bridge spans with the same order as truck travelling direction in each case. The locations are almost evenly distributed in order to cover most of case scenarios, which include loading near piers and abutments, loading closed to instrumented tie plates, loading at mid-spans, etc. The effectiveness of selecting of locations will also be evaluated further in this study.

The marks on the plots in the following figures through the rest of this section are representing the locations where replicated truck loads are applied on FE model. The stress value is assumed to be zero when the load is on abutments and interior pier 1 and 3. The differences between theoretically computed and field monitoring results of stresses are evaluated at critical locations during the comparison as well.

4.3.1 Primary Girder Response

As illustrated above, strain gages were installed on the bottom and top flanges of the girder at Locations A and B (on the south girder) and Location C (on the north girder). Sensors A1, B1, and C1 are on the top girder flange, and sensors A2, B2, and C2 are on the bottom girder flange. Presented in Figure 4-5, Figure 4-6 and Figure 4-7 are the stress comparison between crawl test data and finite element results at similar locations at each location, respectively. Note that the dashed lines in the following figures are representing the interior piers.

The comparison of stress in top and bottom flange of the girder at Location A is plotted in Figure 4-5. The two results are in the same stress range and with the similar shapes of curvature, both of which reverse in sign once in the third span, almost at the same location. This is consistent with the expected influence line for a four-span bridge and the given sensor location. The peak stress for each plot is achieved at identical location, which is closed to the interior pier 2 (the one in the middle). The selecting of locations to apply truck load on ABAQUS model is proved to be effective.

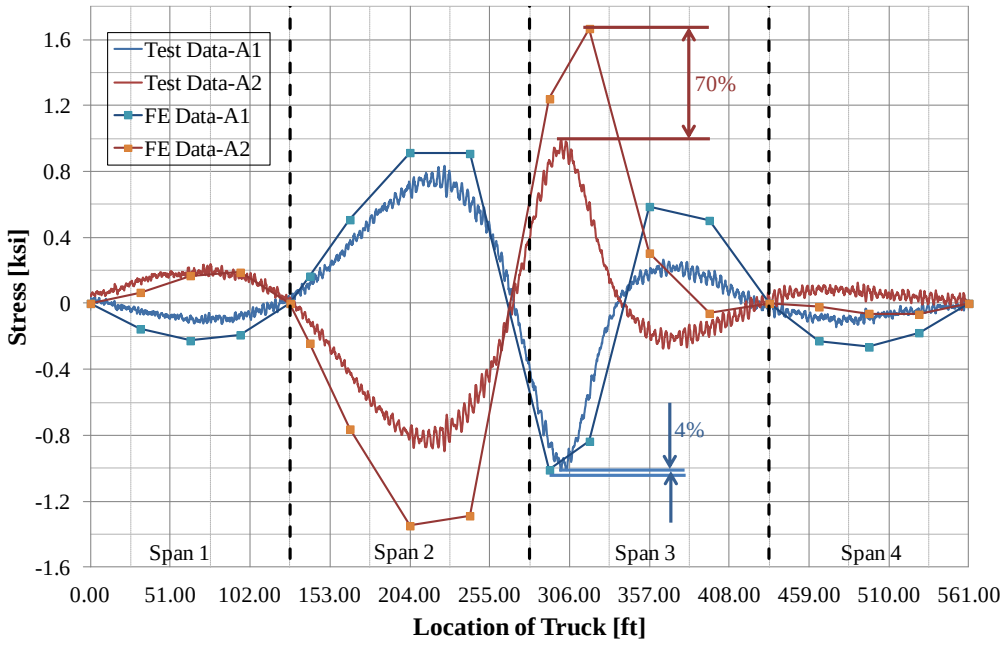

Figure 4-5: Computed and measured stress in the top and bottom girder flange at locations at Location A

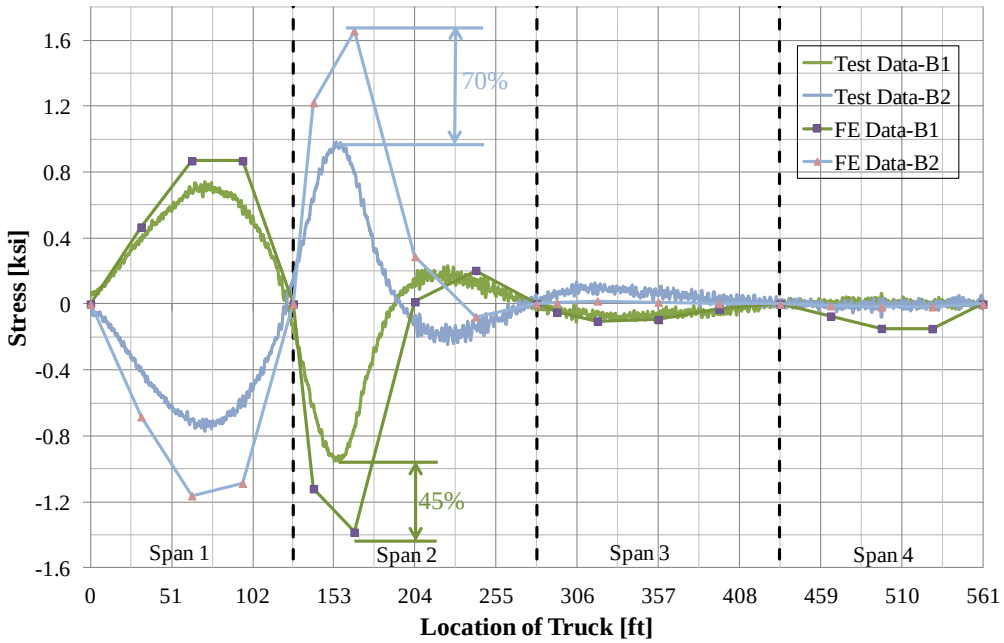

Figure 4-6: Computed and measured stress in the top and bottom girder flange at locations at Location B

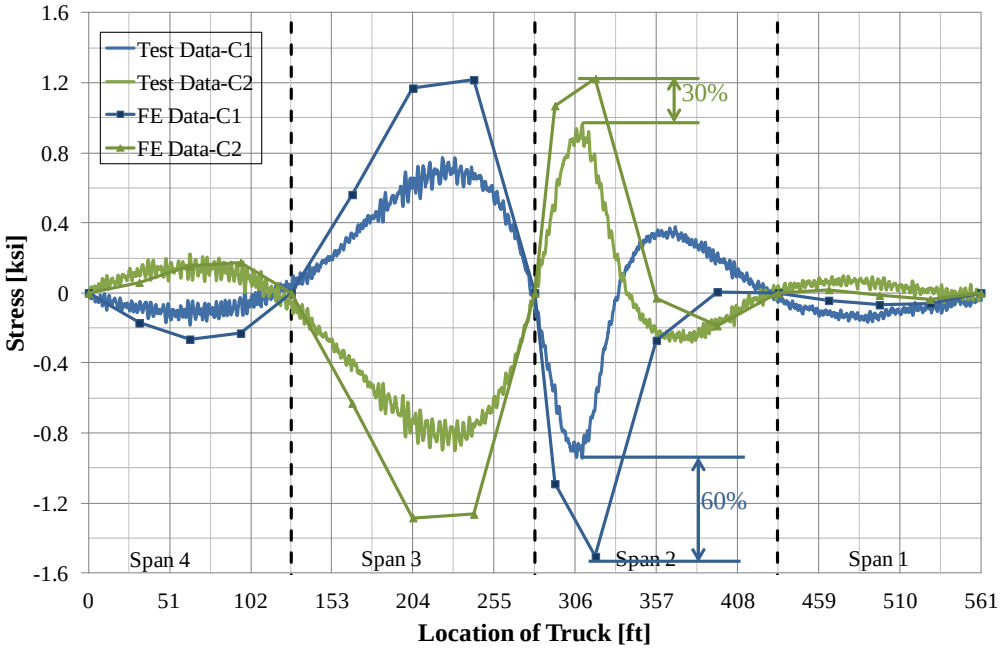

Figure 4-7: Computed and measured stress in the top and bottom girder flange at locations at Location C

The errors are collected at the location where test truck/simulated load is near instrumented floor beam to girder to cantilever bracket connection in each case. As illustrated in percentage in above three figures, the model generally gives more accurate estimate of the measured stress variations in the top girder flange than bottom flange. There is 4% of error in top flange at Location A and 45% of error at Location B, versus 70% in bottom flange case.

As clarified previously, during the procedure of developing FE model, the height of girder section was inevitably reduced due to assembly, which would change the overall flexural stiffness of the bridge. As for the integrity of the cross-section of the bridge, the parapets were not modeled, which would also affect the structural stiffness. Together the two recognized factors cause the discrepancy in similarity.

4.3.2 Tie Plate Response

Similar plots compare the estimated and measured stress in tie plate at Location A, B and C. All gages were oriented along the axis of the tie plate, which is transverse to the bridge axis. They are installed 1 inch from the side of the tie plate and directly above the exterior edge of the girder flange.

Shown in Figure 4-8 are estimated and measured stress on the tie plate at Location A, when the test truck/simulated load was applied on the eastbound right lane, prior to removal of the tie plate-to-girder flange bolts. The errors (35% of peak tensile stress and 5% of peak compressive stress) are measured near Location A, which are relatively small compared to the girder case (e.g. Figure 4-5). Recall that to simulate the loading condition, all together the six concentrated loads in ABAQUS are applied at twelve locations along the bridge spans with the same order as truck travelling direction in each case. The locations are almost evenly distributed in order to cover most of case scenarios, which include loading near piers and abutments, loading closed to instrumented tie plates, loading at mid-spans, etc. Based on observation, it is believed that the correlation would improve (i.e. the curve will be smoother) if more loading cases were examined as part of the ABAQUS model.

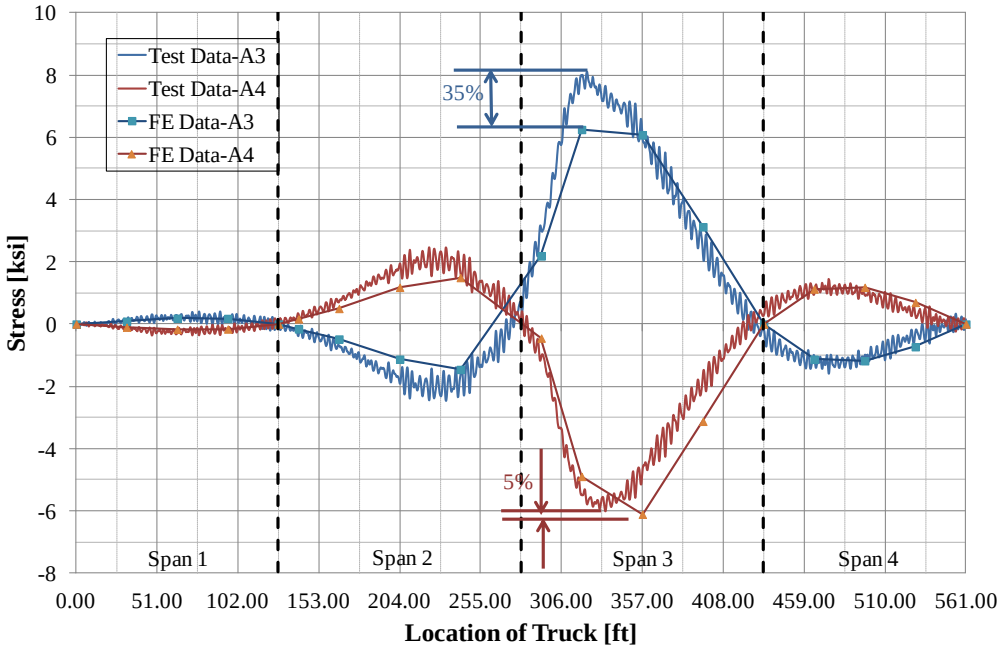

Figure 4-8: Computed and measured stress in the tie plate at locations at Location A before bolt removal

A similar procedure for comparison has been conducted for Location B, with the load on eastbound far right lane. As shown in Figure 4-9, after the tie plate was replaced, the girder is free to move longitudinally relative to the tie plate, the stresses are significantly reduced from the as-built condition (shown in Figure 4-10). The estimated result successfully catches the peak tensile and compressive stress, both of them occurred when load was applied near Location B. The analytical plot generally matches well with field measurement result along the bridge span, with a small margin of error. The error rate is as low as 10%.

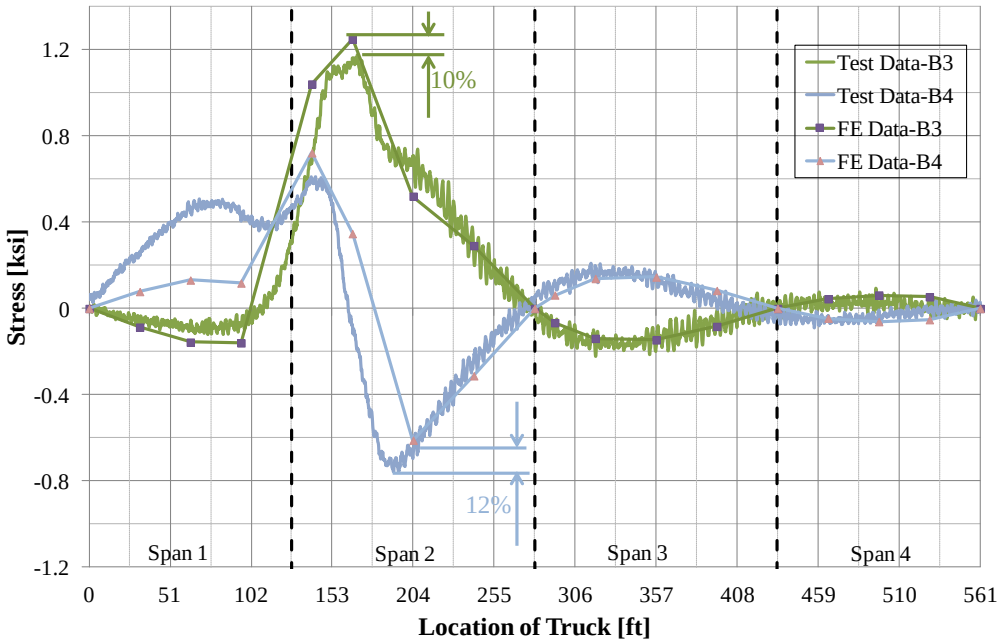

Figure 4-9: Computed and measured stress in the tie plate at locations at Location B

Figure 4-10 provides correlation between finite element model and strain gage results, which is similar as Location A. The load was on westbound right lane, passing span 4 through 1 in an order. Again, the model agrees well with field data, it also provides evidence that reducing the interval of loading cases would more precisely predict the peak stress.

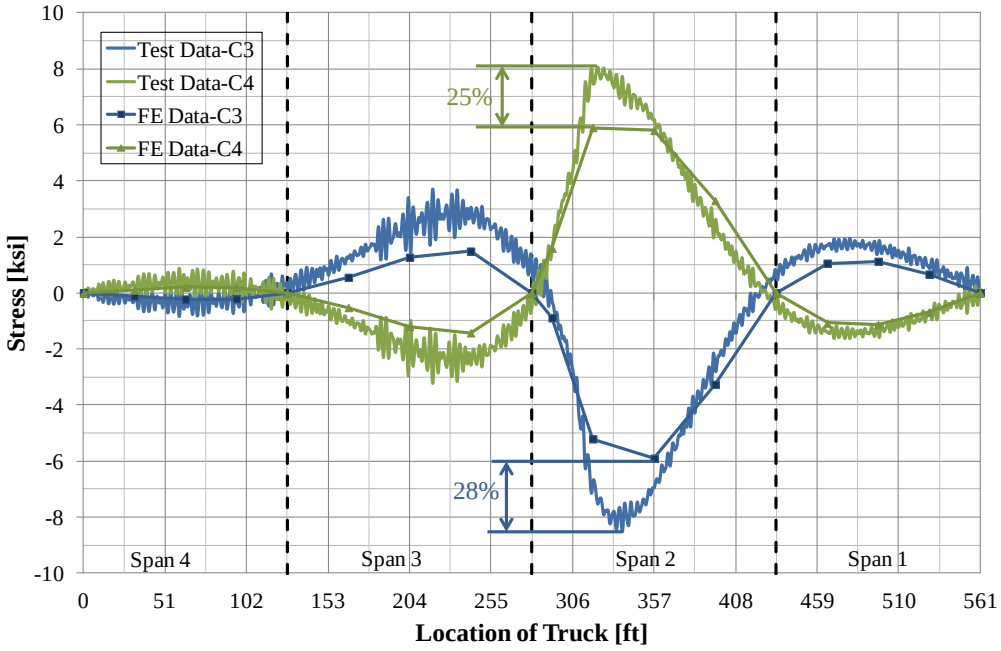

Figure 4-10: Computed and measured stress in the tie plate at locations at Location C

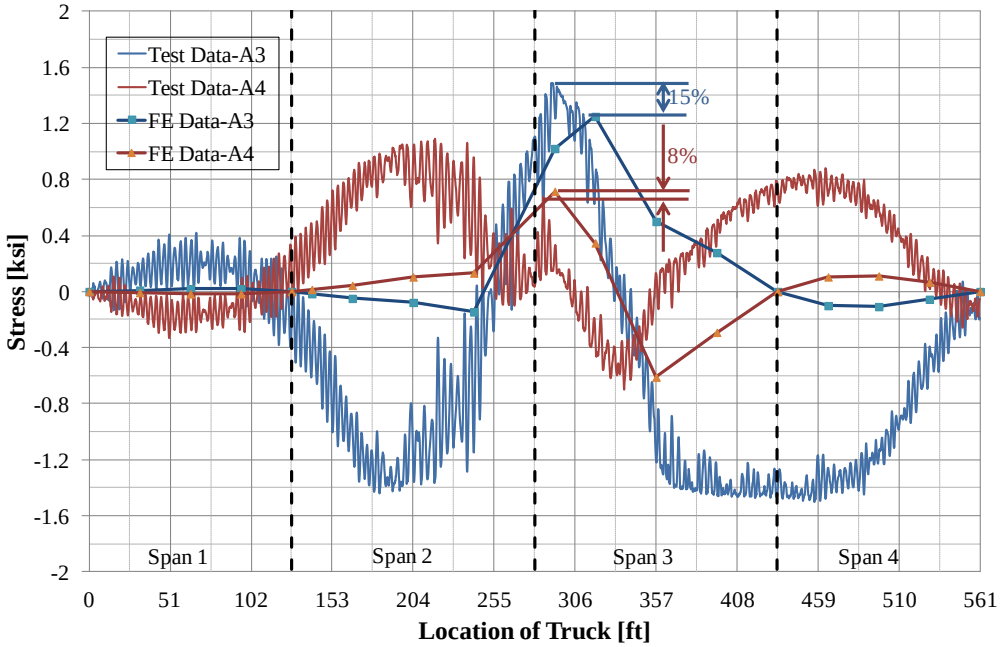

Figure 4-11: Computed and measured stress in the tie plate at locations at Location A after bolt removal

Above figure shows unstable correlation between computed and measured stresses in tie plate at Location A after seven of eight tie plate-to-girder flange bolts were removed from the connection. The stresses in both plots are significantly reduced due to release of the constraint. The error recorded when load was passing Location A are 15% of actual stress on the east side of the tie plate, and 8% on the west side, which are significantly lower than the average error rate.

The failure of estimation could be attributed to the difference between in-situ condition of tie plate connection and constraint in ABAQUS model. Although the incompletion of unbolting was modeled as well in FE model, by leaving one tie constraint at similar location, the in-situ condition was suspected to be somewhat between complete unbolted and fully connected, given the fact that the nut on the bolt was removed however the bolt itself remained in place.

FEA shows agreeable match of displacement location-history of tie plate at Location A after bolt removal (ABR) compared to LVDT data (shown in Figure 4-12). The theoretical analysis succeeded in catching the slope, though the predicted maxim and minim value of the relative longitudinal displacement between the centerline of the tie plate at the girder and the connection points at the stringers on either end are conservative. The plots of LVDT results of both before and after unbolting cases show some levels of deflection when the load applied right above the interior support. Since the senor was attached to the stringer it is suspected that the relative deflection was not properly measured.

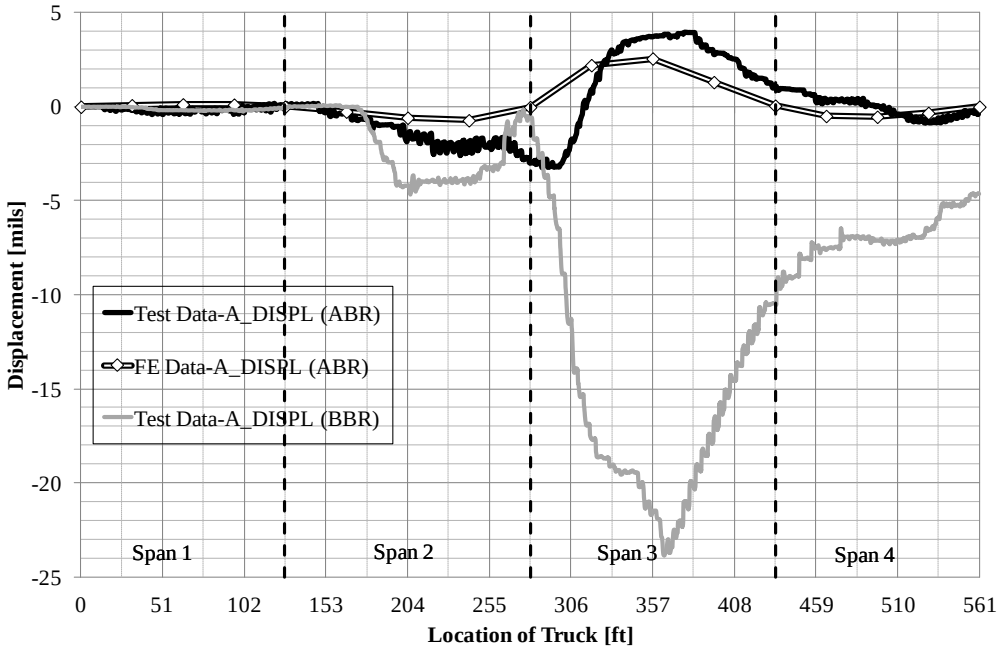

Figure 4-12: Displacement location-history plot for test data and FEA of tie plate at Location A before bolt removal (BBR), after bolt removal (ABR)

Since a part of study scope is to predict the effectiveness of the retrofits, meanwhile the model is success in matching analytical data with field test data in Figure 4-9 and Figure 4-12, where the cracked region that was retrofitted with a new plate prior to installation of instrumentation and monitoring. The retrofit strategy has been evaluated through controlled-load testing and FEM, which agree well with each other. The objective of using FEM to assess the effectiveness of the retrofits has been accomplished.

4.3.3 Cantilever Bracket Web Response

As discussed in the instrumentation plan, strain gages were installed on the web of the cantilever bracket adjacent to the cope at the top flange of the girder at Location A with the test truck in the eastbound acceleration lane (far right lane) prior to the removal of the tie plate-to-girder

connection bolts. Strain gages A5 and A7 are vertically oriented back-to-back on the web at the cope. Strain gages A6 and A8 are horizontally oriented back-to-back on the web (see Figure 4-4). The finite element model is adjusted accordingly. The elements at similar location as where stain gages were installed are targeted.

Shown in Figure 4-13 are the comparison plots for the four sets of data. The twelve loading cases cover most of the critical stress changes along the overall bridge span and precisely catch the locations where peak tensile and compressive stress occurred. Furthermore, a better correlation between the finite element model and the test results was obtained for vertically oriented stress (presented by A5 and A7). Higher error rate of data comparison for horizontal stress could be attributed to the discrepancy in connection angle simulation of cantilever bracket web region, which is originally modeled to accommodate the potential stress concentration.

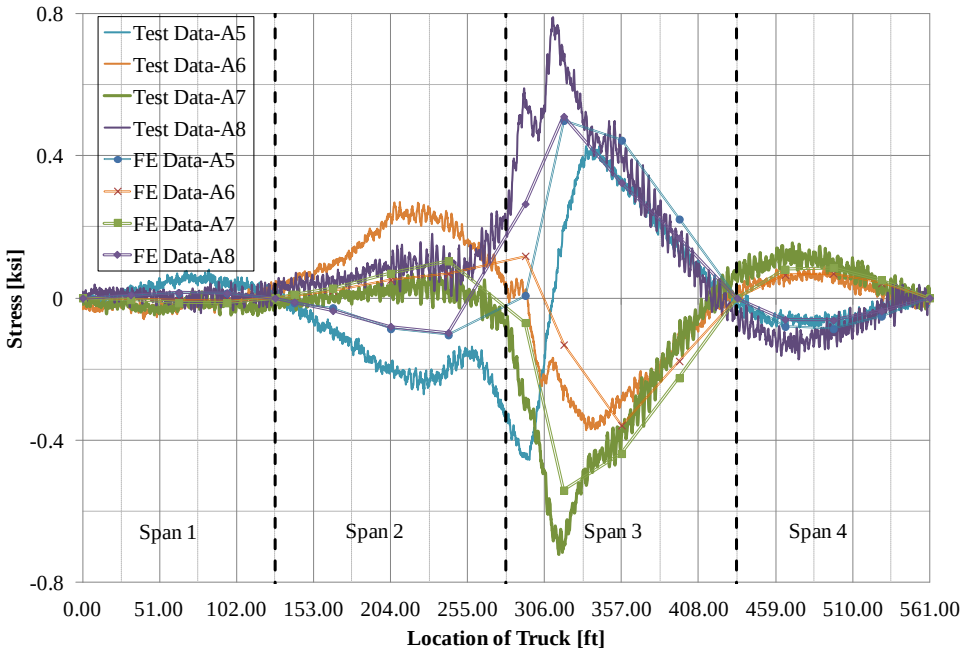

Figure 4-13: Computed and measured stress in the cantilever bracket web at locations at Location A before bolt removal

Presented in discussion on crawl testing results, removal of the tie plate-to-girder connection removes the restraint between the tie plate and the girder, which results in longitudinal displacement on the floor beam and cantilever bracket webs causing the region to bend out of plane. This additional demand can initiate vertical fatigue cracking along the connection angle of the web region. The long-term monitoring results confirmed the high risk.

Due to the complexity of bridge's three-dimensional deformation and constitutive relationships, the simplified linear-elastic model has limitation in prediction of horizontally oriented stresses. Only two sets of vertical stresses are plotted in Figure 4-14 to validate the performance of FE model after retrofit procedure had taken place at Location B. As shown, the value of theoretically computed peak stress is closed to the corresponding test one.

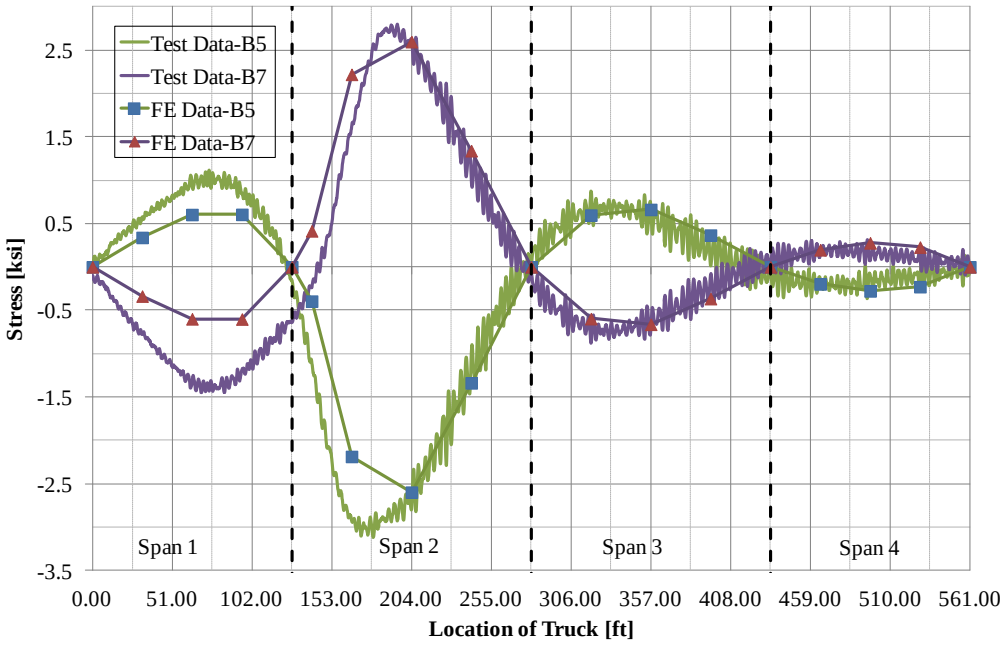

Figure 4-14: Computed and measured vertically-oriented stress in the cantilever bracket web at locations at Location B

Finally Location A has been evaluated for both before and after constraint removal cases. Indicated in Figure 4-15 and Figure 4-16, the inaccuracy of estimation could be caused by inadequately detailed simulation of incomplete unbolting of tie plate. In both cases, the FE model failed to catch the significant drop of vertical stress value when the loads were closed to Location A, which could be caused by enhanced web connection.

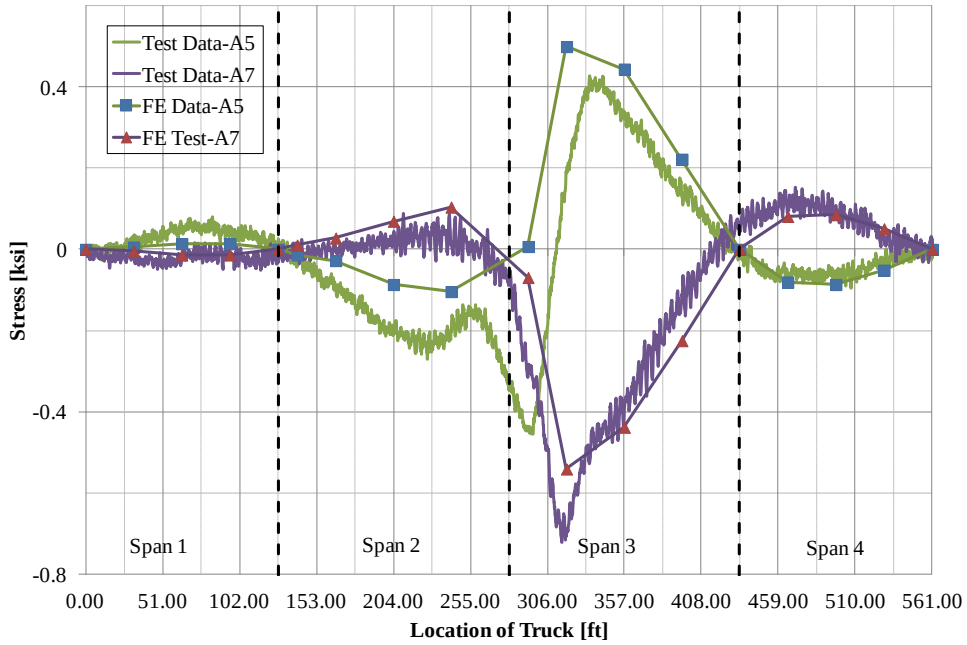

Figure 4-15: Computed and measured vertically-oriented stress in the cantilever bracket web at locations at Location A before bolt removal

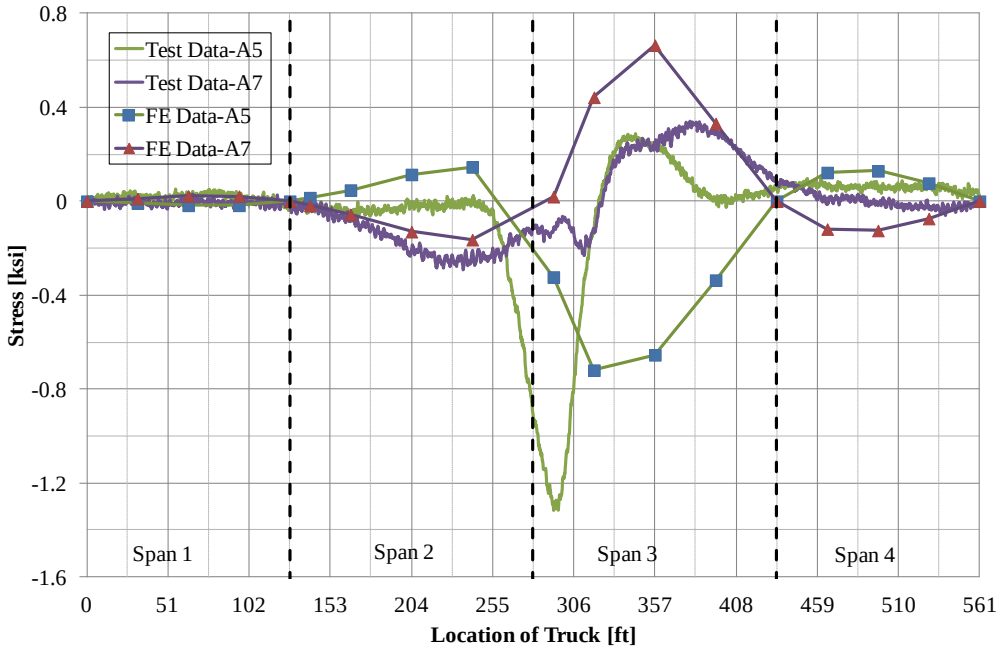

Figure 4-16: Computed and measured vertically-oriented stress in the cantilever bracket web at locations at Location A after bolt removal

4.4 Adjustment of FE Model

Parapets are added to FE model to evaluate its affect on structural integrity and furthermore overall flexural stiffness which may cause the stress change in tie plate.

Modeled with shell element, the simulated parapets are assigned with steel properties and actual height and width obtained from shop details. They are merged with deck at edges as shown in Figure 4-17. Note that the web of cantilever bracket is not shaped as original shop details, the lower edge remains uncut. It is believed that this may not cause increase of structural stiffness when the bridge is subjected to vertical load.

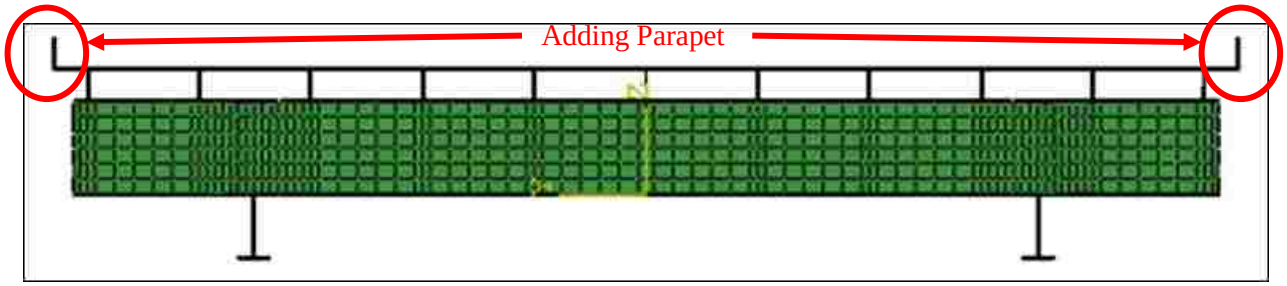

Figure 4-17: Bridge cross-section after adding parapets to FE model

Figure 4-18 presents the comparison of stress in the top and bottom girder flange at locations at Location A prior to and after adding parapets to FE model. To some extent the parapets enhance the structural integrity, however, the influence on the analytical results are negligible.

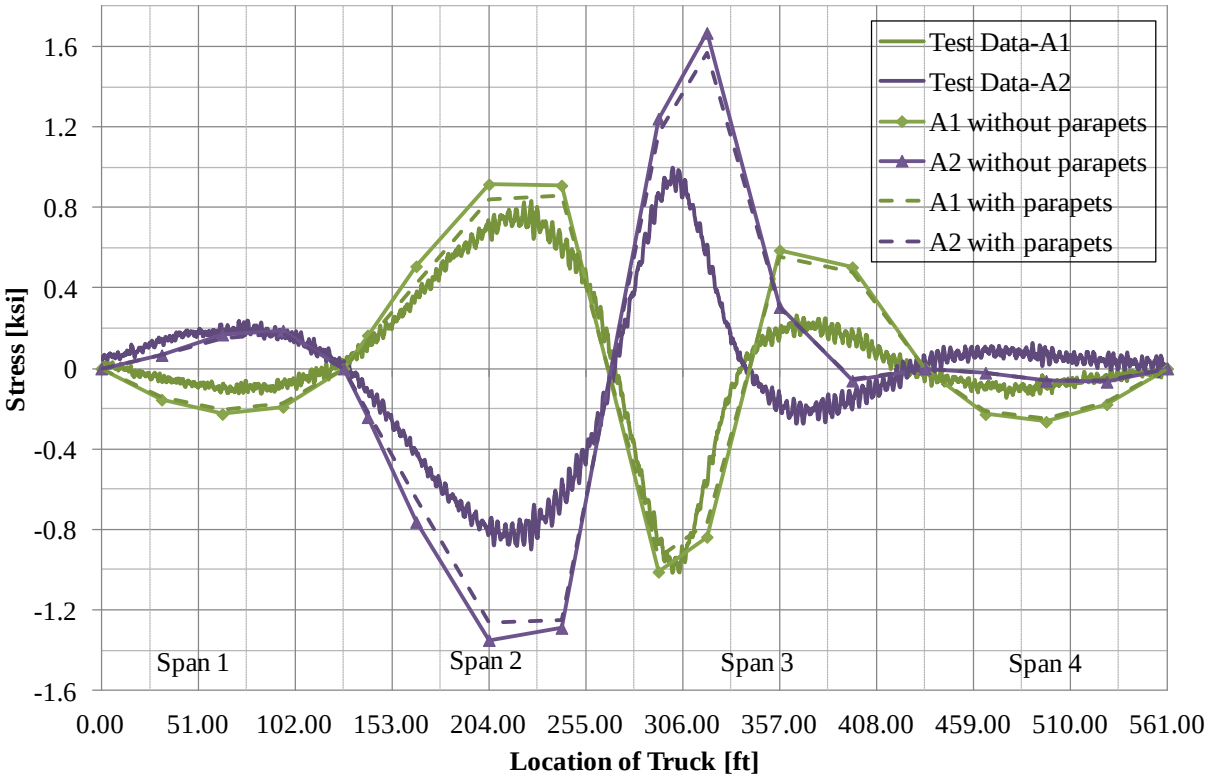

Figure 4-18: Stress in the top and bottom girder flange at locations at Location A without and with parapets

An alternative method to evaluate the change in stiffness is to comparing the frequencies of two models to the actual bridge natural frequency, which is 1.92Hz from field monitoring. Appling gravity (32.2 ft/s^2) as loading condition to FE model, totally ten (10) modes are computed. Shown in Figure 4-19 is the one closest to bridge deformation in service. The calculated frequency for model without parapets is 1.55 Hz, while for model with parapets is 1.57 Hz. The more flexible the model is the lower frequency it has.

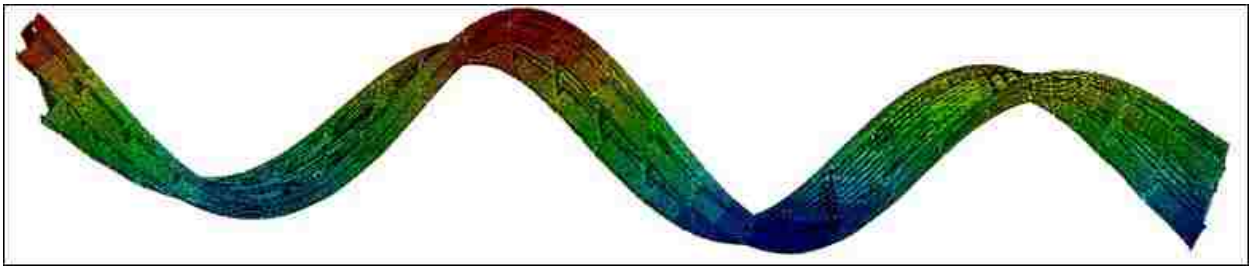

Figure 4-19: Model (with parapets) exaggerated deformed shape with frequency of 1.57 Hz

Both results indicate that the parapet is not the primary contributor to the change of structural stiffness.

The deck system of the bridge (concrete deck and stringers) is stiff against the in-plane deflection or deformation of the deck. This results in the bending of the tie plate. Adding the composite action of the parapet to the deck would not change the situation of tie plate bending.

Based on above evaluation, the model is not significantly influenced by adding parapet to deck system. In order to maintain the efficiency of calculation operation, the FE model remains without parapet during the remaining investigation.

4.5 Summary of Comparison

A study of the deformations of the overall bridge system (component by component) confirms qualitatively that the tie plate is bending in the horizontal plane, which validates the feasibility and the rationality of the finite element model.

The validation of the computed results is reported in section 4.3. The accuracy of the comparison supports that the in-plane tie plate bending can be computed using FE model and analysis, specifically in Figure 4-8 and Figure 4-10. Furthermore, FEM provides satisfactory

results in predicting the feasibility and effectiveness of the retrofits, shown in Figure 4-9 and Figure 4-14. The selection of load applying locations is proven to be effective and representative, though more intensive distribution would increase the accuracy of estimation.

The out-of-plane bending of cantilever bracket web plates, on the other hand, cannot be predicted with sufficiently accurate results due to local restraints provided by built-up sections and riveted plates. In addition, the discrepancy between the measured and predicted girder stress could be attributed to simplifications in the variation of actual girder section properties over their lengths that were incorporated in the model.

5. Examination of Bridge System using FEM

A finite element model was presented previously to provide insight on the cracking of the tie plates and evaluation of a repair technique. The model takes into account the effect of girder length and size, the controlled test truck loads, the riveting of tie plates and the connection of cantilever brackets. Some comparisons with field test data are reported to validate the efficiency of the proposed model.

A series of research based on modification of current simulated bridge system is conducted in this section. The cause of tie plate in-plane bending is determined through the investigations of span length. In addition, parametric studies are conducted to assess the potential of this failure mode for bridges with different skewness and stringer spacing.

5.1 Cause of Tie-Plate Bending

Studies in field measurement and FEA indicate that the tie plates are subjected to in-plane bending stresses. Figure 5-1 shows schematically that the high cyclic stresses in tie-plate are caused by in-plane displacement of the tie-plate, which generated by flexural bending of the girder. X-axis is parallel with longitudinal girder, the positive direction represents truck traveling direction on eastbound. Y-axis indicates vertical deflection; its positive direction is opposite to load applying direction. Both axes in this 2-D sketch are consistent with global coordinates in FE model. Correspondingly, dx and dy are considered as longitudinal and vertical deflection of girder, respectively. After taking the height of girder cross-section into consideration and assuming that the neutral axis of girder cross-section and the axis of zero

rotation of girder coincide with each other, the first sketch of girder major deformation can be magnified at one floor beam (the second sketch in Figure 5-1). Δ is the displacement at tie plate with respect to its associated girder.

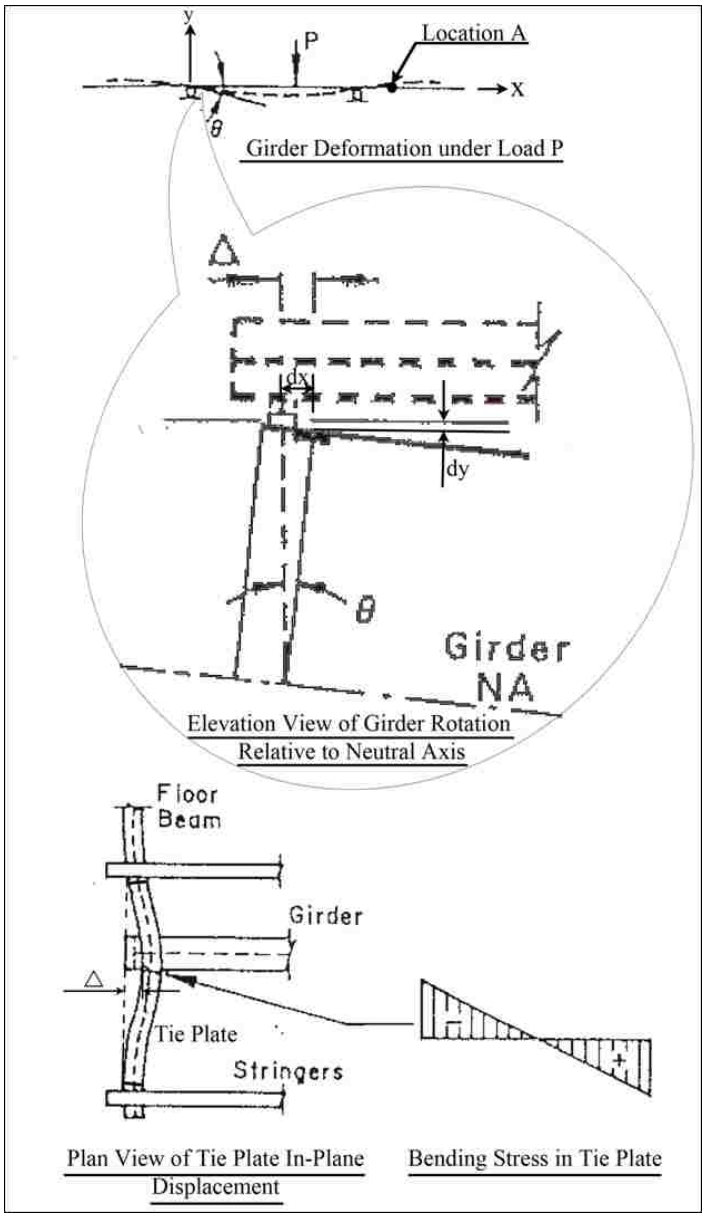

Figure 5-1: Sketch of tie plate bending due to global action [Fisher 1984, Page 188]

5.1.1 Girder Rotation

To study the link between the rotation of girder and the in-plane bending of tie plate, the influence lines of dy/dx and the measured in-plane bending stress of tie-plate at Location A (over floor beam 13) with bolt-connected to girder were collected under the same twelve loading cases as Section 4.3. It is expected that the girder slope of dy/dx is the indicator of the magnitude of in-plane bending of the tie-plates.

The stresses of tie plate are obtained from field measurement data A3 and from similar location on FE model, which represent the in-plane bending stress of the tie plate one inch from east side of the tie plate above the outside edge of girder top flange. dy/dx can be obtained by relative longitudinal displacements between top and bottom flange of girder divided by the distance between the central lines of those two flanges.

As shown in Figure 5-2, the in-plane bending of tie plate is compatible with the change in slope of the main longitudinal girder. The influence line for Location A agrees with the measured stress response. As predicted, the primary cracking occurred at locations that experienced the largest changes in rotation.

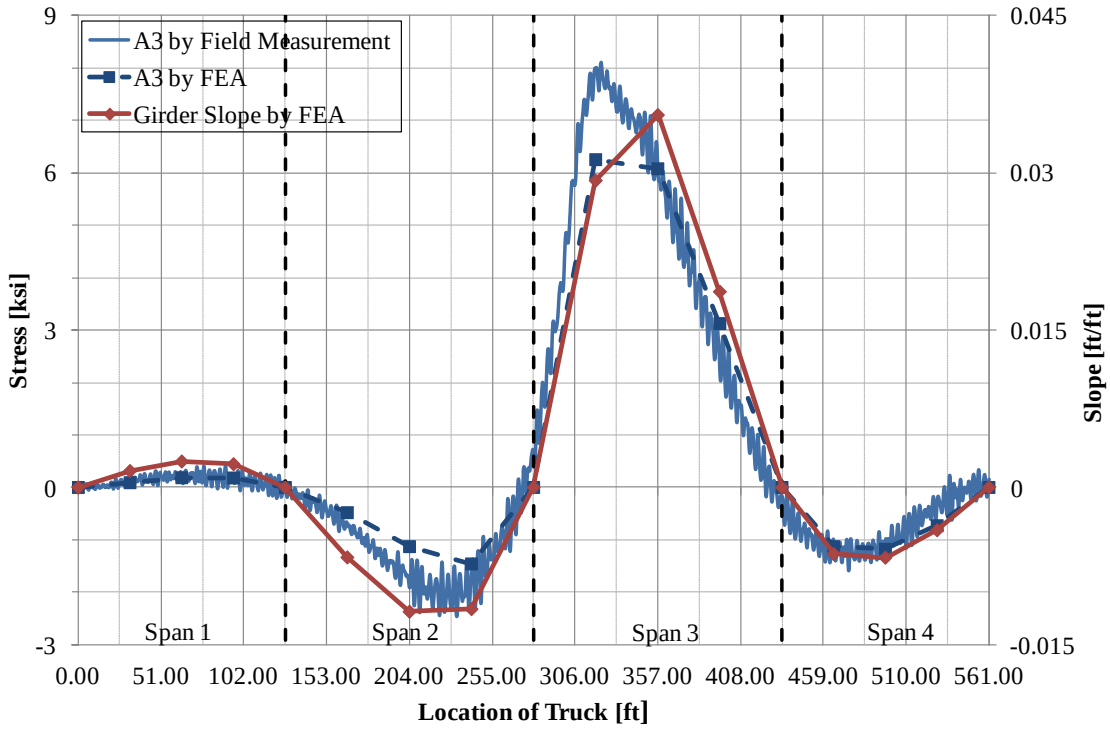

Figure 5-2: Comparison of stress history in tie plate with influence line for girder slope for Location A (floor beam 13)

After raising the attention on the difference between theoretical and practical methods to access girder slope, further insight on the possible effects of the point of zero rotation of girder at different floor beams is achieved by applying one random loading case and investigating girder rotation at each floor beam. Measured by distance from the central line of girder bottom flange, Figure 5-3 shows neutral axis and zero rotation location of south girder at span 3 when the replicated truck load is acting at that span, right above the girder. Featured points on x coordinate represent floor beams, which are aligned with Pier 2 and 3 at the end and number 13 through 17 in between. As a reference, the stress envelope of tie plates connecting floor beam system to girder at span 3 is included in Figure 5-3 and presented in another coordinate.

This typical case indicates opposite to sketch in Figure 5-1, the neutral axis and the axis of zero rotation do not coincide with each other due to actual boundary condition in practice. The non-composite cross-section of girder is symmetric, with the height of 10 ft, the neutral axis of girder over two end piers is the same as the geometric center of girder cross-section. The locations of zero rotation of girder, however, are variable at different floor beams. Recall that the tops of girder and floor beam are at the same elevation (shop drawing in Figure 2-3) and the floor beam height is 6 ft, which sum up to 4 ft between the bottom flanges of floor beam and girder. When girder rotates with respect to its geometry center, large rotation is produced resulting high bending stress at tie plate. When floor beam interferes with girder rotation causing girder rotating relative to floor beam bottom flange, the connecting tie plate becomes less vulnerable to girder rotation. Then when the center of floor beam becomes the new center of rotation, the relative movement between girder top flange and tie plate continues to induce in-plane bending, though the magnitude is not as large as the one controlled by main girder rotation.

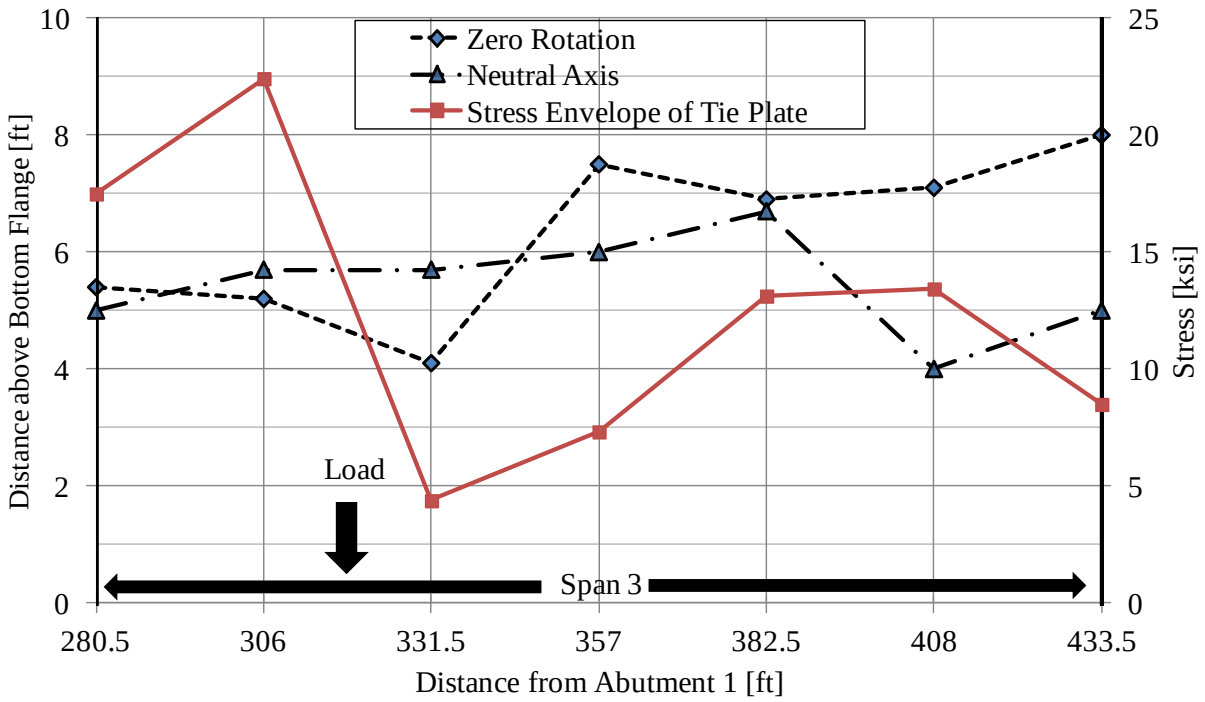

Figure 5-3: Neutral axis and zero rotation location of south girder and stress envelope of the associated tie plate

5.1.2 Stress and Displacement Envelops

Furthermore, the data of stresses and displacements at tie plates along the entire length of the south girder were collected from all eastbound replicated test load positions. Figure 5-4 and Figure 5-5 provide the envelopes of the maximum and minimum in-plane displacements and bending stresses at each tie plate. The in-plane displacements of the tie plates in the middle of each span are relatively small. Correspondingly, the more highly stressed tie plates are near the piers and abutments. These behaviors can be seen to be compatible with the change in slope of the main longitudinal girder.

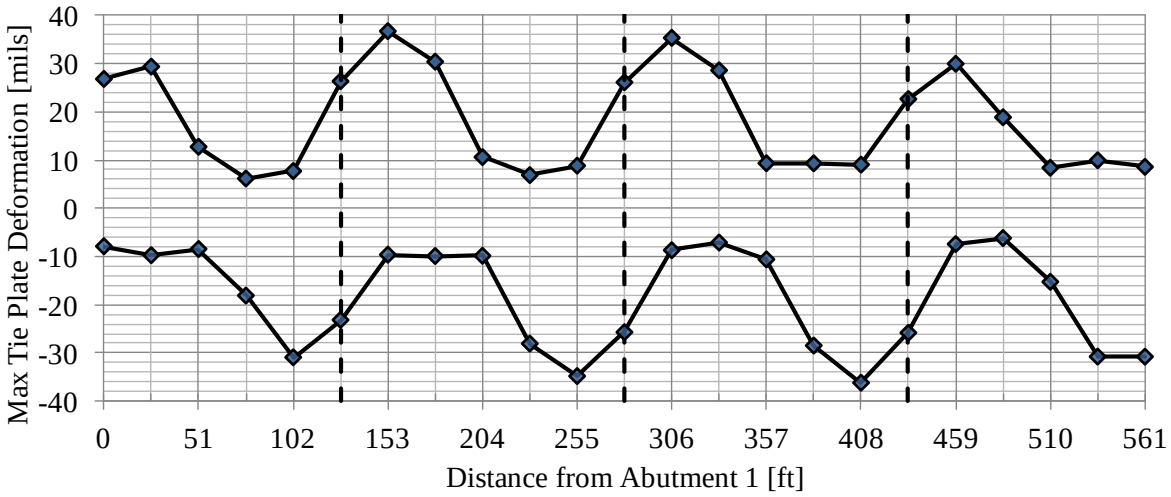

Figure 5-4: Envelope of horizontal displacement at each tie plate over the length of the bridge

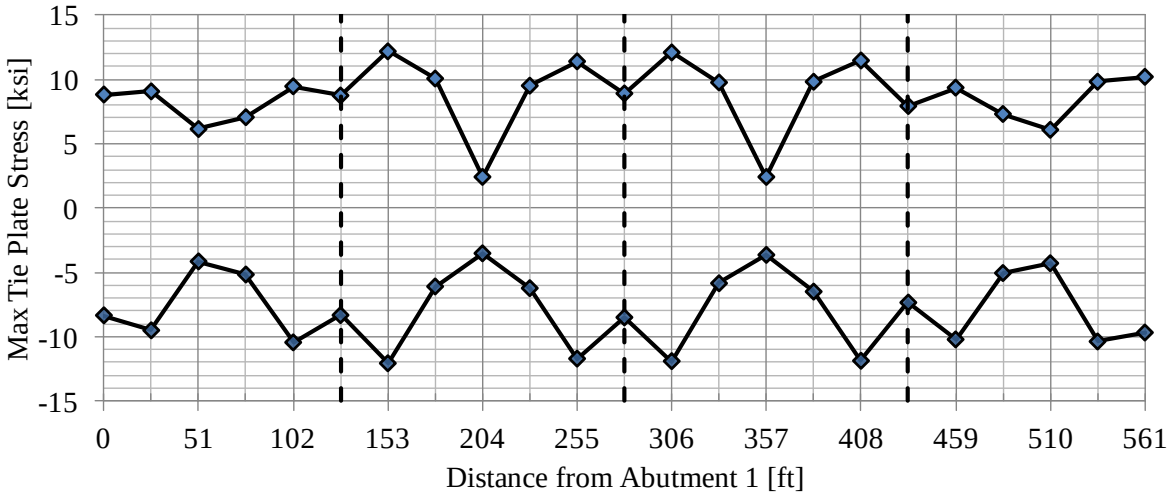

Figure 5-5: Envelope of normal stress at each tie plate over the length of the bridge

A variation of span length is made to compare the resulting stress at tie plate to Figure 5-5. The bridge was originally designed with four continuous spans, end span lengths are 127.5 feet and interior span lengths are 153 feet. By changing the boundary condition (support location) of

finite element model, a “new” bridge model was developed. The supports are remain skewed at an angle of 63-degree, the end lengths are 127.5 feet and interior span lengths are 102 feet.

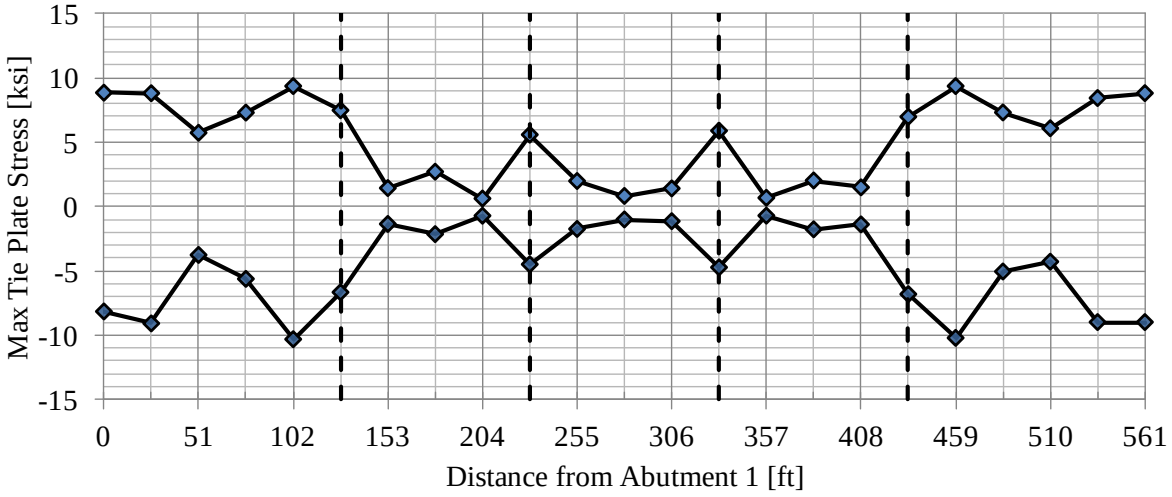

Figure 5-6: Envelope of normal stress at each tie plate after shortening the span length

As shown in Figure 5-6, decreasing the length of interior spans reduces the girder slope therein and consequently the bending of the tie plate. The stresses in tie plate have reduced dramatically, while the one along exterior span remains in the same stress range.

In summary, results in sub-section 5.1 indicate that the rotation (slope) of the girder is a main factor causing tie-plate bending, which further confirm that tie-plate bending is due to its relative movement in compliance with the top flange of the girder and that the deck is rigid with respect to the displacement of the girder and tie plate.

5.2 Examination of Skew

It is under a suspicion that skewness of the bridge might have a strong effect on the tie plate stresses. With the same loading conditions as the ones in case study, the effectiveness of skew is examined with three different skewness arrangements as follow:

- Remain current arrangement as the basic case.
- Shift one side of the bridge, including abutments, piers and a girder, to make the bridge "right".
- Make all the floor beams intersecting the girders at an angle for the skewed bridge.

The plan view of above all three girder to floor beam to stringer arrangements are shown in Figure 5-7. To eliminate variables, the spacing of floor beam, girder and stringer is remaining the same in all three cases, respectively. The supports are shown with red dots. Figure 5-8 summaries the stress variation at tie plate associated with floor beam 13 (Location A) when tie plate is bolt-connected to girder top flange in all above three proposals.

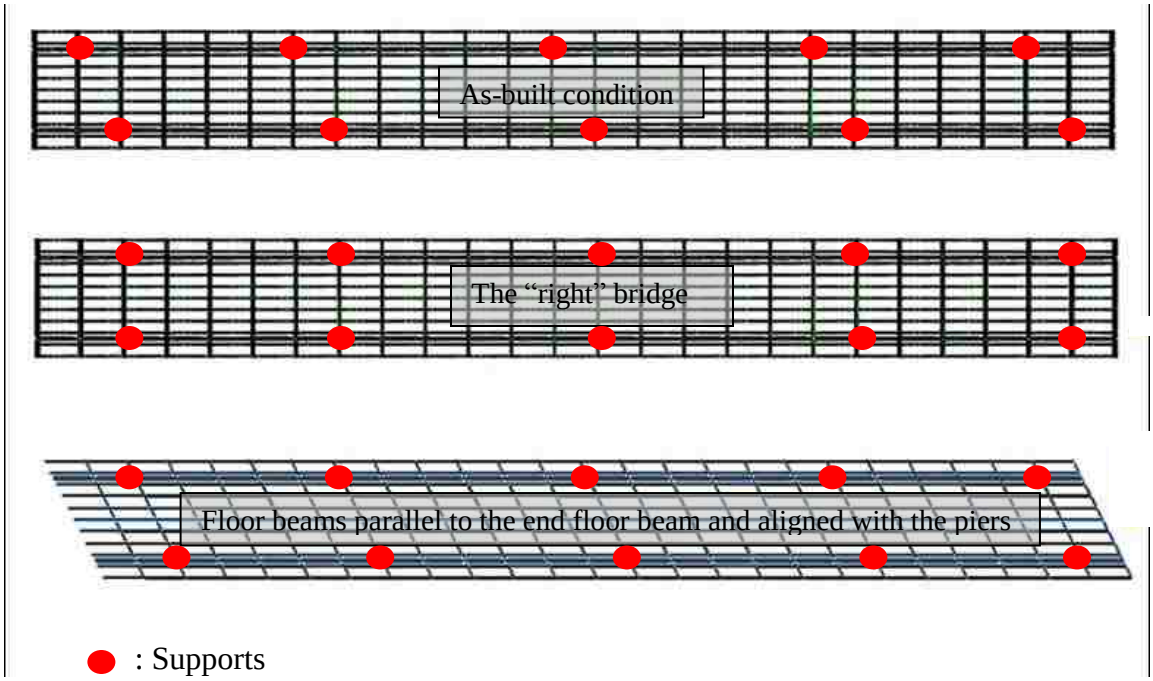

Figure 5-7: Plan views of three proposals for skewness investigation

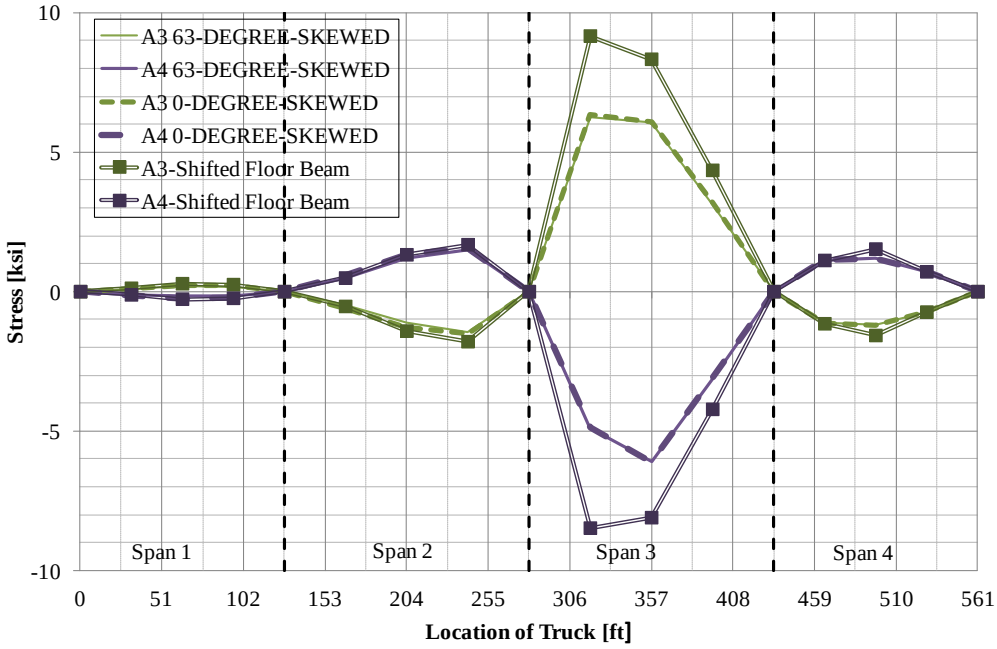

Figure 5-8: Comparison of stress in tie plate at Location A with three skewness arrangements

5.2.1 The “Right” Bridge

In this plan, the piers supporting north girder are shifted eastward, meeting the corresponding piers under south girder at the same floor beam, making the floor beams, except those at the bridge ends, are all perpendicular to the girders. As presented in bold green and purple dashed lines in Figure 5-8, the "right" bridge of the same geometry has about the same magnitude of tie plate bending stresses.

The result is acceptable given the discussion made in section 3.1.1. The far right lane loading produces the highest stresses in the south girder (Locations A). The shifting of supports at north girder may not initiate significant stress change in tie plates over south girder. This might extend the FEA results from previous case study to broader application field, providing reference for future investigation on bridges with different degree of skewness.

5.2.2 Floor Beams Parallel to Abutments

A bridge model of the same dimension and geometry as the existing one but with all floor beams parallel to the end ones is developed in ABAQUS program. The modified FE model sustains the same level of accuracy by remaining the mesh sizes and tie constrains at connection region. Figure 5-9 demonstrates that as the longitudinal girder rotates inward, the top of the transverse floor beam’s web, which is enhanced by angles and connected to the longitudinal girder, is pulled toward the center of the span. The stringers, which are connected to the top flange of the transverse floor beam, provide lateral bracing restraint and resist the inward movement of the transverse floor beam. This forces the tie plate to bend in the horizontal plane, creating tension

on the leading edge of the tie plate and compression on the trailing edge of the tie plate. Compared with Figure 4-3, floor beam is susceptible to torsion, resulting higher in-plane bending demand. The legend at the lower right corner presents in-plane bending stress at girder top flange, with the unit of ksf. The stress at the corresponding tie plate at Location A plotted in Figure 5-8 is revealing of significant increase when truck load is travelling nearby, due to the contribution of torsion of floor beam system.

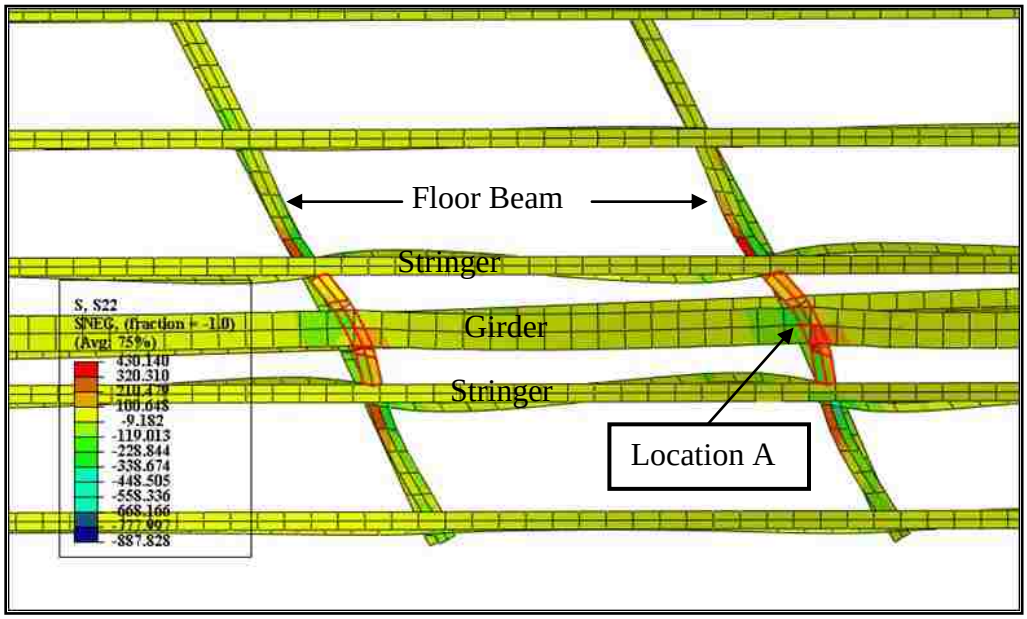

Figure 5-9: Magnified plan view of floor beam system deformation and structural components' interaction

The qualitative and some quantitative comparison might provide reference to future design and examination of skewed steel plate girder system. Torsion of floor beam system should be eliminated in order to secure the maximum value of stress range being kept at a level which is less than the fatigue limit of the structural detail.

5.3 Examination of Stringer Spacing

Parametric study in this section is conducted with a goal of determining the link between in-plane bending of tie plate and the spacing of its adjacent stringers. By examining the magnitude of tie plate bending stresses with variable constrains provided by floor beam and stringer, an argument is made regarding the suspicion of the defect in the bridge design. This proposal is executed on current finite element model by lengthening and shortening the spacing of the stringers adjacent to the tie plates over south and north girder, under the assumption that the change of stringer spacing does not make the deck system too rigid or too soft to change the behavior of the main girders.

To begin this study, the stringers-to-floor-beam connections are considered functioning as the end supports of the tie-plate. The sketch of simplified fixed-end beam is shown in Figure 5-10. S_{max} is directly proportional to the displacement (Δ), is directly proportional to the distance c (as in M_c/I) and is inversely proportional to the [square of the length of the beam, (L^2)]. When the displacement (Δ) due to global action and the distance c of the tie-plate remain unchanged, increasing the spacing between stringers (L) will reduce the maximum stress (S_{max}) in the plate.

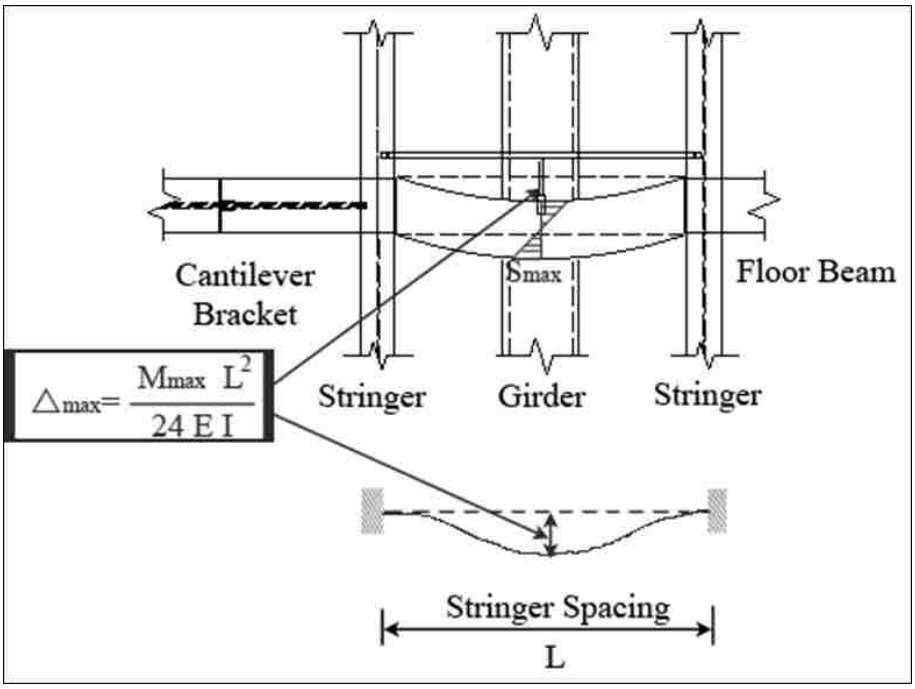

Figure 5-10: Plan view of stringer-to-floor-beam connection and fixed-end beam theory

The modified FE model sustains the same level of accuracy by remaining the mesh sizes and tie constrains at connection region. Based on current element size at the top flanges of cantilever bracket, girder and floor beam, the spacing (L) between the adjacent stringers is changed from the current value of 7.125 ft. to 4.06 ft., 10.57 ft. and 13.02 ft., respectively. The bottom flange of stringer is merged to the top flange of the supporting girder. To verify the attachment methods of the intersecting area, the relative longitudinal displacement between the centerline of the tie plate at the girder and the connection points at the stringers on either end is checked through four different spacing cases. It is expected that the displacement is almost the same due to global girder rotation.

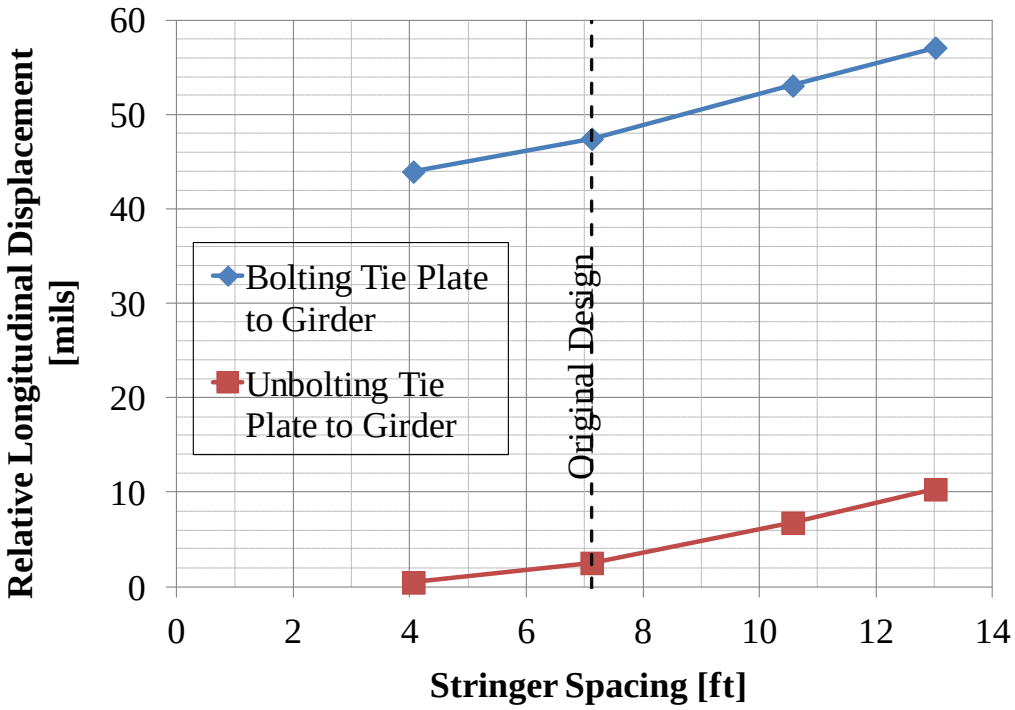

Figure 5-11: Relative displacement between tie plate and stringers at Location A with tie plate connected and not connected to girder using FEA

The displacement variation (Δ) with distance (L) is plotted in Figure 5-11. Both bolting and unbolting cases are considered. The black dashed line represents the original design of 7.125 ft. It is proved previously by results from controlled loading test (section 3.1.2) that removal of the bolts resulted in significantly reduced displacement of the tie plate. Within 9 ft. of distance lengthening, the relative movement between tie plate and restraining stringers on either side raises from 44 mils to 57 mils when the tie plate is bolted to the girder flange, and from 0.5 mils to 10.3 mils when it's not. As increasing of stringer spacing, the tie plate responses with more deformed shape relative to adjacent stringers, yet the development is within a small range.

Recall the discussion in section 5.1: tie plate in-plane bending is mainly caused by the rotation (slope) of the girder, the relationship between longitudinal displacement at top flange of girder

and horizontal bending of tie plate is illustrated in Figure 5-1. Considering the depth of girder, which is 10 ft., 10-mils discrepancy based on fundamental theory is acceptable in practice. Thus, the assembling method of new stringer-to-floor-beam arrangement is confirmed. The stress-spacing (S-L) relationship in four spacing cases with the tie plate connected and not connected to the girder flange is further investigated.

Figure 5-12 shows exaggerated deformed tie plate associated with floor beam system. Measured with local coordinate, the tie plate bending stress is reduced when increasing the distance between the stringers for this bridge. The Maximum and minimum bending stress of tie plate vs. stringer spacing at Location A with tie plate connected and not connected to girder is shown in Figure 5-13. As expected, the spacing gets bigger, the stress or moment gets lower.

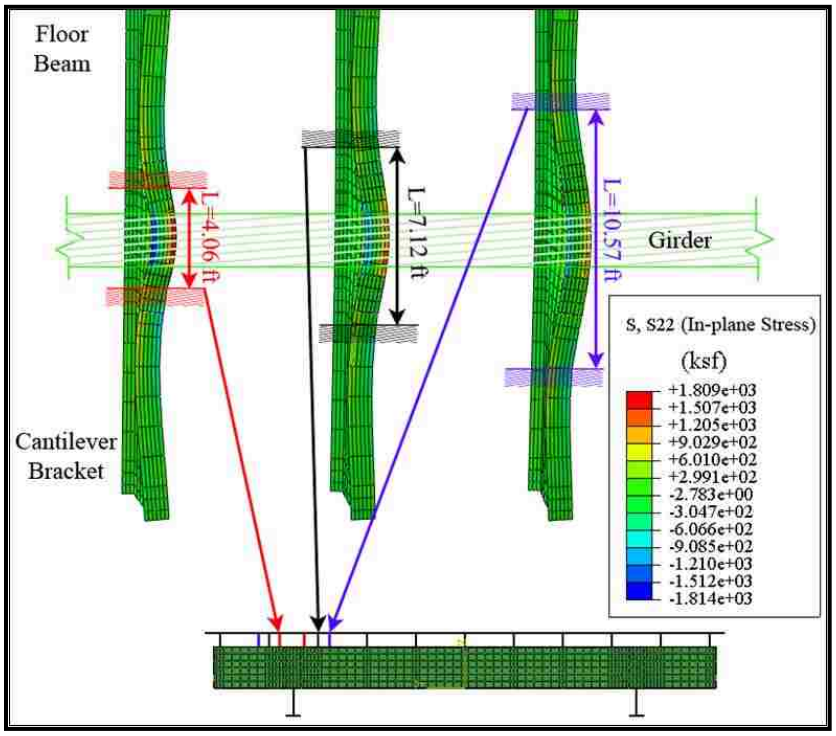

Figure 5-12: Bending stress in tie plate with stringer fixed at various spacing when the tie plate is bolted to girder

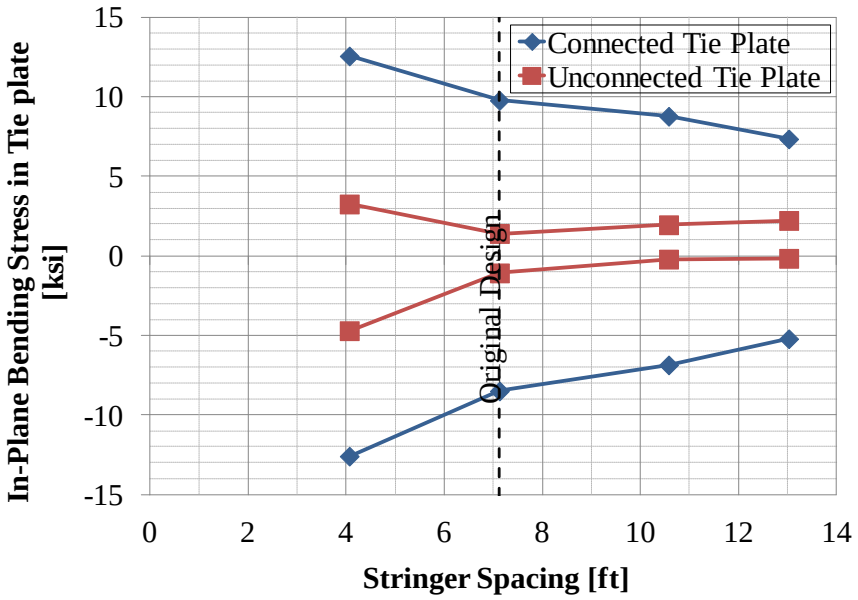

Figure 5-13: Maximum and minimum bending stress of tie plate vs. stringer spacing at Location A with tie plate connected and not connected to girder

A procedure of estimating tie-plate bending stresses by design computation is conducted with the results compared to FEA in Figure 5-15. Based on the envelope of girder slope at the tie-plate shown in Figure 5-14, the corresponding horizontal displacement of the tie-plate can be computed by hand. Then the in-plane bending stress of the tie plate one inch from east side of the tie plate above the outside edge of girder top flange can be computed. The hand calculation results agree with FEA, which confirms the assumption made regarding stringer constraining towards tie plate. The detailed calculation sheet is attached to Appendix B: Mathcad Computation Sheet.

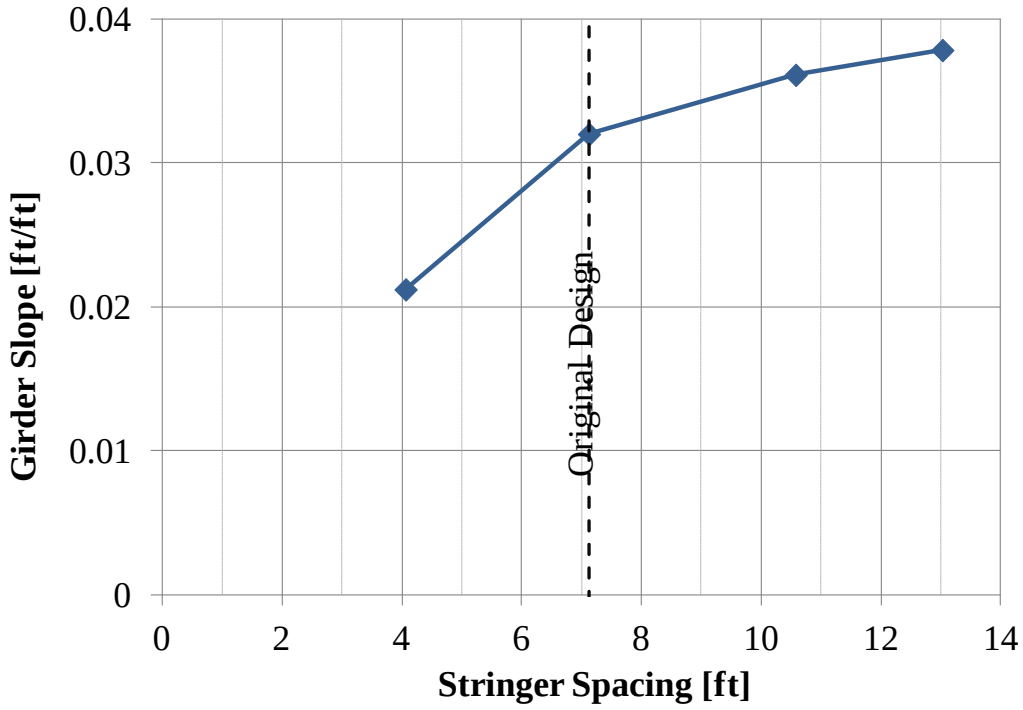

Figure 5-14: The envelope of girder slope at the tie-plate

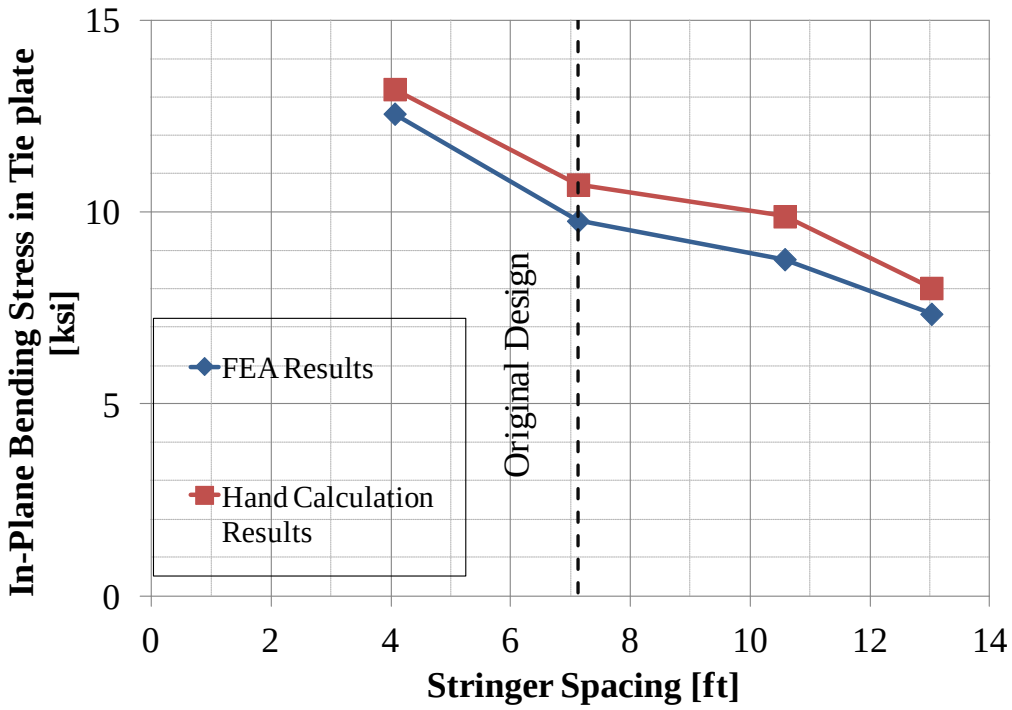

Figure 5-15: Estimation of maximum bending stress by design computation of tie plate at Location A with tie plate connected to girder

This parametric study would provide reference to future design and rehabilitation of steel plate girder bridge system:

1) As increasing of stringer spacing, the tie plate responses with more deformed shape relative to adjacent stringers, which should remain unchanged due to global action and the distance c of the tie-plate, yet the discrepancy is acceptable in practice.
2) Removal of the bolts between tie plate and girder top flange results in significantly reduced in-plane bending stress of the tie plate.
3) Stress of tie plate is increasing significantly when its adjacent stringers approaching to each other.

4) After disconnecting the tie plate to girder top flange underneath, the girder is free to move longitudinally relative to the tie plate. Subsequently, the bending stress at tie plate is less sensitive to the change of constraints on either side.
5) Girder is undergoing severe rotation as its adjacent stringers moving towards each other.
6) The stringers-to-floor-beam connections can be considered functioning as the end supports of the tie-plate. The bending stress of tie plate can be calculated following design procedure.

5.4 Summary of Parametric Studies

The rotation (slope) of the girder is a main factor causing tie-plate bending, which further confirms that tie-plate bending is due to its relative movement in compliance with the top flange of the girder and that the deck is rigid with respect to the displacement of the girder and tie plate.

The qualitative and some quantitative comparisons are conducted to prove that skewness of floor beam system may contribute to the tie plate in-plane bending stress. Furthmore, torsion of floor beam system should be eliminated in order to secure the maximum value of stress range being kept at a level which is less than the fatigue limit of the structural detail.

After disconnecting the tie plate to girder top flange underneath, the girder is free to move longitudinally relative to the tie plate. Subsequently, tie plate is less sensitive to the change of constraints on either side. Girder is undergoing severe rotation initiating stress of tie plate is increasing significantly as its adjacent stringers moving towards each other. The stringers-to-floor-beam connections can be considered functioning as the end supports of the tie-plate. The bending stress of tie plate can be calculated following design procedure.

6. Recommendation for Retrofit

The maximum and minimum in-plane displacements and bending stresses at each tie plate are obtained previously in sub-section 5.1.2. The stress range for tie plates is discussed in this section. The locations with high bending demand are further identified. The recommended retrofit strategies are evaluated under the aid of FEA.

6.1 Recommended Retrofit Location

To evaluate the likelihood of cracking at each tie plate on the bridge, Figure 6-1 illustrates the predicted stress ranges for the tie plates over south girder under the replicated test truck load. The estimated stress range of each tie plate is obtained by adding the absolute values of maximum and minimum in-plane bending stresses plotted in Figure 5-5. The locations marked with red crosses have already exhibited cracking, which are floor beam #2, #7 (Location B) and #22. The stresses at location B is the higher stress location predicted by analysis, providing confirmation of field inspection results. Other locations of potential crack formation can be identified, such as Location A and Location C. Note that the tie plate at Location A was over the south girder at the first floor beam east of Pier 2, and the tie plate at Location C was over the north girder at the first floor beam west of Pier 2, those two tie plates were located symmetrically at two sides of the center of Pier 2.

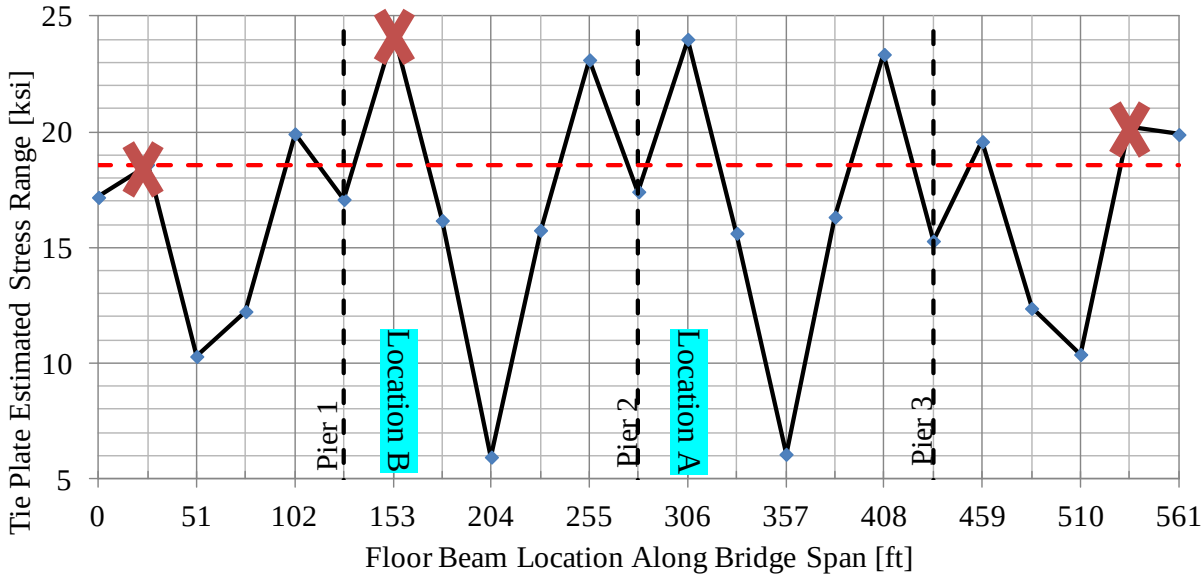

Figure 6-1: Estimated stress range for tie plates over south girder

Recall in section 3.2.3, the field evaluation revealed that fatigue cracking of Location C should have already occurred at tie plate. Note that the tie plate at Location C was over the north girder at the first floor beam west of Pier 2. Again, the FE model gives accurate prediction of location where tie plate with high risk.

Validated by field inspection and long-term monitoring program, tie plates with potential fatigue failures are identified by the parametric study. Shown in Figure 6-1, the dividing line illustrated as the red dashed line is representing the cracked region. As a minimum, all tie plates with stress ranges higher than the cracked regions should be unbolted. Based on these results a minimum of nine tie plates are likely to have fatigue failures in the near future.

6.2 Recommended Retrofit Procedures

FEM not only can be adopted to identify the locations of tie plate with high in-plane bending demand, but also to evaluate the effectiveness of proposed retrofit methods both qualitatively and quantificationally. During the following subsections, two optional rehabilitation paths are proposed and examined. The details of suggested retrofit procedures are shown in Figure 6-2, respectively.

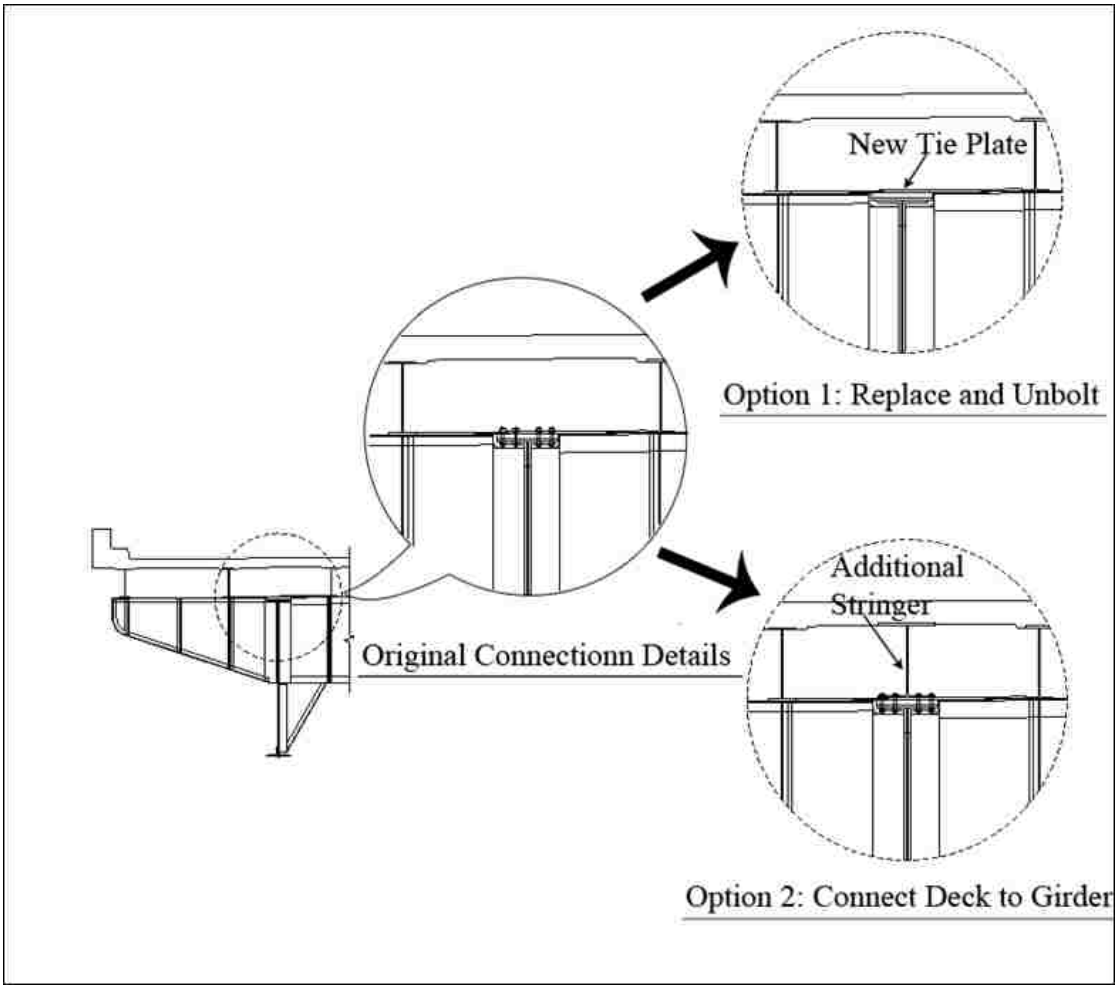

Figure 6-2: Recommended retrofit strategies

6.2.1 “Softening”

Based on the results presented in section 6.1, many of the un-fractured tie plates will likely fracture in the next few years. To reduce the likelihood of future crack formation of the tie plate, the study in section 3.1.2 has shown that disconnecting the tie plate from the girder will give the plate an infinite fatigue life. This can be achieved by either unbolting the existing tie plate-to-girder connection or through installation of a new plate that does not include a girder connection. By removing the bolts connecting the tie plate and girder, the retrofitting procedure for this bridge "softens" the zone of girder to floor beam connection, allowing the top flange of the floor beam and the tie plate to be freed from the top flange of the girder. This reduces the horizontal in-plane bending of the tie plate and reduces its stresses, which is proved by plots in Figure 6-3. This procedure is relatively less expensive.

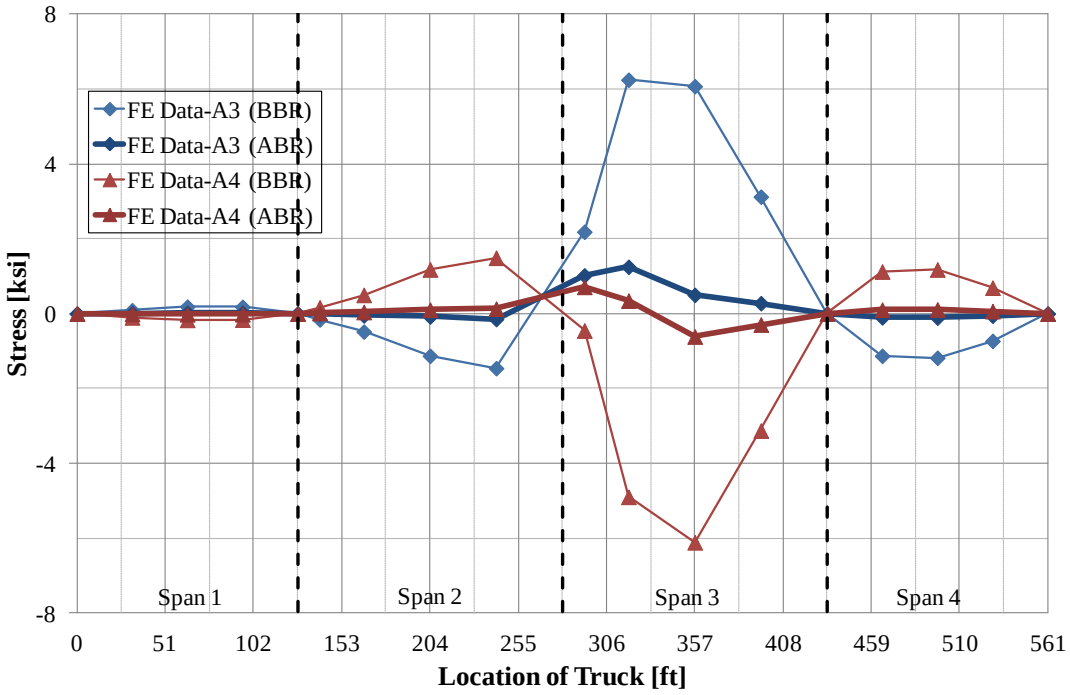

Figure 6-3: Stress in tie plate at Location A prior to and after bolt removal (BBR)/ (ABR)

6.2.2 "Stiffening"

The results of field measurement and the finite element analysis indicated that the tie plates were subjected to in-plane bending stresses. Figure 3-3 and Figure 5-4 show the in-plane displacement that was introduced into the tie plates. This behavior can be seen to be compatible with the change in slope of the main longitudinal girder. The primary cracking occurred at locations that experienced the largest changes in rotation. An improvement method is proposed by making the girder composite with the deck through adding a stringer directly above the girder to increase the stiffness in the longitudinal direction (sketched in Figure 6-2). Thus, the modified girder, the stringers and the deck do not have relative displacement at the elevation of the top

flange of the floor beams. This procedure is described as "stiffening", opposite to previously discussed "softening" method. The caveat to this repair strategy is that it is very expensive.

FEM is also used in predicting the feasibility and effectiveness of this proposed retrofit strategy. Modeled with shell element, the simulated additional stringers are assigned with steel properties and the same height and width as existing stringer. The elevation view of the modified cross-section is shown in Figure 6-4. The top flange of the new stringer is merged with above deck, while the bottom flange are tie constrained with tie plate and the rest of the girder. The location of tie constrain between stringer and girder is selected based on shop details of stringer to floor beam connection, while the location of tie constrain between stringer and tie plate is engineered considering the bottom flange width, tie plate size, existing bolts and both spacing. Figure 6-5 is the comparison of stresses in tie plates at Location A prior to bolt removal between without and with additional stringers case. The stress decreases as the overall flexural stiffness being enhanced. The problem of in-plane bending of the tie plate is eliminated.

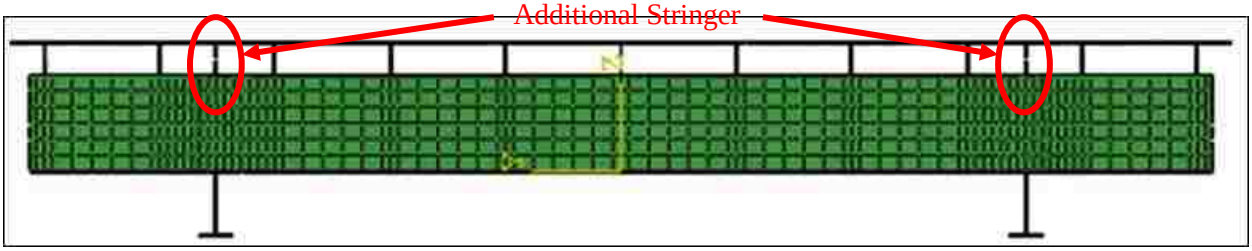

Figure 6-4: Bridge cross-section after adding additional stringers to FE model

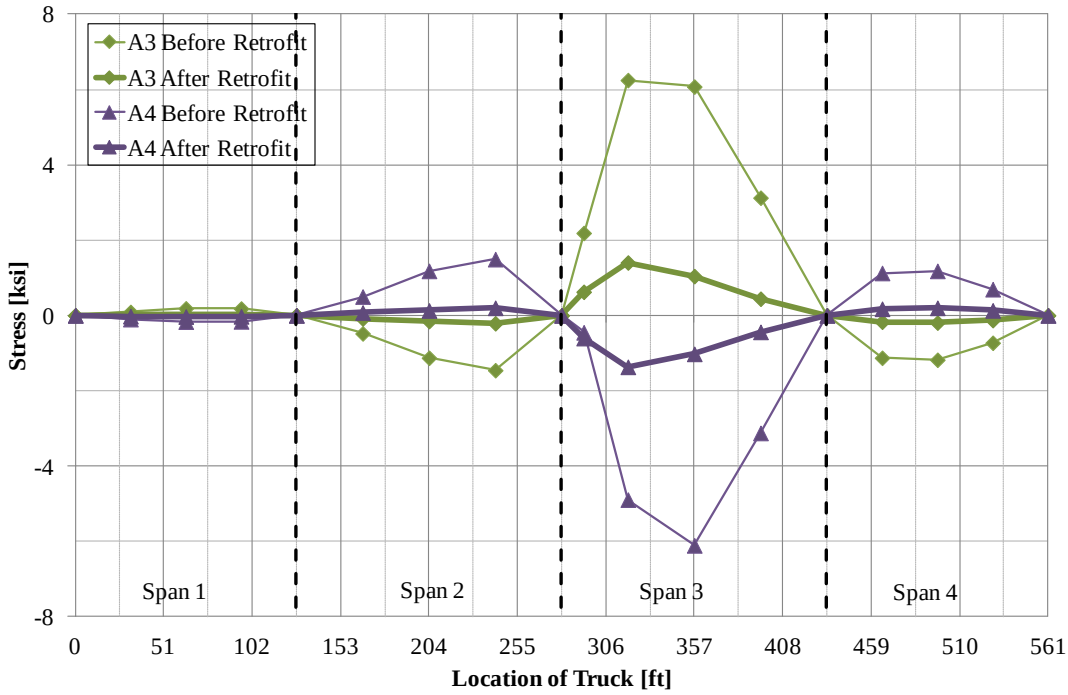

Figure 6-5: Stress in tie plate at Location A prior to bolt removal without and with additional stringers

6.3 Summary

In general, FEA results agree with both "softening" and "stiffening" methods. The peak stresses at tie plate change significantly from 6 ksi to less than 2 ksi in both modifications. "Softening" is achieved by removing the bolts between the tie plate and girder, which is proved to reduce the restraint in the tie plate and associated stresses. "Stiffening" is performed by modifying the girders and connecting it to the bridge deck, the in-plane bending of tie plate induced by the relative displacement between stringers and the deck is effectively decreased.

The first repair strategy is more cost-effective, while in the meantime, the caveat to it is that unbolting the girder-to-tie plate connection will cause an increase in the floor beam and

cantilever bracket stresses. It is possible that the increase in stresses may result in fatigue cracking of the web region of the floor beam or cantilever bracket. To execute the second proposal, the concrete deck has to be replaced beforehand, which will cost more personnel and facility input.

7. Conclusions and Limitations

This study is initiated by the inspection of the bridge carrying State Route 422 over the Schuylkill River, which revealed fractures on the tie plates connecting the cantilever floor brackets and floor beams. The bridge consisted of a reinforced concrete bridge deck supported on steel stringers, which were in turn supported on floor beams. The floor beams framed into two continuous girders. This system created a separation between the concrete deck and the girder top flange. As a result of this construction detail the flexural deformations of the girder top flange and the bridge deck were incompatible, which produced in-plane bending of the tie plate.

A field testing was conducted to identify the cause of the. The results indicate that removal of the bolts between the tie plate and girder will reduce the restraint in the tie plate and the associated stresses. The stresses in the web however increase. Due to the complexity of the built-up floor beam and cantilever bracket it is possible that the highest stress region was not measured. If a higher region of stress exists in the retrofitted connection (particularly at a rivet hole) a crack of the web region could occur.

An analytical study illustrated the cause of the high cyclic stresses on the tie plates. The study of the deformations of the overall bridge system (component by component) confirms qualitatively that the tie plate is bending in the horizontal plane, which validates the feasibility and the rationality of the finite element model.

The validation of the computed results is also reported. The accuracy of the comparison supports that the in-plane tie plate bending can be computed using FE model and analysis. Furthermore, FEM provides satisfactory results in predicting the feasibility and effectiveness of the retrofits. The selection of load applying locations is proven to be effective and representative, though more intensive distribution would increase the accuracy of estimation.

The out-of-plane bending of cantilever bracket web plates, on the other hand, cannot be predicted with sufficiently accurate results due to local restraints provided by built-up sections and riveted plates. In addition, the discrepancy between the measured and predicted girder stress could be attributed to simplifications in the variation of actual girder section properties over their lengths that were incorporated in the model.

Parametric studies show that the rotation of the girder is a main factor causing tie-plate bending, which further confirm that tie-plate bending is due to its relative movement in compliance with the top flange of the girder and that the deck is rigid with respect to the displacement of the girder and tie plate.

The qualitative and some quantitative comparison provide reference to future design and examination of skewed steel plate girder system. Torsion of floor beam system should be eliminated in order to secure the maximum value of stress range being kept at a level which is less than the fatigue limit of the structural detail.

Girder is undergoing severe rotation resulting stress of tie plate increasing significantly as the adjacent stringers approaching to each other. The stringers-to-floor-beam connections can be

considered functioning as the end supports of the tie-plate. The bending stress of tie plate can be calculated following design procedure.

FEA results agree with both “softening” and “stiffening” methods. The first repair strategy is more cost-effective, while in the meantime, the caveat to it is that unbolting the girder-to-tie plate connection will cause an increase in the floor beam and cantilever bracket stresses. It is possible that the increase in stresses may result in fatigue cracking of the web region of the floor beam or cantilever bracket. To execute the second proposal, the concrete deck has to be replaced beforehand, which will cost more personnel and facility input.

References

Fisher J.W., 1984, "Fatigue and Fracture in Steel Bridges: Case Studies," John Wiley and Sons, Inc. New York, NY, USA.

Demers, C.E., Fisher, J.W., 1989, "Lehigh Canal and River Bridge, Pennsylvania. A Survey of Localized Cracking in Steel Bridges 1981 to 1988," ATLSS Report No.89-01, Lehigh University, Bethlehem, PA, USA.

Fisher J.W., Yen, B.T., Kaufmann, E.J., and Ma, Z., 1995, "Crack Evaluation and Repair of Cantilever Backet Tie Plates of Edison Bridge," Vol. 2, Fourth International Bridge Engineering Conference, San Francisco, California.

Naito, C.J., Hodgson, I.C., Yen, B.T., Kaufmann, E.J., and Li, X., 2010, "Evaluation of Cracked Tie Plates on the Bridge Carrying SR422 over the Schuylkill River Cumru Township, Berks County PA," ATLSS Report No. 10-08, ATLSS Center, Lehigh University, 77 pages.

Nowak A. S., Sanli A. and Eom J., 1999, "Bridge Girder Distribution Factors for Live Load," Structural Engineering in the 21st Century; Proceedings of the 1999 Structures Congress, New Orleans, LA, USA.

Shenton H. W., Jones R., and Howel, D., 2004, "A Web-Based System for Measuring Live Load Strain in Bridges," Structural Materials Technology VI, an NDT Conference, Buffalo, NY, USA.

Bhattacharya B., Li D., Chajes M. and Hastings J., 2004, "Reliability-Based Load and Resistance Factor Rating Using In-Service Data," ASCE Journal of Bridge Engineering, Vol. 10, No. 5, 530-543.

Chajes M.J., and Shenton H.W. III, 2005, "Using Diagnostic Load Test for Accurate Load Rating of Typical Bridges," Proceedings of the 2005 Structures Congress and the 2005 Forensic Engineering Symposium, New York, NY, USA.

Zhao Y. and Roddis W. M., 2003, "Finite Element Study of Distortion-Induced Fatigue in Welded Steel Bridges," TRB, National Research Council, Washington, D.C., USA

Barrett A. S., Kim H., and Frank K. H., 2009, "Field Test and Finite Element of I-345 Bridge in Dallas," Report No. FHWA/TX-10/5-4124-01-2, 170 pages.

Troiano G. P. Jr, DeWolf J. T., 2009, "Field Strain Monitoring to Evaluate Unexpected Cracking in a Non-Redundant Steel Plate Girder Bridge," Report No.CT-2251-2-09-4, University of Connecticut, CT, USA.

Miner M.A., 1945, "Cumulative Damage in Fatigue," Journal of Applied Mechanics, 12(3): 159-64.

AASHTO, 2008. American Association of State Highway and Transportation Officials, "LRFD Bridge Design Specifications," 4th Edition, Washington, D.C.

ABAQUS Version 6.9.3

Connor R.J., Fisher J.W., Hodgson I.C., Bowman C.A. 2004, "Results of field monitoring prototype floor-beam connection retrofit details on the Birmingham Bridge," final report, ATLSS Report No. 04-04, Lehigh University, Bethlehem, PA.

Appendix A: Instrumentation Details

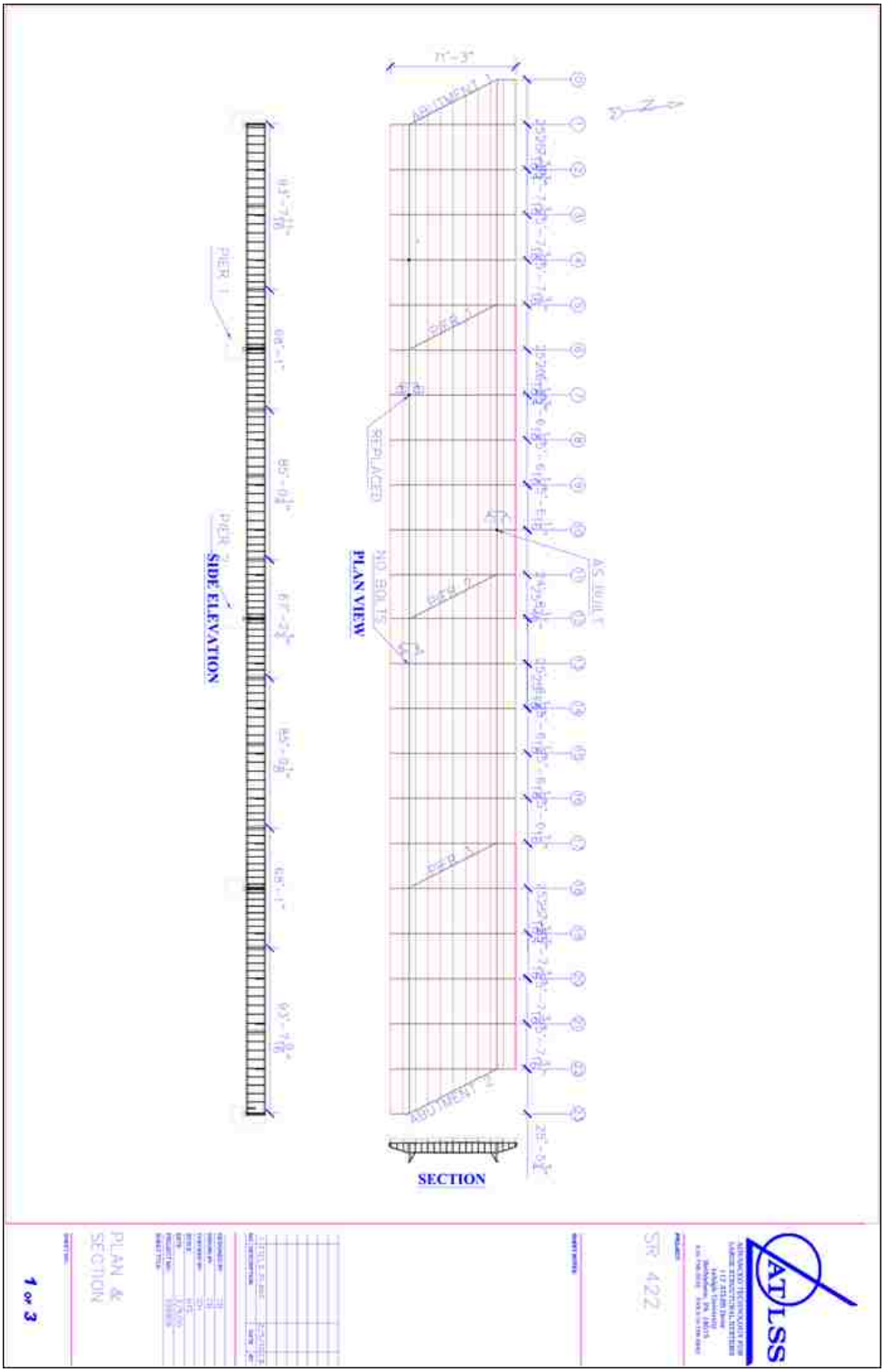
SIDE ELEVATION
PLAN VIEW
SECTION
PLAN & SECTION
1 of 3
SR 422
ATLSS

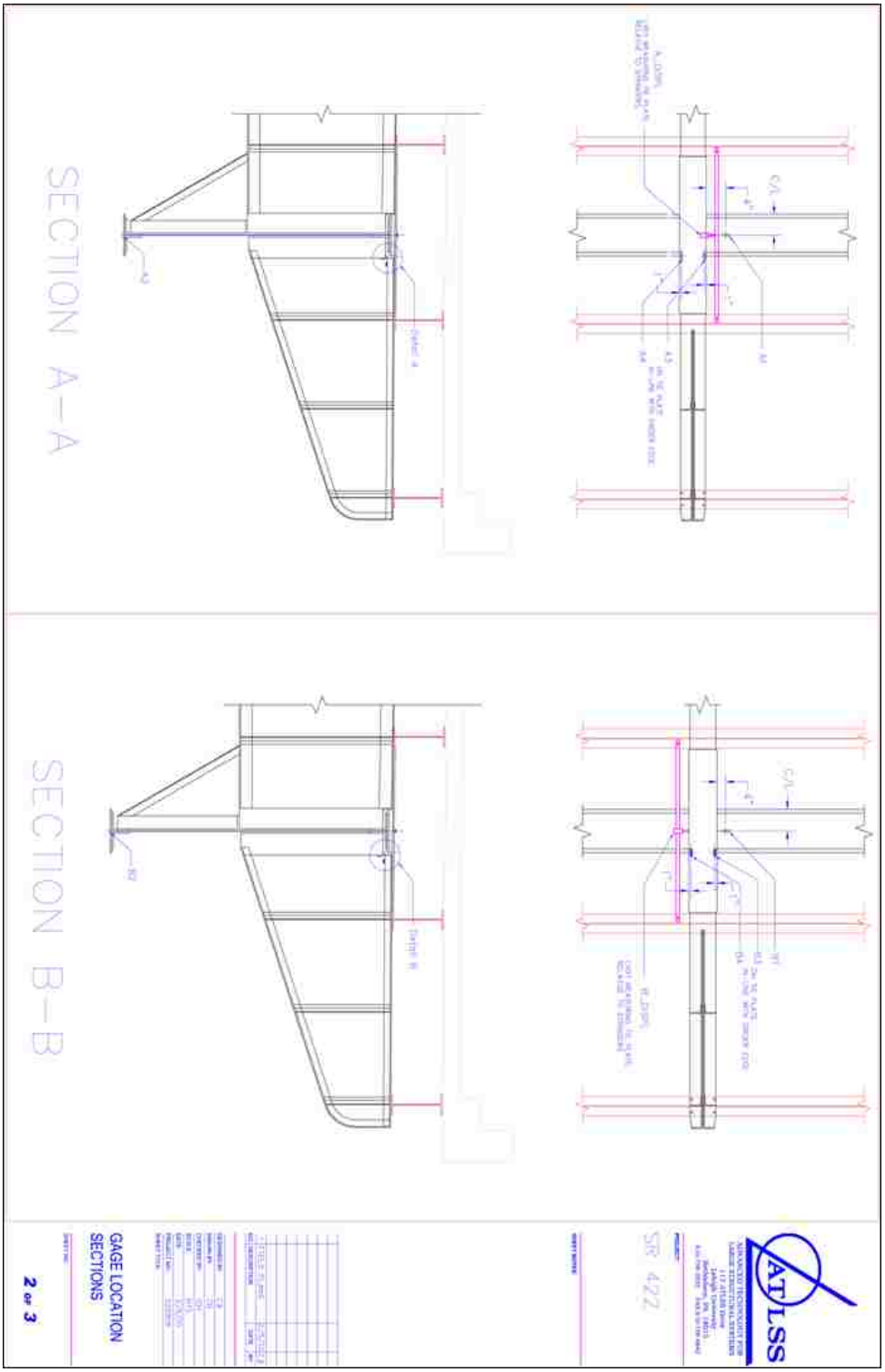
SECTION A–A
SECTION B–B
GAGE LOCATION SECTIONS
2 of 3
SR 422
ATLSS

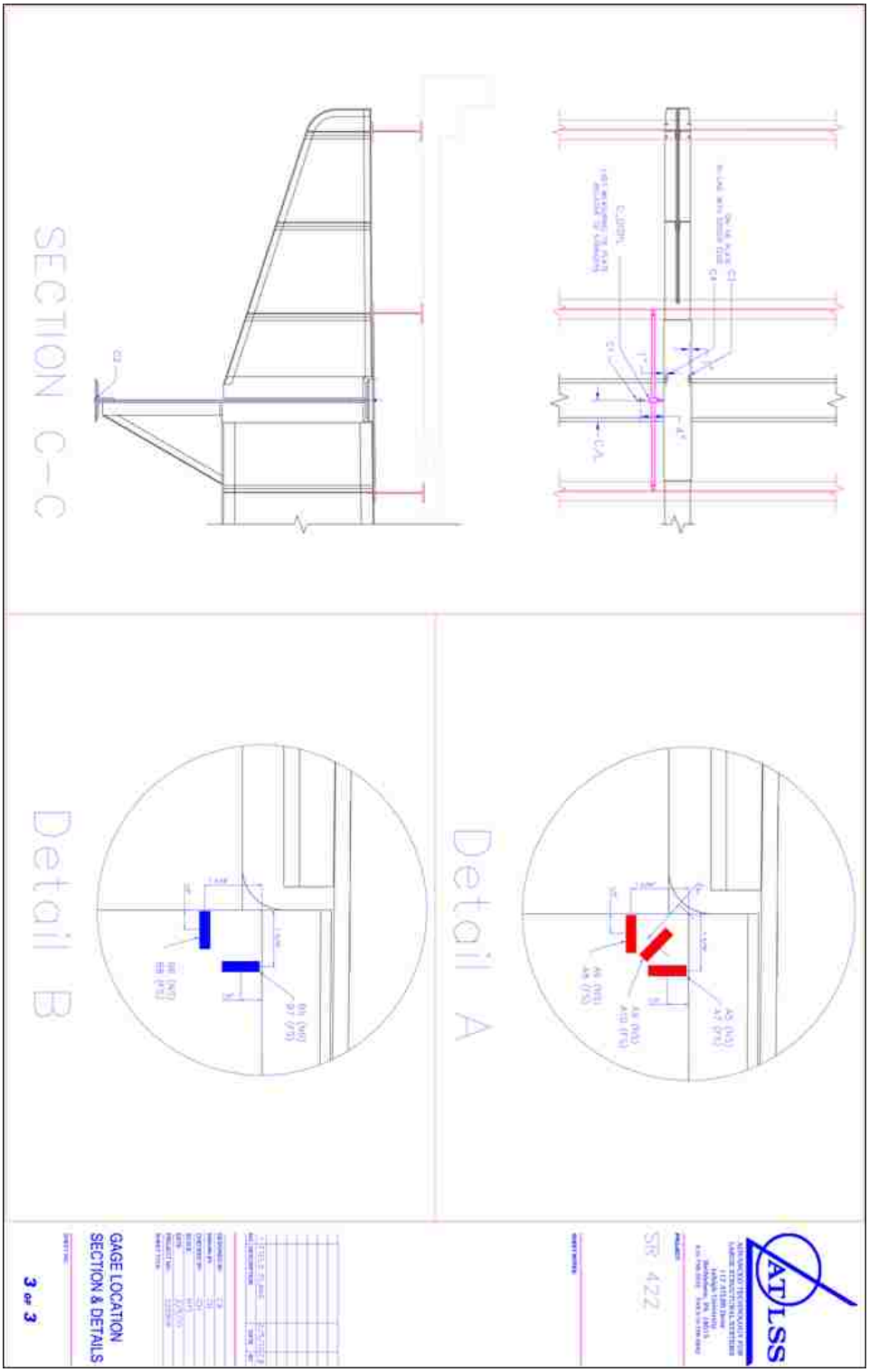
SECTION C-C
Detail A
Detail B
ATLSS
SR 422
GAGE LOCATION
SECTION & DETAILS
3 of 3

Appendix B: Mathcad Computation Sheet

Design Computation of Bending Stress in Tie Plate

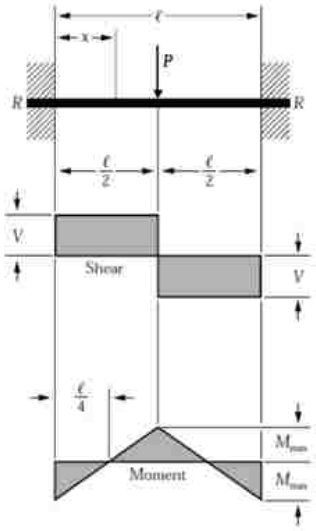

$R = V \ldots = \frac{P}{2}$

M_{max} (at center and ends) $\ldots = \frac{P\ell}{8}$

$M_x \left(\text{when } x < \frac{\ell}{2} \right) \ldots = \frac{P}{8}(4x - \ell)$

Δ_{max} (at center) $\ldots = \frac{P\ell^3}{192EI}$

$\Delta_x \left(\text{when } x < \frac{\ell}{2} \right) \ldots = \frac{Px^2}{48EI}(3\ell - 4x)$

h := 10ft Girder height

E := 29000ksi Young's modulus

d := 1ft Tie plate width

I Moment of inertia of tie plate

θ Girder rotation

L Stringer spacing

x Distance between location under study and stringer

Δ Tie plate in-plane displacement

$Mmax := \frac{24 \cdot E \cdot I \cdot \Delta}{L^2}$ Maximum in-plane bending moment of tie plate

$Mx := Mmax \cdot \frac{4x - L}{L}$ Moment at location under study

$\sigma max := \frac{Mmax \cdot \frac{d}{2}}{I}$ Maximum in-plane bending stress of tie plate

$\sigma x := \frac{Mx \cdot \frac{d}{2}}{I}$ Stress at location under study

Case 1: stringer spacing = 4.06 ft

$\theta := 0.00037\,rad \qquad L := 4.0625 \cdot ft \qquad x := 1.1875 ft$

$\Delta := h \cdot \tan(\theta) = 3.7 \times 10^{-3} \cdot ft$

$\sigma x := \frac{12 \cdot E \cdot d \cdot \Delta}{(L)^2} \cdot \frac{(4 \cdot x - L)}{L} = 13.203\,ksi$

Case 2: stringer spacing = 7.125 ft

$\theta := 0.000558311\,rad \qquad L := 7.125 ft \qquad x := 2.28 ft$

$\Delta := h \cdot \tan(\theta) = 5.583 \times 10^{-3} \cdot ft$

$\sigma x := \frac{12 \cdot E \cdot d \cdot \Delta}{(L)^2} \cdot \frac{(4 \cdot x - L)}{L} = 10.716\,ksi$

Case 3: stringer spacing = 10.57 ft

$\theta := 0.00062\,rad \qquad L := 10.575 ft \qquad x := 4 ft$

$\Delta := h \cdot \tan(\theta) = 6.2 \times 10^{-3} \cdot ft$

$\sigma x := \frac{12 \cdot E \cdot d \cdot \Delta}{(L)^2} \cdot \frac{(4 \cdot x - L)}{L} = 9.898\,ksi$

Case 4: stringer spacing = 13.02 ft

$\theta := 0.00066\,rad \qquad L := 13.025 ft \qquad x := 5.23 ft$

$\Delta := h \cdot \tan(\theta) = 6.6 \times 10^{-3} \cdot ft$

$\sigma x := \frac{12 \cdot E \cdot d \cdot \Delta}{(L)^2} \cdot \frac{(4 \cdot x - L)}{L} = 8.206\,ksi$

Vita

EDUCATION

Lehigh University, **Master of Science** in Civil Engineering (Expected in May, 2012), Department of Civil and Environmental Engineering, Bethlehem, PA, 08/ 2009 ~ 05/2012

Tongji University, **Bachelor of Science** in Civil Engineering, Shanghai, China, 09/2005 ~ 06/2009

ENGINEERING EXPERIENCES

Graduate Research Assistant of ATLSS (Advanced Technology for Large Structural Systems), Lehigh University, worked on PennDOT bridge projects, 04/2010~04/2012

- **Master of Science Thesis** "Fatigue Failure Evaluation of Tie Plates due to Secondary Deformations on Steel Plate Girder Bridges"
- Performed field inspection, collected and analyzed test data
- Developed Finite Element (ABAQUS) and SAP2000 Model to evaluate fatigue and fracture failure and to produce retrofit approaches, parametric studies, etc. **FE Model analysis's results match actual test data very well**. **PennDOT conducted retrofit procedure based on FEA results**
- Assisted with writing forensic report

Undergraduate Research Assistant of State Key Laboratory for Disaster Reduction in Civil Engineering on The Shaking Table Testing Division of Tongji University (TJST), worked on performance of reinforced concrete structure strengthened by new material, 09/2007~05/2009

- Bachelor of Science Thesis "An Initial Study on Performance of Damaged Interior Column-Beam-Slab Subassemblies Strengthened by New Reinforcement Material"
- Designed RC beam-to-column connection
- Assisted with reinforcement assembling and casting
- Developed ANSYS 3D FEM to predict shear performance
- Calculated cracking load and ultimate load, and composed report and paper

WORK EXPERIENCES

Intern in KCI Technologies, Inc., Sparks, MD, 01/2010

- Assisted in shop drawing preparation and review for transportation department
- Observed of entry-level design tasks related to engineering projects
- Introduced to an advanced computer-based technology, Building Information Modeling (BIM), learned to use REVIT
- Field trip to a steel mill, worked with superintendents and site safety managers

Intern in Shijingshan Construction Company, Beijing, China, 05/2008~08/2008

- Worked as a member of the on-site team for the construction management of a multi-purpose reinforced concrete building
- Performed acceptance and quality control tests for concrete pours
- Created plan, elevation, and detail drawings using AutoCAD for a number of projects
- Designed the parking lot for a residential area in Shijingshan, Beijing
- Assistant in cost estimates

COURSE DESIGN PRACTICES

Term Project of Structural Safety and Risk on Bridge Fatigue Reliability Assessment

The Big Beam Contest, PCI Engineering Student Design Competition, 2011 (**served as team leader, won second price**)

Term Project of Highway Design

Term Project of Finite Element Analysis on Arch Bridge Design

Design Project of A Steel Single Story Industrial Building, Zhejing Province, China

Group work on Designing a Concrete Single-Story Industrial Building and Construction Organization

PUBLICATION AND PRESENTATION

Fatigue Crack Formation and Repair Strategies for Steel Cantilever Bracket Tie Plates, ASCE Journal of Bridge Engineering, doi:10.1061/(ASCE)BE.1943-5592.0000391, March 2012

Presentation in 2011 Transportation Research Board 90th Annual Meeting, Washington D.C.

Study on Performance of Reinforced Concrete Structure Strengthened by New Material, Earthquake Resistant Engineering and Retrofitting, 2009, 31(6)

ADDITIONAL EXPERIENCE

Assistant in "IABMAS 2010, the Fifth International Conference on Bridge Maintenance, Safety and Management", Philadelphia, PA

Assistant in the Fritz Engineering Laboratory 100th Anniversary, Lehigh University

AWARD

Scholarship of Transportation Infrastructure Solution, Awarded by Associated Pennsylvania Constructors (APC), 10/2010

COMPUTER SKILLS

Revit, MS Office, Microstation, Mathcad, AutoCAD**,** SAP2000, ABAQUS, ANSYS, LARSA, STAAD, MATLAB, Visual Basic, SQL Server